

REMOVAL OF VOLATILE ORGANIC COMPOUNDS (VOCs) FROM AIR AND WATER USING CARBON NANOMATERIALS

**A Thesis Submitted to
Babu Banarasi Das University
for the Degree of**

**Doctor of Philosophy
in
Environmental Science**

**By
Ila Srivastava**

**Under the Supervision of
Dr. Pramod Kumar Singh**

**Under the Co-Supervision of
Dr. Nalini Sankararamakrishnan**

**Department of Chemistry,
School of Applied Sciences
Babu Banarasi Das University,
Lucknow-226028 (U.P.) India
June, 2018**

CERTIFICATE OF THE SUPERVISOR(S)

This is to certify that the thesis, entitled **“Removal of volatile organic compounds (VOCs) from air and water using carbon nanomaterials”** submitted by Ila Srivastava for the award of Degree of Doctor Philosophy to Babu Banarasi Das University, Lucknow and IIT Kanpur, are record of authentic work carried out by IlaSrivastava under my supervision. To the best of our knowledge, the matter embodied in this thesis is the original work of the candidate and has not been submitted elsewhere for the award of any other degree or diploma.

Signature

(Dr. NaliniSankararamakrishnan)
(Scientist)
Centre for Environmental
Science and Engineering)
Indian Institute of Technology (IIT),
Kanpur, Uttar Pradesh
India - 208016

Signature

(Dr. Pramod Kumar Singh)
(Associate Professor)
Department of Environmental Science
School of Applied Science,
BabuBanarashi Das, University,
Lucknow, Uttar Pradesh,
India - 226028

Date:

DECLARATION BY THE CANDIDATE

I, hereby, declare that the work presented in this thesis, entitled“**Removal of volatile organic compounds (VOCs) from air and water using carbon nanomaterials**”. in fulfillment of the requirements for the award of Degree of Doctor of Philosophy of Babu Banarasi Das University, Lucknow is an authentic record of my own research work carried out under the supervision of **Dr. Pramod Kumar Singh** (Associate Professor) Department of Environmental Science, Babu Banarashi Das, University, Lucknow, Uttar Pradesh, India- 226028 and **Dr. Nalini Sankararamakrishnan**, (Scientist), Centre for Environmental Science &Engineering, IIT Kanpur,Uttar Pradesh, India- 208016.

I also declare that the work embodied in the present thesis is my original work and has not been submitted by me for any other Degree or Diploma of any university or institution.

Date:-----

Name & Signature of theCandidate
Ila Srivastava
Environmental Science
School of Applied Science
Babau Banarasi Das, University
Lucknow, UP, India- 226028

ACKNOWLEDGEMENT

I honestly precise my deep sense of gratitude to my thesis supervisor, Dr. Pramod Kumar Singh, (Associate Professor), BabuBanarasi Das, University, Lucknow, Uttar Pradesh, India, and co-supervisor, Dr. NaliniSankararamakrishnan, (Scientist), Centre for Environmental Science & Engineering, IIT Kanpur, UP, India, for providing me an opportunity to do research under his supervision, mentoring and being a continuous source of motivation for me throughout the research period for his expert guidance, continuous encouragement and inspiration throughout the course of thesis work. I am sincerely thankful for his intellectual support and creative criticism, which led me to generate my own ideas and made my work interesting and enjoyable.

I precise my gratefulness to my Ph.D. events committee member Dr. Ahmad Ali, (Dean School of Applied Science and Coordinator of Ph.D. program) for her time to time informative moral support and timely help throughout my research period like presentation, exam and other activity.

I am thankful to faculty members of Centre for Environmental Science and Engineering Dr. Tarun Gupta for their help and guidance. I am indebted to all of them and IIT Kanpur for giving me the fundamentals and chance to implement them.

I would also like to express my thanks to my respected faculty members Dr. Shalini G. Pratap, Dr. Manisha T. Sharma, Dr. C.P. Pandey, Dr. Monika Gupta, Department of Chemistry, BabuBanarasi Das, University, for their timely support, motivation and care during the study period and management committee and members of BBDU which support me and other special thanks to Mr. Mayank, for help starting to till to encourage me.

I would like to thank help me for doing research work and thesis writing Dr. KartikyaShukla, Associate professor, Jounpur University, Dr. Dharam Singh, Head, Environmental Science, CSJMU, Kanpur and Dr. JatinSrivastava, Assistant Professor, Global Institute of Lucknow, for lending a helping hand by valuable inputs, extending valuable inputs, discussions, helping in writing of thesis to submission and motivation during the course of the study.

I would like to thanks my seniors Dr. DivyaChauhan, Dr. Sruti Mishra, Dr. Anil Shankhwar, Mr. Vinay Kumar, Miss. NeetuPanday, for being the Stress-busters and staying by me through the thick and thin of things. Thanks to them for transforming moments of uncertainties and sulkiness into uplifting ones.

I am also thankful to my friends Mr. Anil Kumar, Mr. RanjeetVerma, Mr. PokhrajSahu, Mr. LalJi, Mr. Sanjai Kumarand Mr. Nafeesh Ali for their friendly behavior, cooperation and help during my thesis work.

I have no words to express my respect for my parents and my brothers, who have sacrificed their comforts for me and have been continuous source of inspiration in my difficult time, my father Mr. Vishnu Kumar Srivastava and mother Miss. SeemaSrivastava, my brother Mr. OshoSrivastava and my brother wife Miss. JanaviSrivastava. I am sure that I would not have had the strength to complete the task successfully. I thank them for their patience and bearing with me for shunning most of the domestic responsibilities during this period. Finally I would like to thank everyone who had helped me in an along my research work.

ILA SRIVASTAVA

PREFACE

Volatile organic compounds namely toluene(T), ethylbenzene (E) and o-xylene (X) are widely used in various industrial processes. TEX is the primary pollutants that convert into secondary air pollutants and result in disastrous condition that claim a number of lives. Huge amounts of TEX are discharged into the air and further TEX contaminated wastewater is discharged into surrounding water bodies from various industries. TEX are carcinogenic, toxic, and flammable substances, presence of greater amounts of these carcinogenic solvents in water bodies may affect air/water quality and thus endanger both public health and wellbeing.

To address the afore mentioned problems efforts were made to synthesize carbon nanotubes (LCNT) and carbon microspheres (LCM) indigenously by floating catalytic chemical vapor deposition method. In this method, ferrocene dissolved in benzene acted as the hydrocarbon source and the material was prepared without any additional substrate. Further functionalization of the prepared carbon materials was carried out by oxidation using nitric acid to produce oxidized carbon nanotubes (LCNT-OX) and oxidized carbon microspheres (LCM-OX). The prepared adsorbents were evaluated for the removal of TEX from both air and water matrices.

The prepared carbon composites were characterized by various techniques including Scanning Electron Microscopy (SEM), Transmission electron microscopy (TEM), Fourier Transform Infrared spectroscopy (FTIR), Brunauer–Emmett–Teller (BET) surface analyzer, Raman, and X-ray photoelectron spectroscopy (XPS).

The hexagonal arrays of sp²-like carbon atoms in the tubular graphene sheets on the surfaces of CNTs provide a favorable morphological structure for adsorbing aromatic compounds. The prepared CNTs ranged from 50 to 80 nm in width and few micrometers in length. The specific surface area of LCNT and LCM was found to be

99.8 and 7.22 m²/g respectively. Further upon oxidation with nitric acid opening of pores lead to increased surface area. Thus the surface of LCNT-OX and LCM-OX was found to be 121.68 and 12.70 m²/g respectively. Further pore size distribution of the composites revealed higher percentage of mesopores in all the adsorbents.

The adsorption kinetics of TEX over various prepared carbon composites in water followed Pseudo Second Order Kinetics with regression coefficients >0.99. Langmuir and Freundlich isotherms were used to model the obtained equilibrium data and various isotherm constants were evaluated. The main novelty in this work is the preparation of CNTs without any substrate. Adsorption properties of TEX as a function of equilibration time, pH initial TEX concentrations were evaluated.

The removal TEX from ground water matrix without depreciation in sorption capacity, faster kinetics, dynamic equilibrium and recyclability studies advocate the applicability of carbon composites in filter cartridges and wastewater treatment units. Recyclability studies were demonstrated for 5 cycles without any decrease in the sorption capacity. Column studies revealed that 50 bed volumes of (950 ml) of 30 ppm toluene containing distilled water could be treated reducing the concentration from 30 ppm to below detection limit using 3 mg of LCNT. The prepared material was applied to the successful removal of Toluene, ethyl benzene and O-Xylene from aqueous solutions.

Adsorption of TEX by lab CNTs were found to be constant irrespective of initial pH of the aqueous solution. The rate of adsorption of TEX on lab CNTs was very fast and within 20 min equilibrium was reached. Maximum adsorption capacity of LCNT, LCNT-OX, LCM and LCM-OX towards o-xylene were found to be 47.17, 72.46, 24.27 and 47.16 mg/g, respectively. It was found that using static adsorption test the TEX adsorption capacity for the carbon composites were in the order of

LCNT-OX >LCNT, LCM-OX >LCM. LCNT-OX for O-Xylene was revealed the best % removal (76).

However, for O-Xylene and ethyl-benzene were attained the maximum contact time ($T_e = 164$ min) and overall result as per capacity was followed the following pattern: O-Xylene > Ethyl-Benzene > Toluene.

Experiments were conducted for the removal of TEX from air. Three different initial concentrations of TEX were studied namely 100, 300, and 700 ppm. Weight of the adsorbent for this method was maintained at 3g. It was found that similar to water, experiments with air revealed higher uptake capacity of LCNT-OX compared to other adsorbents. Further uptake capacity of O-Xylene was high compared to ethyl benzene and toluene.

Thus it is evident that prepared adsorbents is efficient in removing TEX from both air and water matrices and hence the prepared adsorbents could be used to remove other VOCs as well.

**DEVOTED
TO
MYFAMILY
AND
TEACHERS**

“Reduce air pollution & increase your life span”

TABLE OF CONTENTS

Topic	Page No
Title	i
Supervisor`s Certificate	ii
Declaration by Candidate	iii
Acknowledgements	iv-v
Preface	vi-viii
Dedication	ix
TABLE OF CONTENTS	x-xv
LIST OF TABLES	xvi
LIST OF THE FIGURES	xvii-xix
CHAPTER- 1 INTRODUCTION	1-14
1.1. Introduction	1-13
1.1. Aims and Objectives	14
CHAPTER- 2 REVIEW LITERATURE	15-40
2.1. Introduction	15
2.2. Volatile organic compounds	15-17
2.3. VOC sources, effect and contamination of water and air (Global Perspective.	18-26

2.4. Various method and techniques for VOCs from air and water streams	26-34
2.5. Various adsorbents used for VOC Adsorption	34-40
CHAPTER- 3 MATERIAL AND METHODS	41-58
3.1. Quality assurance	41
3.1.1. Chemicals	42
3.1.2. Instruments and Accessories	42
3.2. Preparation of LCNTs using floating catalytic chemical vapor deposition technique	42-44
3.2.1. Preparation of Oxidized LCNTs (LCNT-OX)	44-45
3.3. Preparation of carbon Microspheres (LCM) using floating catalytic chemical vapor deposition (CVD) technique	45
3.3.1. Preparation of Oxidized LCM (LCM-OX)	45-46
3.4. Preparation of Alkali carbon microsphere (ACM)	46
3.5. Field electron scanning electron (FE-SEM) microscopy	46-48
3.5.1. Transmission electron microscopy	48
3.5.2. Raman spectroscopy	48-50
3.5.3. X-ray diffraction analysis	50-51
3.5.4. X-ray photoelectron spectroscopy analysis	51-52
3.5.5. Fourier Transform Infrared spectroscopy	52
3.5.6. BET Surface area and total pore volume analysis	53
3.6. pH studies	53-54
3.7. Kinetic studies	54
3.8. Equilibrium isotherm studies	54-55

3.9. Column or dynamic study for VOCs determination	55-56
3.10. Gas Chromatography	56-57
3.11. Model for VOCs adsorption	57-58
CHAPTER- 4 RESULTS	59-95
4.1. Introduction	59
4.2. Characterization of carbon composites SEM images of (a) CNT, (b) LCNT-OX, (c) and (d) TEM images of LCNT, (e) SEM Image of LCM (f) TEM image of LCM	60
4.2.1. SEM and TEM analysis	60-61
4.2.2. BET analysis	62-63
4.2.3. XRD analysis	64-65
4.2.4. FTIR analysis	65-66
4.2.5. Raman analysis	66-68
4.2.6. XPS analysis	68-69
4.2.6.1. Studies on (TEX) removal	70
4.2.6.2. Effect of initial pH	70
4.2.6.3. Effect of kinetics	71-72
4.2.6.4. Adsorption Isotherm	73-77
4.2.6.5. Static sorption	78
4.2.6.6. Column studies	78-79
4.2.6.7. Recyclability studies	79-81
4.2.6.8. Applicability in ground water matrix	81-82
4.3. TEX Analysis of air experiment	83
4.3.1. Introduction	83

4.3.2. Characterization of mesoporous carbon microspheres	83
4.3.2.1. BET analysis and BET Isotherm	83-84
4.3.2.2. Calibration curve for TEX	84-86
4.3.2.3. Breakthrough curves	86-87
4.3.2.4. Breakthrough curves CMS, CNT-Plain, and CNT-OX with Toluene low concentration:	87
4.3.2.5.. Breakthrough curves CMS, CNT-Plain, and CNT-OX with Ethylbenzene low concentration:	87-88
4.3.2.6. Breakthrough curves CMS, CNT-Plain, and CNT-OX with o-xylene low concentration:	88-89
4.3.2.7. Breakthrough curves CMS, CNT-Plain, and CNT-OX with toluene medium concentration:	89-90
4.3.2.8. Breakthrough curves CMS, CNT-Plain, and CNT-OX with Ethylbenzene medium concentration:	90-91
4.3.2.9. Breakthrough curves CMS, CNT-Plain, and CNT-OX with o-xylene medium concentration:	91-92
4.3.2.10. Breakthrough curves CMS, CNT-Plain, and CNT-OX with toluene high concentration:	92-93
4.3.2.11. Breakthrough curves CMS, CNT-Plain, and CNT-OX with Ethylbenzene high concentration:	93-94
4.3.2.12. Breakthrough curves CMS, CNT-Plain, and CNT-OX with o-xylene high	94-95
CHAPTER – 5 DISCUSSION	96-116
5.1. Introduction	96-97

5.2. Characterization of carbon composites SEM images of (a) CNT, (b) LCNT-OX, (c) and (d) TEM images of LCNT, (e) SEM Image of LCM (f) TEM image of LCM	98
5.2.1. SEM and TEM analysis	98
5.2.2. BET analysis	98-99
5.2.3. XRD analysis	99
5.2.4. FTIR analysis	99-100
5.2.5. Raman analysis	100
5.2.6. XPS analysis	100-101
5.2.6.1. Studies on (TEX) removal	101
5.2.6.2. Effect of initial pH	101
5.2.6.3. Effect of kinetics	101-103
5.2.6.4. Adsorption Isotherm	103-105
5.2.6.5. Static sorption	105-106
5.2.6.6. Column studies	106-108
5.2.6.7. Recyclability studies	108
5.2.6.8. Applicability in ground water matrix	108-109
5.3. TEX Analysis of air experiment	109
5.3.1. Introduction	109-110
5.3.2. Characterization of mesoporous carbon microspheres	110
5.3.2.1. BET analysis and BET Isotherm	110-111
5.3.2.2. Calibration curve for TEX	111
5.3.2.3. Breakthrough curves	111
5.3.2.4. Breakthrough curves CMS, CNT-Plain, and CNT-OX with	111-112

Toluene low concentration:	
5.3.2.5.. Breakthrough curves CMS, CNT-Plain, and CNT-OX with Ethylbenzene low concentration:	112
5.3.2.6. Breakthrough curves CMS, CNT-Plain, and CNT-OX with o-xylene low concentration:	113
5.3.2.7. Breakthrough curves CMS, CNT-Plain, and CNT-OX with toluene medium concentration:	113-114
5.3.2.8. Breakthrough curves CMS, CNT-Plain, and CNT-OX with Ethylbenzene medium concentration:	114
5.3.2.9. Breakthrough curves CMS, CNT-Plain, and CNT-OX with 0-xylene medium concentration:	114-115
5.3.2.10. Breakthrough curves CMS, CNT-Plain, and CNT-OX with toluene high concentration:	115
5.3.2.11. Breakthrough curves CMS, CNT-Plain, and CNT-OX with Ethylbenzene high concentration:	115-116
5.3.2.12. Breakthrough curves CMS, CNT-Plain, and CNT-OX with o-xylene high	116
CHAPTER 6 SUMMARY AND CANCLUSION	117-119
REFERENCES	120-139
LIST OF PUBLICATIONS	140-141

LIST OF TABLES

Table No.	Title Name	Page No
1	Physico-chemical properties of Benzene, Toluene and Xylene	5
2	List of 62 VOCs (as per EPA Standard Method to15/17)	17
3	Specific surface area and pore volumes of various carbon composites	63
4	Raman spectra of LCNT, LCNT-OX, LCM and LCM-OX	68
5	Kinetic parameters for TEX sorption using LCNT, LCNT-OX, LCM and LCM-OX	72
6	Langmuir Isotherm Constants for o-Xylene	76
7	Freundlich Isotherm Constants	76
8	Langmuir Isotherm Constants for o-Xylene	77
9	Comparative studies of carbon composites reported in the literature for the removal of o-xylene from aqueous phase	77
10	Static sorption test of carbon composites	78
11	Recyclability Studies	80
12	Applicability to Ground water	81
13	Effect of contact time in Breakthrough curves	86

LIST OF THE FIGURES

Figure No.	Title of Figures	Page No
1	Showing effect of VOCs on different part of Human	26
2	Showing the external image of CVD machine during reaction	43
3	Showing image of internal CVD machine during reaction	44
4	Schematic representation of preparation of CNT-OX	45
5	Schematic representation of preparation of LCM-OX	46
6	Column Study	56
7	Gas Chromatography External image with all accessories	57
8	Experimental model for VOCs adsorption from air contamination	58
9	SEM images of (a) LCNT, (b) LCNT-OX, (c) and (d) TEM images of LCNT, (e) SEM Image of LCM (f) TEM image of LCM	61
10	X-ray diffraction pattern of (a) LCNT and LCNT-OX	64
11	X-ray diffraction pattern of (b) LCM and LCM-OX	65
12	FTIR spectra of LCNT, LCNT-OX, LCM and LCM-OX	66
13	Raman Spectra of LCNT, LCNT-OX, LCM and LCM-OX	67
14	XPS Survey spectra of LCNT, LCNT-OX, LCM and LCM-OX	69
15	Effect of initial pH on the sorption behavior of TEX using LCNT	70
16	Kinetics of adsorption of LCNT, LCNT-OX, LCM and LCM-OX with (a) Toluene, (b) Ethyl Benzene and (c) O-Xylene	71
17	Equilibrium Isotherms of (a) LCNT and LCNT-OX, (b) LCM and LCM-OX and (c) P-CNT with TEX	74

18	Line arised Langmuir isotherm plots of (a) LCNT and LCNT-OX; (b) LCM and LCM-OX and (c) P-CNT with o-Xylene	75
19	Breakthrough curve of LCNT-OX with Toluene	79
20	Recyclability Studies	81
21	Applicability to Ground water	82
22	BET Isotherm (a) Adsorption and Desorption	83
23	BET Isotherm (b) Adsorption and Desorption	84
24	Calibration curve for Ethylbenzene	85
25	Calibration curve for Toluene	85
26	Calibration curve for O-Xylene	86
27	Breakthrough curve of CMS, CNT-Plain, and CNT-OX with Toluene, (100ppm)	87
28	26 Breakthrough curve of CMS, CNT-Plain, and CNT-OX with (b) Ethylbenzene, (100 ppm)	88
29	Breakthrough curve of CMS, CNT-Plain, and CNT-OX with (b) O-Xylene, (100 ppm)	89
30	28 Breakthrough curve of CMS, CNT-Plain, and CNT-OX with (b) Toluene, (300 ppm)	90
31	Breakthrough curve of CMS, CNT-Plain, and CNT-OX with (b) Ethylbenzene, (300 ppm)	91
32	Breakthrough curve of CMS, CNT-Plain, and CNT-OX with (b) O-Xylene, (300 ppm)	92

33	Breakthrough curve of CMS, CNT-Plain, and CNT-OX with (b) Toluene, (700 ppm)	93
34	Breakthrough curve of CMS, CNT-Plain, and CNT-OX with (b) Ethylbenzene, (700 ppm)	94
35	Breakthrough curve of CMS, CNT-Plain, and CNT-OX with (b) O- Xylene, (700 ppm)	95

Chapter 1

Introduction

CHAPTER - 1

INRODUCTION

1.1. Introduction

In atmosphere or around us present several air pollutants which play an important role to causing health problems, like volatile organic compounds (VOCs) are the major pollutants like benzene, toluene, ethylbenzene and xylene (BTEX) because of toxicity behavior. VOCs are defined as - organic compounds having vapor pressure equal to or greater than 0.1 mm Hg (USEPA, 1990). These pollutants are emitted from natural as well as anthropogenically sources. Pollution of water, soil and air is a worldwide issue for the eco – environment and human society.

In fact the widespread use of new products and materials in our days has resulted in increased concentrations of indoor pollutants, especially of volatile organic compounds (VOCs), which pollute indoor air and maybe affect human health. As a result, the air of all kinds of indoor spaces is frequently analyzed for VOCs (Brown et al., 1994). Unfortunately, this common practice suffers from the lack of a standardized procedure to calculate the VOCs value from the results of the analysis.

The organic compounds that evaporate easily are recognized together as volatile organic compounds. Technically such compounds are defined as organic compounds with a vapour pressure of 1300 Pascal (about 1% atmospheric pressure at sea level). These compounds may include several aromatic hydrocarbons and considered into the common category due to their similar physical behavior in the atmosphere. These compounds have a boiling point range with lower limit between 50°C and 100°C and an upper limit between 240°C and 260°C where the higher refer to polar compound.

The major How to cite this paper: Mèçabih, Z. (2010) Adsorption-Desorption of BTEX (Benzene, Toluene, ethylbenzene and O-Xylene) on Fe, Fe-Al Pillared Clay.

41 VOCs, the benzene, toluene and xylene (BTX) volatile compounds are significant environmental concern and are listed as priority pollutants by the United States Environmental Protection Agency (US EPA, 2000)

Mostly VOCs come out as evaporative emissions during handling, storage and use and as part of incomplete or partially burnt hydrocarbons mostly along with exhaust gases from vehicles. There are thousands of different VOCs produced and used in our daily lives. Sources of VOCs like transport: vehicular exhaust, fuel filling station, fuel adulteration, railways, airways. Industries : major industrial units - refinery, petrochemical etc, industrial estates, medium scale chemical industries, domestic emissions - domestic combustion unit, commercial combustion units. Paints, varnishes, moth balls, solvents, gasoline, newspaper, upholstery, fabrics, cooking, cleaning, chemicals, vinyl floors, carpets, photocopying, sealing, adhesives, caulks, cosmetics, air fresheners, fuel oil, and environmental tobacco smoke etc.

VOCs frequently found in the atmosphere are alcohols, ethers, ketones, aldehydes, esters, acids, alkanes, cyclic hydrocarbons, alkenes and terpenes, aromatic hydrocarbons, halocarbons including trichloroethylene etc. (Levin *et al.*, 2006). These are emitted into the atmosphere from a variety of sources, including vehicles, fossil fuel combustion, steel-making, petroleum refining, fuel refilling, industrial and residential solvent use, paint application, manufacturing of synthetic materials (plastics, carpets etc.), food processing, agricultural activities and wood processing and burning (Manahan, 1994). These VOCs were settled down in the soil and water but due to evaporation behavior these pollutants tabulated in atmosphere air that were very toxic. The concentrations of VOCs were toxic more in ambient air and water substances.

The most commonly occurring chemicals of this class are benzene, toluene,

ethylbenzene and xylene (BTEX). Table1 show Physical-chemical properties of Benzene, Toluene and Xylene. The BTEX compounds are harmful toxic pollutants causing exposure related health effects in human beings. This group of VOCs is evidently carcinogenic in human beings. Due to the health aspects of BTEX compounds, it is becoming extremely important to screen their presence and to determine prevailing concentration in the ambient environment. Acute-eye irritation / watering, nose irritation, throat irritation, headache, nausea/vomiting, dizziness, asthma exacerbation chronic–cancer, liver damage, kidney damage, and central nervous system damage.

Long term exposure to benzene causes Leukaemia in human beings. In animal studies, leukemia, lymphomas and other types of tumors are observed. Exposure to benzene is linked to genetic changes, increased proliferation of bone marrow cells and occurrence of certain chromosomal aberrations in humans and animals. USEPA has classified benzene as group a human carcinogen. In addition a number of non-cancer effects are associated with Benzene exposure such as disorders of blood, harmful effects of bone marrow, anaemia and reduced abilities of blood to clot, damage to immune system and acts as a reproductive and developmental toxicant.

WHO estimates a 4 in 1 million risk of leukaemia on exposure to benzene to a concentration of $1\mu\text{g}/\text{m}^3$ (0.31ppb). High levels of benzene exposure produce haematotoxic effects like leucopenia, lymphopenia and anaemia; neurotoxic symptoms; ventricular tachycardia and respiratory failure. Toluene in comparison to benzene is less toxic and may cause drowsiness, impaired coordination etc. High dose exposure of toluene can produce kidney and liver damage and hyperplasia of bone marrow, anaemia, and depression in central nervous system which may lead to impairment of coordination and slowed reaction time. Acute xylene exposure may be

marked by dizziness, weakness, headache, nausea, vomiting, breathing difficulty and loss of coordination. In severe exposure, there is visual blurring, tremors, heart beat irregularities, paralysis and loss of consciousness.

Benzene is extensively utilized as industrial solvent in manufacturing of lacquers, varnishes and paint. Benzene escapes from mineral oil and petrol during storage, transport, loading, unloading or during filling of petrol in motor vehicles. High concentrations of Benzene are encountered in the vicinity of petrol filling stations, fuel tank storage sites, coking plant in the vicinity of refineries. Major Benzene emission originates from the motor vehicles. Benzene is present in both exhaust and evaporative emissions. Motor vehicles account for approximately 85% of the total benzene emissions. The remaining is attributed to stationary sources (15%). Benzene is a component of gasoline. Another important source of benzene in air is active smoking of tobacco. As per EPA's estimate active smoking Central Pollution Control Board, 2002 accounts for roughly half of the total population exposure to benzene, which is over and above that from motor vehicles.

Benzene is quite stable in atmosphere and the only important reaction in the lower atmosphere is the reaction with OH radical. This reaction too is very slow. Benzene is one of the ingredients of petroleum product. Benzene hydrocarbons can be condensed and washed out to the coke-oven gas. Crude oil contains benzene and its homologues account for 3.9%-4.8%. In USA Benzene is also produced from olefins. Benzene in the motor fuel is in fact burnt in the combustion process, but at the same time there is an additional amount of benzene produced through dealkylation which is emitted. Benzene is mainly used as raw material for the production of substituted aromatic hydrocarbons.

Table 1: Physical-chemical properties of Benzene, Toluene and Xylene

Properties	Benzene	Toluene	o-Xylene	m-Xylene	p-Xylene
Physical form (20°C)	Clear colour less liquid	Clear colour less liquid	Colour less liquid	Colour less liquid	Colour less liquid
Flash Point(0°C)	-11.1°C	4.4°C	30°C	25°C	25°C
Flammable limits	1.3-7.1%	1.17-7.1%	-	-	-
Melting/ Freezing point	5.5°C	-95°C	-25.2°C	-47.9°C	13.3°C
Boiling Point (760 mm of Hg)	80.1°C	110.6°C	144.4°C	139.1°C	138.3°C
Density (g/ml) (20°C)	0.878	0.8669	0.876	0.860	0.857
Vapour pressure (26°C)	13.3 kPa	28.7 mmHg	0.66	0.79	0.86
Solubilities	Water:1800 mg/ lt at 25°C; Nonaq. Solvents: miscible with most	Freshwater: 535 mg/ lt at 25°C Seawater:380mg/lt at25°C	Water:142 mg/ lt	Water:156 mg/lt	Water:185 mg/lt

Benzene is found in the air from emissions from burning coal and oil, gasoline service stations, and motor vehicle exhaust. Acute (short-term) inhalation exposure of humans to benzene may cause drowsiness, dizziness, headaches, as well as eye, skin, and respiratory tract irritation, and, at high levels, unconsciousness. Chronic (long-term) inhalation exposure has caused various disorders in the blood, including reduced numbers of red blood cells and aplastic anemia, in occupational settings. Reproductive effects have been reported for women exposed by inhalation to high levels, and adverse effects on the developing fetus have been observed in animal tests. Increased incidence of leukemia (cancer of the tissues that form white blood cells) have been observed in humans occupationally exposed to benzene. EPA has classified benzene as known human carcinogen for all routes of exposure.

Toluene is added to gasoline, used to produce benzene, and used as a solvent. Exposure to toluene may occur from breathing ambient or indoor air affected by such sources. The central nervous system (CNS) is the primary target organ for toluene toxicity in both humans and animals for acute (short-term) and chronic (long-term) exposures. CNS dysfunction and narcosis have been frequently observed in humans acutely exposed to elevated airborne levels of toluene; symptoms include fatigue, sleepiness, headaches, and nausea.

CNS depression has been reported to occur in chronic abusers exposed to high levels of toluene. Chronic inhalation exposure of humans to toluene also causes irritation of the upper respiratory tract and eyes, sore throat, dizziness, and headache. Human studies have reported developmental effects, such as CNS dysfunction, attention deficits, and minor craniofacial and limb anomalies, in the children of pregnant women exposed to high levels of toluene or mixed solvents by inhalation. EPA has concluded that that there is inadequate information to assess the

carcinogenic potential of toluene.

Commercial or mixed xylene usually contains about 40-65% m-xylene and up to 20% each of o-xylene and p-xylene and ethylbenzene. Xylenes are released into the atmosphere as fugitive emissions from industrial sources, from auto exhaust, and through volatilization from their use as solvents. Acute (short term) inhalation exposure to mixed xylenes in humans results in irritation of the eyes, nose, and throat, gastrointestinal effects, eye irritation, and neurological effects. Chronic (long-term) inhalation exposure of humans to mixed xylenes results primarily in central nervous system (CNS) effects, such as headache, dizziness, fatigue, tremors, and incoordination; respiratory, cardiovascular, and kidney effects have also been reported. EPA has classified mixed xylenes as a Group D, not classifiable as to human carcinogenicity.

Several treatment technologies include adsorption, ion exchange, reduction, reduction followed by chemical precipitation; electrochemical precipitation, membrane separation, solvent extraction, bio-sorption, etc. have been adopted to remove volatile organic compounds (VOCs): benzene, toluene, ethylbenzene and xylene. The capability of such technique is greatly dependent on the development of suitable adsorptive materials. Many adsorbents have been used to remove benzene, toluene, ethylbenzene and xylene from air and water such as metal oxide nanoparticles, dendrimers, zeolites and carbon nanotubes.

Among the several hundreds of VOCs, most of the VOCs in ambient air are benzene, toluene, ethylbenzene, xylene, trichloroethylene and heptane. These compounds are carcinogenic, mutagenic and teratogenic to human health and also harmful to the skin, central nervous system, kidney and liver. It causes drowsiness, dizziness, headaches, tremors, confusion, and unconsciousness, leading to anemia at

high concentration (WHO, 2000). The United States Environmental Protection Agency (USEPA, 1990) has enlisted these compounds in the group of hazardous air pollutants (HAPs). HAPs (also known as toxic air pollutants or air toxics) are those pollutants that cause or may cause cancer or other serious health effects.

There are many adsorbents available for the removal of benzene, toluene, ethylbenzene and xylene still there is a need for an adsorbent which is ecofriendly, high removal capacity, operates at neutral pH, chemical stability and can applies in large scale. The adsorbents described above are cost effective and applied in small scale, however, carbon based adsorbents are economical, ecofriendly, used in large scale industries.

However carbon nanotubes (CNTs) are a promising third generation of carbonaceous adsorbents. CNTs are allotropes of carbon exhibiting regular arrangement of carbon atoms bonded in single or multiple graphene sheets rolled in cylinders about a common axis. Naturally, CNTs have characteristic “tubular” voids along their axes formed by a single layer of carbon atoms bonded together.

The removal of volatile organic compounds (VOCs) from nano carbon tube technology treatment processes occurs through several mechanisms. These include absorption, adsorption onto solids, evaporation and air tripping or volatilization to the atmosphere. A variety of researchers have developed relationships between oxygen transfer into the water and VOC removal by air stripping (Roberts, et. al., 1984; Hsieh, et. al., 1993 a, b).

VOCs have significant effect on indoor and outdoor air quality along with other air pollutants including oxides of nitrogen (NO_x), oxides of carbon (CO and CO_2) and particulate matter. The United States Environmental Protection Agency (USEPA, 1990) has found concentrations of VOCs in indoor air commonly to be 2 to 5

times greater than in outdoor air and sometimes far greater. People generally spend more than 80% of their time in an indoor environment such as home, office, hotels etc. Therefore, exposure through indoor air could be high and it may result in adverse health effects (Wang *et al.*, 2007).

Consequently, effective air cleaning techniques are necessary for controlling the indoor air quality. Various methods are available to minimize pollutants from the environment which includes: source control, increase in ventilation and air purification system. Methods for air cleaning can be divided into two categories, i.e. combustible and non-combustible processes (Carp *et al.*, 2004). In non-combustible processes, VOCs released with the waste gas are collected. Contemporary techniques in this area include adsorption, condensation and biological filtration. In combustible processes, VOCs in the gas phase are destroyed by thermal and catalytic incineration. Both of these technologies have disadvantages and limitations in practical applications.

A significant nanoparticle discovery that came to light in 1991 was carbon nanotubes. Where buckyballs are round, nanotubes are cylinders that haven't folded around to create a sphere. Carbon nanotubes are composed of carbon atoms linked in hexagonal shapes, with each carbon atom covalently bonded to three other carbon atoms. Carbon nanotubes have diameters as small as 1 nm and lengths up to several centimeters. Although, like buckyballs, carbon nanotubes are strong, they are not brittle. They can be bent, and when released, they will spring back to their original shape. The carbon atoms in nanotubes are great at forming covalent bonds with many other types of atoms for several reasons:

Carbon atoms have a natural capacity to form covalent bonds with many other elements because of a property called electronegativity. Electronegativity is a

measure of how strongly an atom holds onto electrons orbiting about it. The electronegativity of carbon (2.5) is about in the middle of the range of electronegativity of various substances from potassium (0.8) to fluorine. Because carbon has electronegativity in the middle of the range, it can form stable covalent bonds with a large number of elements. All the carbon atoms in nanotubes are on the surface of the nanotube and therefore accessible to other atoms. The carbon atoms in nanotubes are bonded to only three other atoms, so they have the capability to bond to a fourth atom.

Techniques have been developed to produce carbon nanotubes in sizable quantities, including arc discharge, laser ablation, high-pressure carbon monoxide disproportionation, and chemical vapor deposition (CVD). Most of these processes take place in a vacuum or with process gases. CVD growth of CNTs can occur in vacuum or at atmospheric pressure. Large quantities of nanotubes can be synthesized by these methods; advances in catalysis and continuous growth are making CNTs more commercially viable (Takeuchi, 2014). CVD technique can be achieved by taking a carbon source in the gas phase and using an energy source, such as plasma or a resistively heated coil, to transfer energy to a gaseous carbon molecule.

During this study we found the best method for carbonization date to be used for removal BTEX from water, air and wastewater. Also, we studied both the isothermal and kinetics adsorption models. To understand the mechanism of adsorption and other variables like pH, concentration and contact time have been studied. Carbon nanostructures are a relatively new class of synthesized carbonaceous material. Moreover, in most studies, carbon nanotubes (CNTs) have been used as adsorbents and other carbon nanostructures like carbon nanofiber as well as carbon nanoporous have been studied very limited.

On the other hand, as carbon nano-structures can vary significantly in shape, size, morphology, and impurity (e.g., metal, amorphous carbon and O-containing groups), which can influence their adsorptive properties, more studies are still required for a better understanding of the molecular interactions of carbon nanotubes and organic contaminants with different properties. This study has been concentrated on testing the adsorption of BTEX. Through this study, comparisons of different kinds of carbon nano-materials and oxidized CNTs have been compared to find out the conventional sorbents for organic contaminants.

Volatile organic compounds (VOCs) are one of the most important environmental pollutants that cause adverse effects on human health and environment, even at very low concentrations (Uria-Tellaetxe et al., 2016). Recently, a large amount of the volatile organic compounds from process industries such as oil refining, paint, pharmaceuticals, solvent in manufacturing, transportation and exhaust vehicles can be released into the atmosphere (Mohammed et al., 2015). It has been well documented that many of these compounds, such as benzene, are well-known to cause leukemia, carcinogenic and mutagenic in human body (Chen et al., 2015). Benzene is the most important risk factor in workplace air and caused the acute myeloid leukemia in humans (Carlos-Wallace et al., 2016).

In gas phase, a few studies showed that the carbon nanotubes as a favorite sorbent absorbed benzene vapor from environmental and workplace air as a pollution removal technique. In addition, the adsorption of BTEXs (benzene, toluene, ethylbenzene and xylenes) on carbon structures including SWCNT, MWCNT (2 types), nanoporous carbon, carbon nanofibers, double-walled carbon nanotubes and activated carbon were studied (Jahangiri et al., 2011). In this study, the structure and surface properties of the carbons were examined, however, the important adsorption

parameters such as flow rate, initial concentration, temperature and humidity were assumed constant (Jahangiri et al., 2011). Over the last two decades, the multi-wall carbon nanotubes (MWCNTs) have been extensively studied in different applications of nanotechnology due to their extraordinary properties and wide variety of applications such as mechanical, electrical, optical and sensing (Popov, 2004). Benzene is a highly volatile aromatic compound usually component of mineral oil, petrol, coking plant and other products.

The BTEX (Benzene Toluene, ethylbenzene and Xylene) compounds are harmful toxic pollutants causing exposure related health effects in human beings. These groups of volatile organic compounds (VOCs) are evidently carcinogenic in human beings. The exposure of Benzene may cause respiratory disorders, narcosis, changes in blood pattern, anemia, leucopenia and leukemia. Toluene in comparison to Benzene is less toxic may cause drowsiness, impaired coordination etc.. High dose exposure of toluene can produce kidney and liver damage and hyperplasia of bone marrow, anaemia, depression in central nervous system which may lead to impairment of coordination and slowed reaction time.

Acute Xylene exposure may be marked by dizziness, weakness, headache, nausea, vomiting, breathing difficulty and loss of coordination. In severe exposure, there are visual luring, tremors, heart beat irregularities, paralysis and loss of consciousness. Due to exposure associated health aspects of BTX compounds, it is becoming increasingly important to screen their presence and to determine prevailing concentration in the ambient, environment. In this study, the experimental parameters affecting on the benzene removal from air such as, temperature, flow rate and relationship between temperature/humidity/benzene concentrations were studied and optimized.

The performance of the proposed method in bench scale was evaluated by GC-FID and. Removal of benzene, toluene and xylene from air has yet not been reported extensively and there are seldom any reports in the literature on the use of functionalized CNTs towards benzene, toluene, ethylbenzene and xylene. Thus the topic of the proposed research work aims at the preparation of CNTs indigenously and functionalizes it with various ligands for the selective removal of benzene, toluene, ethylbenzene and xylene from water /air at lower and higher concentrations. Efforts will also be taken to recycle the adsorbent and recover the adsorbed. Thus Topic of the proposed research work will be carried out to investigate and develop novel adsorbents for the removal of benzene, toluene, ethylbenzene and xylene from contaminated air and water.

1.2. Aims and Objectives

The present work entitled “Removal of volatile organic compounds (VOCs) from air and water using carbon nanomaterials.” aims at the preparation of CNTs indigenously with various legand for the removal of toluene, ethlbenzene, o-xylene from air and water at lower and higher concentration.

The main objectives of the proposed research work are:

- Indigenous preparation of CNTs using floating catalytic chemical vtecapor deposition technique.
- Characterization of CNTs produced by various techniques including Scanning Electron Microscopy and X- Ray Energy Dispersive (SEM and EDAX), Transmission electron microscopy (TEM), Fourier Transform Infrared spectroscopy (FTIR) BET surface analyzer, Raman, and X-ray photoelectron spectroscopy (XPS).
- Optimization of various parameters including pH, equilibrium time, adsorbent dose in batch reactors by dissolving known amount of VOCs in water.
- Kinetic and Isotherm modeling of batch data.
- Design of column reactor for VOC removal.
- Experiments to study to breakthrough capacity in column mode in air samples.

Chapter 2

Review of Literature

CHAPTER - 2

LITERATURE REVIEW

2.1. Introduction

This chapter review with an extensive literature survey on the present research work. This literature provides a background and guide for help to the entire study. This chapter includes the review on historical appraisal for VOCs pollution in air and water, activated carbon nanotubes, activated carbon preparation methods, application of activated carbon, characterization of carbon nano material, wastewater treatment methods, air treatment, and effect of process parameters on activated carbon preparation and adsorption studies (isotherm and kinetics). Survey matter shows that there is a large variety of ways to calculate a VOC value from the results of an analysis (eg, De Bortoli et al., 1986; Krause et al., 1987; Molhave, 1992; Rothweiler et al., 1992; Seifert, 1990; Wallace et al., 1991).

2.2. Volatile Organic Compounds

According to EU Directive 1999/13/ EC or Solvent Emissions Directive (EU, 1999), VOCs are functionally defined as organic compounds having at 293.15 K (i.e., 20°C) a vapor pressure of 0.01 kPa or more, and having a corresponding volatility under particular conditions of use. The EU Paint Directive, 2004/42/EC (EU, 2004) on the other hand, uses that boiling point, rather than its volatility in its definition of VOCs and defines VOC , an organic compound having an initial boiling point lower than and equal to 250 °C at an atmospheric pressure of 101.3 kPa. Same, the European Eco-labelling scheme,

2002/739/EC (EU, 2002) for paints and varnishes defines VOCs as any organic compounds having the boiling point (or initial boiling point) lower than and equal to 250°C.

Air contain 62 VOCs according to the EPA Standard show Table 2 and 23 added VOCs (1, 1-dichloroethylene, dichloromethane, trans-1, 2-dichloroethylene, cis-1, 2- Dichloroethylene, chloroform, 1, 1, 1-trichloroethane, carbon tetrachloride, 1, 2- Dichloroethane, benzene, tichloroethylene, 1, 2-dichloropropane, bromodichloromethane, Cis-1, 3- dichloropropene, toluene, trans-1, 3-dichloropropene, 1, 1, 2-trichloroethane, Tetrachloroethylene, dibromochloromethane, m-xylene, p-xylene, o-xylene, bromoform, And p-dichlorobenzene). Rodenas et al. (2005 and 2011) analyzed adsorption of mixtures of benzene and toluene at low concentrations on a wide variety of activated carbon. F. Pourfayaz et al. (2014) Removal of volatile organic compounds (VOCs) especially benzene, toluene, ethylbenzene and xylenes (BTEX).

Table 2: List of 62 VOCs (as per EPA Standard Method to15/17)

Acetone	Ethylidibromide(1,1-Dibromoethane)	Ethanol
Benzene	4-Ethyltoluene	Ethylacetate
Benzylchloride	Trichlorofluoromethane(Freon11)	Ethylbenzene
Bromoform	Dichlorodifluoromethane(Freon12)	1,4-Dioxane
Bromomethane	1,1,2-trichloro-1,2,2-trifluoroethane	Propylene
Bromodichloromethane	1,2-Dichlorotetrafluoroethane(Freon	Styrene
1,3-Butadiene	Hexachloro-1,3-butadiene	Carbondisulfide
2-Butanone(MEK)	2-Hexanone(MBK)	Carbontetrachlor
Dibromochloromethane	4-Methyl-2-pentanone(MIBK)	Chlorobenzene
1,2-Dichlorobenzene	Methylenechloride	Chlorethane
1,3-Dichlorobenzene	Methyl-tert-butylether(MTBE)	Chloroform
1,4-Dichlorobenzene	2-Propanol	Cyclohexane
1,1-Dichloroethane	1,1,2,2-Tetrachloroethane	Chloromethane
1,2-Dichloroethane	Tetrachloroethene	Heptane
1,1-Dichloroethene	Tetrahydrofuran	Toluene
cis-1,2-Dichloroethene	1,1,1-Trichloroethane	o-Xylene
trans-1,2-Dichloroethene	1,1,2-Trichloroethane	m-Xylene
1,2-Dichloropropane	Trichloroethene	p-Xylene
cis-1,3-Dichloropropene	1,2,4-Trichlorobenzene	Vinylacetate
trans-1,3-	1,2,4-Trimethylbenzene	Vinylchloride
Hexane	1,3,5-Trimethylbenzene	-

2.3. VOC Sources, effect and Contamination of Water and air (Global Perspective):

Volatile organic compounds (VOCs) are important air and water pollutants emitted largely by industries, vehicles and domestic cooking using fossil fuels, especially bio-fuels. Many other VOCs (e.g. benzene, ethylbenzene and n-decane) are toxic and some are carcinogenic, mutagenic or teratogenic (Edgerton et al., 1989; Burstyn et al., 2007; You et al., 2008). Besides health effects, VOCs can combine with nitrogen oxides leading to production of secondary air pollutants (ozone, peroxy-acetyl nitrates and organic aerosols) (Carp et al., 2004; USEPA 2006; Song et al., 2007).

Out of several VOCs, the common VOCs which are toxic and present in the appreciable quantities in ambient air include benzene, toluene, ethylbenzene and xylene (BTEX) (Lau and Chan, 2003; Lü et al., 2006; Zhang et al., 2012). The major sources of BTEX are vehicular exhausts and evaporation losses from handling, distributing and storing of solvents (Srivastava et al., 2005; Choi et al., 2009; Dutta et al., 2009).

Among atmospheric pollutants emitted by industry, volatile organic compounds (VOC) may achieve particular relevance for the specific sources, such as petroleum Water, Air, and Pollution by Gariazzo et al., 2005 refineries and petrochemical plants. In particular, benzene is one of the most toxic pollutants with a proven carcinogenic and Figure. 1 Showing effect of VOCs on different part of Human effect associated with the inhalation of benzene-contaminated air (Ott et al., 1978). An attempt to evaluate the exposure to VOC compounds from an industrial complex was reported by Park et al. (2004). They

monitored higher toluene, m + p-xylene and o-xylene “personal air” concentrations for children attending a school very close to the industrial complex, with respect to another group living far away. In general, a main problem in linking the environmental pollution to health effects is the current lack of data about the actual exposure to hazardous pollutants.

The major source is emission from motor vehicles and evaporation losses during the handling distribution and storage of petrol. As the CPCB survey during 1988-89 five Metro cities account for 35% of total vehicular population in India. 2 Wheelers in 5 Metros only account for 23% of all 2 Wheelers in India. Two-wheelers have grown in number accounting for 68.8% of all vehicles in 1995 against 8.8% in 1951 in India. Delhi alone accounts 1/8th of Total Vehicle Population (TVP) in India. The total number of vehicles in Delhi (27.0 lacs) was more than number of vehicles in cities of Mumbai (7.24 lacs), Calcutta (5.61 lacs) and Chennai (8.12 lacs) put together during 1995. The total no. of 2 Wheelers in Delhi (14.03 lacs) was about one and half times of other three Metros i.e. Mumbai (2.46), Calcutta (2.22) & Chennai (4.61) put together during 1993.

The total number of vehicles in Delhi was 30 lacs as on March 31, 1998, which has grown up to more than 34.25 lacs as on July 2001. (Out of which CNG vehicle constitute 2450 Buses, 1178 Mini-Buses, 27,263 Three-Wheeler, 1993 Taxis). Diesel vehicles constitutes about 6% of total vehicles. Two wheelers owing to predominate category (i.e. about 2/3rd of total vehicular population in Delhi need utmost attention. In the petrol driven two-wheeler the emission of benzene is significant because about 20-30% of fuel is coming out

as unburnt hydrocarbon. Gasoline consumption in Delhi has shown a growth of 247% during 1997-98 against 1980-81 as compare to Diesel consumption growth of 150% only.

About 50% of benzene is absorbed by inhalation & absorption of it via skin is limited. The high lipophilicity and low water solubility of benzene favour its distribution to fat-rich tissues. Benzene distributed by blood accumulates in fat-rich tissues like adipose tissue bone marrow & liver. Benzene is readily absorbed by the body during inhalation or ingestion and is rapidly distributed throughout the body, particularly in fatty tissues. Metabolism occurs primarily in liver and to less extent in the bone marrow, producing intermediates, which account for the toxicity of benzene. In human, half-life of benzene is 1 - 2 days.

Accumulation is not expected for benzene or its metabolites. Benzene is primarily exhaled through the lungs unchanged or excreted as metabolites in the urine. Benzene is oxidized by cytochrome P-450- dependent mixed-function oxidase system. In humans voluntarily exposed to 100ppm (320 mg/m³) benzene for 5 hours, 61% absorbed benzene was metabolised to phenol, 6.4% to catechol & 2% to hydroquinone while 26% was exhaled unmetabolized.

The major part of the metabolites was excreted as sulfate or glucuronic acid conjugates. Metabolites of benzene are responsible for haematotoxicity. The bio-transformation path ways are the formation of phenol via epoxide & catechol via benzene dihydrodiol. Hydro-quinone, catechol and hydroxy hydroquinone are converted to p-benzosemiquinone and p- benzoquinone, to o-benzoquinone and to o- hydroxy-p-benzosemiquinone and hydroxy – p – benzoquinone respectively. The copy of reactions is enclosed. These

metabolites bind covalently to microsomal proteins or mitochondrial DNA metabolism leads to opening of benzene ring & this pathway plays a role of hemotoxicity.

Benzene is ubiquitous in the environment, resulting in the exposure of most humans to trace levels (or more) of this chemical. Exposure in the general population is primarily to air borne benzene and derives from active and passive tobacco smoke, industrial activities, and use of the automobile (gasoline fumes from refilling, etc. and exhaust emissions). Estimates of the daily amounts of benzene consumed in drinking – water and food-stuffs vary considerably and are of the order of $\mu\text{g/day}$. Depending upon the assumptions made with respect to levels of benzene from tobacco products and foodstuffs, estimates for the exposure of the general smoking population in industrialized countries range from 2000 to 3500 μg benzene/day. Adult (70kg) non-smokers are considered to be exposed to about 200 to 1700 μg benzene/ day (about 3 to 25 $\mu\text{g/kg}$ body weight per day). It would be helpful to have more information on total human exposure, particularly in developing countries.

TEX are carcinogenic, toxic, and flammable substances, presence of greater amounts of these carcinogenic solvents in water bodies may affect water quality and thus endanger both public health and wellbeing (Purdom, 1980). Thus it is imperative that cost effective and sustainable wastewater treatment is required for TEX contamination. Conventionally activated carbon is the most widely used adsorbent (Daifullah and Girgis, 2003, Lillo-Rodenas et al. 2005, Wibowo et al. 2007).

Department of the Environment; (Based on rural daily mean of 0.5 ppb and

urban maximum daily mean of 12.2 ppb at Exhibition Road, London. Intake calculated using the World Health Organisation method) About 50% of inhaled Benzene in air is absorbed. Benzene intake based on 24 hour exposure volume of 20 m³ at rest will be 10 mg/day for each 1 mg/m³ benzene in air. The daily adult intake at a typical benzene level of 16 µg/ m³ will, Central Pollution Control Board, 2012, therefore, be about 160 µg. Together with other pollutants, benzene also participate in photochemical process which result in formation of oxidants and smog. Exposure to high level of benzene causes neurotoxic symptoms. Persistent exposure to high level of toxic level of benzene may cause injury to human bone-marrow. Early manifestation of toxicity are anaemia, leucocytopenia or thrombocytopenia.

Benzene is a known human carcinogen (IARC Group). Typical in vehicle and refueling exposure in US in 1987-1991 are reported to be 40 µg/m³ (12ppb) and 288µg/m³ (89ppb), respectively · Occupational Exposure : The major factors controlling industrial exposure to benzene are process technology, worker practices and the efficiency and sophistication of engineering controls. When appropriate engineering controls are in place, available monitoring data indicate that exposures of workers involved in the production, handling and use of benzene and benzene- containing materials which vary from non-detectable levels to approximately 15 mg/m³ (8-h TWA), in addition to the amounts estimated for the general population. In developing countries the exposure can be several times higher.

Due to the nature of the processes involved, a small percentage of workers may be exposed to more than 320 mg benzene/shift. In some developing

countries, benzene exposure may be sufficiently high to cause acute toxicity. Dermal exposure to benzene has generally not been included in these estimates. As regards to permissible level of benzene concentration for occupational exposure, American Conference of Government Industrial Hygienists prescribes a threshold limit value (TLV) of 0.5 ppm (1622 $\mu\text{g}/\text{m}^3$) (TWA). OSHA regulations also call for human exposure limit of less than 0.5 ppm. National Institute of Occupational Safety and Health (NIOSH) suggests Recommended Exposure Limit (REL) of 320 $\mu\text{g}/\text{m}^3$ (0.1ppm).

Long term exposure to benzene in air causes leukaemia in human beings. In animal studies, leukaemias, lymphomas and other types of tumours are observed. Exposure to benzene is linked to genetic changes, increased proliferation of bone marrow cells and occurrence of certain chromosomal aberrations in humans and animals. US EPA has classified benzene as Group A human carcinogen. The International Agency for Research on Cancer (IARC), Lyon (France) has list added benzene as carcinogenic to humans. In addition a number of non-cancer health effects are associated with benzene exposure such as disorders of blood, harmful effects on bone marrow, anaemia and reduced abilities of blood to clot, damage to immune system and a reproductive and developmental toxicant.

WHO estimates a 4 in 1 million risk of leukaemia on exposure to benzene to a concentration of 1 $\mu\text{g}/\text{m}^3$ (0.31 ppb) High levels of benzene exposure produce haematotoxic effects like leucopenia, lymphopenia & anaemia in laboratory animals. Exposure to high levels of benzene causes neurotoxic symptoms. Substances that can induce benzene –metabolizing enzymes are

likely to modify the haematotoxicity of benzene.

It has been found that benzene itself, Phenobarbital, Toluene & ethanol can modify the metabolism & haematotoxicity of benzene if animals are pretreated with these substances. Toluene has been found to inhibit the metabolism of benzene & decrease its haematotoxicity. Ethanol enhances the haematotoxicity of benzene in mice. Acute lethal doses of benzene in experimental animals cause narcosis, ventricular tachycardia and respiratory failure. At benzene concentration above 32 ug/m^3 in air, there is a co-relation between phenol excretion in urine and the level of exposure.

As many VOCs are known to have short-term and long-term adverse effects on human health and comfort, VOCs are frequently determined if occupants report complaints about bad indoor air quality. On the comfort side VOCs are associated with the perception of odours. Adverse health reactions include irritation of mucous membranes, mostly of the eyes, nose and throat, and long-term toxic reactions of various kinds (ECA-IAQ, 1991).

Aydin Berenjian et al. (2012) volatile organic compounds (VOCs) are man-made and/or naturally occurring highly reactive hydrocarbons. World Health Organisation defined VOCs as any organic compound whose boiling point is in the range from (50- 100°C) to (240-260°C), corresponding to having saturation vapour pressures greater than 102 kPa at 25°C (ISO-16000-6, 1989). Many types of VOCs are toxic or even deadly to humans and can be detrimental to the environment. Therefore a multitude of definitions exist globally depending on the context frame used by different organisations such as United Nations Economic Commission for Europe (UNECE) and U.S. Environmental

Protection Agency (EPA).

The international agency for research on cancer (IARC, USA) has classified benzene as A1 group (carcinogenic effect) which can cause many diseases in human such as; lymphoma, aplastic anemia and bone marrow damage (Pearce et al., 2015; Stenehjem et al., 2015). Benzene has been widely used in many petrochemical industries as a solvent in raw product and by-product (Mohammed et al., 2015). The exposure to benzene caused to consider a toxic substance which was strictly monitored around the world (Zhao et al., 2015). As a consequence, the government regulations have been established to reduce occupational and environmental exposure to benzene and other VOCs (Barbieri et al., 2008). In conjunction with, the implementation of high-performance methods to removal and control such emissions are inevitable in industries and environment (Romero-Anaya et al., 2012).

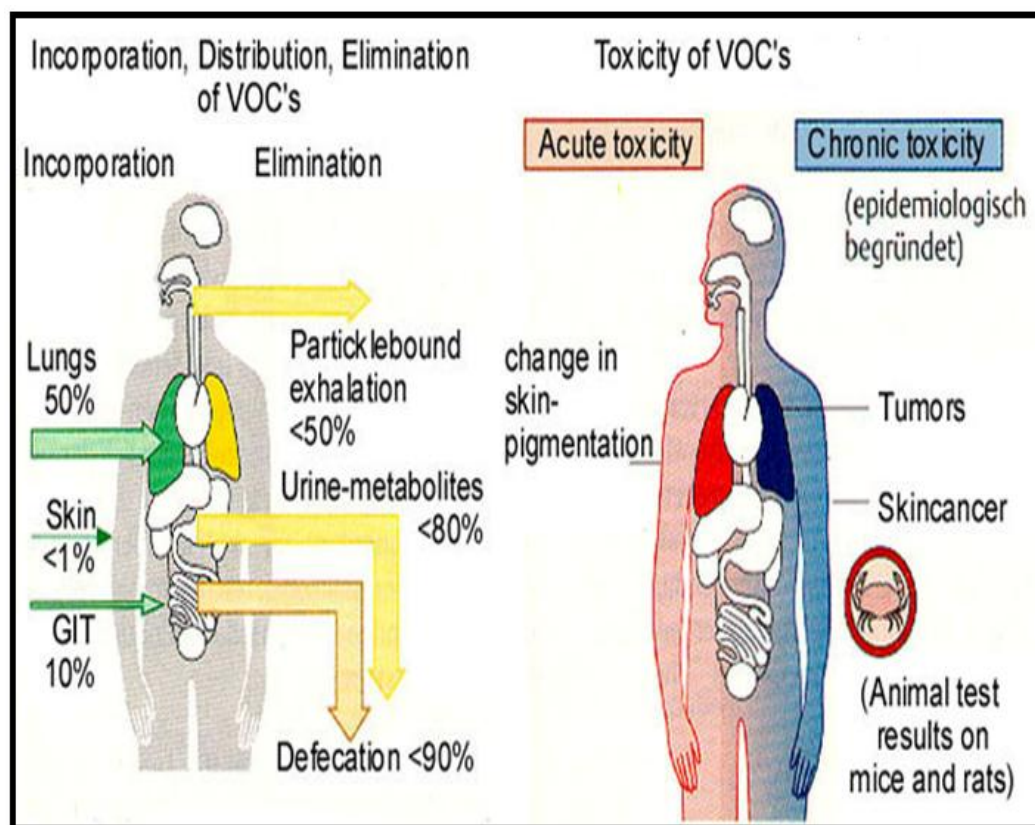


Figure. 1 Showing effect of VOCs on different part of Human

2.4. Various method and techniques for VOCs from air and water streams

Chuang et al. (2008) used a BDR model to assess the effect of temperature on the adsorption and desorption of three VOCs. Compared with the Langmuir isotherm and LDF (with Langmuir) model, the BDR model showed the same trend with both of them, such as the Carbon tetrachloride had a larger k_a/k_d (BDR model) and KL (Langmuir isotherm) and k (LDF with Langmuir) than benzene and Chloroform, and the k_a/k_d values of Carbon tetrachloride and benzene. Based on these parameters adsorption isotherms and breakthrough curves were predicted under various operational conditions. Both experimental and model-predicted data indicated the

both adsorption and desorption rate constants increased whereas equilibrium adsorption constants decreased under the high reaction temperatures.

Xiang et al. (2010) investigated adsorption of dibenzofuran (DBF) on three commercial activated carbons (AC) to correlate the adsorption equilibrium and kinetics with the morphological characteristics of activated carbons. Breakthrough experiment was conducted to determine the isotherm and kinetics of dibenzofuran on the activated carbons. All the experiment runs were performed in a fixed bed with a process temperature of 368 K. The effects of adsorbent morphological properties on kinetics of the adsorption process were studied.

The equilibrium data were found to be satisfactorily fitted to the Langmuir isotherm. An intra-particle diffusion model based on the obtained Langmuir isotherm was developed for predicting fixed bed adsorption of dibenzofuran. The results indicated that this model fit all the breakthrough curves well. The surface diffusion coefficients of dibenzofuran on activated carbon were calculated, or a relationship with the microporosity was found. As it was expected, the dibenzofuran molecule found more kinetic restrictions for diffusion in those the carbons with narrower pore diameter.

The investigated structural characteristics of pelletized MCM-48 using X-ray diffraction, nitrogen adsorption and desorption. The adsorption equilibrium data were also obtained for seven pure vapors (acetone, benzene, cyclohexane, hexane, methanol, MEK and toluene) at 300.15 K for different pelletized MCM-48 using a gravimetric method. Shim, et al. (2006) From experimental and theoretical works on adsorption of nitrogen and VOCs vapor, the following conclusions were reached. The BET surface area and the pore volume were highly dependent on the pelletizing pressure, while the average pore diameter remains unaffected with increasing

pelletizing pressure up to 400 kg/cm². Single species adsorption the isotherm data showed typical type IV of IUPAC classifications.

The adsorption amount of VOC was reduced by around 70% from the parent sample to maximum sample pressed at 500 kg/cm². Adsorption equilibrium data measured at a wide range of pressures were fitted to two hybrid isotherm model equations (Langmuir–Sips and inhomogeneous DA). In accord with column dynamic experiments, the patterns of adsorption breakthrough curves were highly influenced by influent concentration and pelletizing pressures that were closely related with adsorption isotherm shape. The determined mass transfer coefficients of VOCs on pelletized MCM-48 showed that minimum values correspond to the capillary condensation region. Furthermore, the simple dynamic model employed successfully simulated adsorption breakthrough behavior of VOCs under various operating conditions.

The carried out kinetic studies on the adsorption of α -amylase from *Aspergillus oryzae* on anion exchanger, Duolite A-568, and the hydrophobic resin, Duolite XAD-761 in fixed bed. The efficiency with respect to the adsorbate and adsorbent was determined to estimate the performance of the process of adsorption. The effect of flow rate, α -amylase inlet concentration, temperature, and particle size of the packing was analyzed. Bautista, et al. (2003) In addition, the transient response, in the form of experimental breakthrough curves, was fitted using a phenomenological mathematical model accounting for the external-film and pore-diffusion mass-transfer mechanisms as well as axial dispersion along the column. The Langmuir isotherm was included in the model to account for the extent of the equilibrium of adsorption. The developed mathematical model was solved by using orthogonal collocation technique.

The model reproduced adequately the experimental results once the best-fitting parameters were attained. The model described satisfactorily the experimental breakthrough curves and it proved to predict successfully the behavior of a scaled-up bed using the kinetic and equilibrium parameters estimated previously. The shape of the breakthrough curves was sensitive to changes in both the pore diffusion coefficient and the external-film mass-transfer coefficient. This showed the control of both mass-transfer mechanisms. Thus, the mathematical model can be considered a reliable tool for process design and scale-up of similar systems.

They considered the models for the dynamic adsorption of volatile organic compound (VOC) traces in air. They were based on the linear driving force approximation associated with various adsorption isotherms characteristic of the couple VOC-adsorbent (Langmuir, Freundlich, Type V and Dubinin–Astakhov (D–A)). Joly and Perrard (2009) The occurrence of constant pattern breakthrough curves made easier the prediction of breakthrough time, i.e. time necessary for the pollutant concentration at the column outlet to reach a given fraction of its inlet value (e.g. 2%). The necessary and sufficient condition has been given for the existence of such a constant pattern and has been applied to various models associated to the considered adsorption isotherms.

Theoretical results have been illustrated by numerical simulation based on a finite element method, which provided a set of typical behaviours of breakthrough curves with the increase of bed length. For practical applications, the aim was to achieve breakthrough times as long as possible for a given pollutant. This goal can be reached by choosing an adsorbent with a large adsorption capacity and able to yield the steepest possible constant pattern breakthrough curves.

The investigated the nickel (II) ions bio-sorption process by marine algae *Sargassum filipendula* in a fixed bed column for the following experimental conditions: temperature = 30°C and pH = 3.0. The experimental breakthrough curves were obtained for the following chosen flow rates 0.002, 0.004, 0.006, and 0.008 L/min. A mathematical model was developed to describe the nickel ion sorption in a fixed bed column. Borba et al. (2006) The model of three partial differential equations (PDE) had considered the hydrodynamics throughout the fixed bed column as well as the sorption process in liquid and the solid phases. The internal or external mass transfer limitations were considered and The nickel ion sorption kinetics had been studied utilizing Langmuir isotherm.

The PDE of the system were discretized in the form of ordinary differential equations (ODE) and were solved for the given initial and boundary conditions using the finite volume method. A new correlation for external mass transfer coefficient was developed. Some of the model parameters were experimentally determined (dp) where the others such as (KF , KS) were evaluated on the base of experimental data parameters. The identification procedure was based on least square statistical method. The robustness and flexibility of the developed model was checked out using four sets of experimental data and the predictive power of the model was evaluated to be good enough for the all studied cases. The developed model can be useful tool for nickel ion removal process optimization and design of fixed bed columns using biomass of *S. filipendula* as a sorbent.

The analyzed the fixed bed adsorption kinetics to test the validity of the simplified model based on the linear driving force approximation by comparison with the exact model by using the orthogonal collocation method. Park (2004) The axial dispersion, the external film diffusion, and the intra-particle diffusion were

considered to be the major mass transfer phenomena involved with fixed bed adsorption kinetics in that study. It was assumed that a local equilibrium was attained at the fluid-solid interface and the equilibrium can be described by Langmuir isotherm.

A homogeneous particle diffusion model was employed to describe the intra-particle diffusion. Among four LDF models cited in the present study, the model which was based on the parabolic concentration profile in the particle, showed to be best agreement with the exact model. The LDF model based on the parabolic concentration profile deviated to some extent from the exact model in shorter bed. However, the deviation became negligible in a sufficiently long bed, in which the intra-particle concentration profile approaches a symmetric form. As the intraparticle diffusion resistance becomes relatively less important compared to both the axial diffusion resistance and the external diffusion resistance, the LDF model based on the parabolic concentration profile approximates the exact model more closely.

The proposed a new model to describe the removal of volatile organic compounds (VOCs) from a gas stream passing through a bed packed with activated carbon fibers (ACFs). Toluene was used as the test compound. Both pore diffusion and surface diffusion were considered in the model. Cheng et al. (2004) The equilibrium behavior was shown to fit Dubinin–Radushkevich isotherm with the values of parameters K and W_0 of 1.101×10^{-9} and 57.73 kg/m^3 , respectively. Mathematical model was developed which was numerically solved by using finite difference technique. The experimental results showed that this model can predict VOC breakthrough curve.

The performed a simulation of the performance of an activated carbon packed-bed system for adsorption of toluene from air. For a non-switched operation

the time-varying exit toluene concentration of a 30 mm-depth bed was measured. The simulation result was compared with the measured data. San et al. (1998) The computer analysis was based on the modified solid-side resistance model which was originally proposed by Pesaran and Mills. The effects of cycle operating time, regeneration temperature and the adsorption performance were investigated. The maximum removal and corresponding optimum the cycle time were obtained. The influence of the number of the grid points on the accuracy of the numerical scheme was discussed. The effects of tortuosity factor or transfer coefficients on the adsorption were also investigated.

The prepared an adsorption package to simulate adsorption / desorption operation for both single and multi-component systems in an isothermal condition by different mechanisms such as; local adsorption theory and mass transfer resistance (rigorous and approximated methods). Siahpoosh et al. (2009) Different mass transfer resistance mechanisms of pore, solid and bi-dispersed diffusion, together with nonlinear isotherms (Langmuir, Freundlich, Sips and Toth) were taken into account in modeling the fixed bed adsorbers. The Extended Langmuir isotherm was found to the explain properly the binary and ternary mixtures in adsorption/desorption process.

Almost all the mass transfer approximations were explained by the linear driving force, LDF, although the alternative driving force, ADF, approximation was examined in some cases. The numerical solution was the Implicit Method of Lines which converted that partial differential equations to the ODEs then solving them by the Runge-Kutta method. Validation of the models was performed by experimental data derived from the literature for different types of adsorbents and adsorbates. The sensitivity analyses was carried out to find out variation of the breakthrough curves

against some physical and operational parameters such as; temperature, flow rate, initial and inlet concentration or particle adsorbent size. The results revealed excellent agreement of simulated and previously published experimental data

In many cases the available VOC measurements are given as total non-methane hydrocarbons (NMHC), whilst lesser concern is given to their speciation. By contrast, it is necessary to draw attention on the relative importance of individual VOC, to detect compounds acting as tracers for specific industrial processes, and finally to assess the relative contributions of emission sources to pollution by means of source apportionment techniques (Watson et al., 2001).

(Carp et al., 2004) Methods for air cleaning can be divided into two categories, i.e. combustible and non-combustible processes. In non-combustible processes, VOCs released with the waste gas are collected. Increasing levels of VOCs in ambient air, indoor air and industrial premises (Dhada et al., 2012) necessitate that VOC control technologies are developed and further improved. Earlier studies (Deshusses and Webster 2000; Rene et al., 2005), have reported that VOCs from polluted air streams can be controlled by traditional methods such as adsorption, condensation and incineration.

Although these methods use simple techniques, there are certain implementation constraints which include high cost, unpredictable recoveries and difficulty in separating one or more VOCs for reuse/recycle (Jeong et al., 2005). In many cases the available VOC measurements are given as the total non-methane hydrocarbons (NMHC), whilst lesser concern is given to their speciation. By contrast, it is necessary to the draw attention on the relative importance of individual VOC, to detect compounds acting as tracers for specific industrial

processes, and finally to assess the relative contributions of emission sources to pollution by means of source apportionment techniques (Watson et al., 2007).

2.5. Various Adsorbents used for VOC Adsorption

In recent years carbon nano tubes (CNTs) have been found useful in removing various pollutants owing to their large surface area, greater chemical stability, thermal resistance, unique hollow structure and hydrophobic surface. Carbon based nano-composites have found useful in removing many organic pollutants including volatile organic compounds (Agnihotri et al. 2005, Hsu and Lu, 2007) from air streams, 1,2 dichlorobenzene (Fagan et al. 2004, Chen et al. 2007), xylene (Chin et al. 2007, Su et al. 2010), TEX (Yu et al. 2011, 2016), trihalomethanes (Lu et al. 2005, 2006), triazine based pollutant (Engel and Chefetz, 2017), pharmaceuticals (Shan et al. 2016) etc. from various aqueous solutions.

The specific adsorptive capacity of charcoal was recognized by the Scheele at 1773 AD, which measured the volumes of gases, could be adsorbed by carbons derived from different sources. The use of carbon molecular sieves in gas separation, in the particular oxygen and nitrogen, has grown steadily in the past years (Sircar et al 1996). Activated carbons are useful adsorbents due to their porous structures, the presence of various oxygenated functional surface groups depending on the precursor's nature and the procedures used in their preparation, and thus activated carbons show differences in their adsorptive behavior. To produce these carbons, chemical, physical and mixture of both as activating agents are used and a number of activation procedures have been reported in the literature using the above said activating agents. In the general it can be classified either as single stage or two-stage process.

The demonstrated carbon nanotubes with a highly crystalline Structure to be capable of selectively adsorbing aromatic VOCs. Mehdi Jahangiri et al. (2011) the adsorption of benzene, toluene and xylenes (BTX) as appropriate representatives of volatile organic compounds (VOCs) on seven types of different carbon nanostructures were investigated. Sone et al. (2008) In this research, multi-walled carbon nanotubes (MWNT1 and MWNT2), single walled carbon nanotubes (SWCNT), double-walled carbon nanotubes (DWCNT), carbon nano-fibers (CNF), nano-porous carbon and MWNT-COOH, as well as activated the carbon as a conventional sorbent for organic contaminant were studied.

Adsorption is the most versatile and appropriate technique to water and air VOCs pollution compared to different techniques because of its simplicity, ease of operation, flexibility, insensitivity of toxic pollutants, potential of regeneration, low waste generation and considerably low recurring cost (Hosseini, et al. 2011. Carbonaceous materials like carbon mesosphere (CMS) and carbon nano-tubes (CNTs) (Schierz and H. Zanker, 2009) will be foremost and extremely attention grabbing backbone of our proposed research work. The solid adsorbents such as zeolites, silica gel and activated carbons (ACs) which trapped adsorbate materials (BTX) on the surface are widely used.

The different adsorbents, carbon adsorbents such as; graphene oxide, activated carbons, carbon nanotubes and porous carbon have demonstrated more advantage due to the low density, chemical stability, variety of structural forms, high capacity, desire chemical structure, and texture properties (Silvestre-Albero et al., 2010; Seredych and Bandoz, 2010; Dhaouadi et al., 2010; Wang et al., 2010).

The adsorption process using activated carbon to remove organic

contaminants in the gas phase has been widely studied (Zhang et al., 2011) and more information about chemical and physical properties of activated carbon and carbon nanotubes was introduced or compared in electronic supplementary material (ESM, Text S1) (Ahmaruzzaman, 2008; Xiang et al., 2010; Sone et al., 2008; Ren et al., 2011; Pan and Xing, 2008; Agnihotri et al., 2005; Hussain et al., 2008; Chen et al., 2009a; Lin et al., 2009; Gaur and Shim, 2008; Fu and Wang, 2011; Chen et al., 2008; Chen et al., 2009b; Goering et al., 2008; Hyung and Kim, 2008).

The surface modification of MWCNTs with different compounds is the major interest for enhancing sensitivity and ameliorating selectivity to different toxic vapors or gases (Fan et al., 2012; Lu et al., 2006). The sidewall functionalization of MWCNTs not only allows better interactions with gas species, but also leads to improve their surface reactivity and dispersion. In general, it is possible to modify them by non-covalent (Chen et al., 2007; Manoso et al., 2013; Zhang et al., 2011) or the covalent functionalization (Niu et al., 2007; Mu et al., 2014).

The adsorption capacity of the various carbon composites was calculated as the difference between increased weight of weighing bottle containing carbon composites and initial weight of weighing bottle (Yates et al. Technologies (e.g. absorption, adsorption, biofiltration, bio scrubber, thermal oxidation and incineration) to recover or destroy VOCs have progressed significantly. Low temperature Cryogenic recovery is desirable for VOCs concentration >1%; for smaller concentration, the significant amount of liquid nitrogen was required (Gupta and Verma, 2002).

The several decades, many researchers show their interests in searching for low-cost adsorbents with excellent adsorption characteristics, such as zeolites (Blocki, S.W. (1993)), organokaolinite (Egbuchunama, 2016), smectite (Carvalho, 2012), hectorite (Jaynes, 1999), organosilica (Moura, 2011), and montmorillonite (Sharmasarkar, 2000) and (Nourmoradi, 2012).

The characterization of adsorbent material that's used in research work and most intense peak at $2\theta = 26.4$ was observed in the diffraction spectra of both LCNT and LCM which is due to the (002) reflection of sp^2 carbon of carbon composites (Sankararamakrishnan et al. 2016). Oxidized carbon composites (LCNT-OX and LCM-OX), exhibited the peaks around 1720 cm^{-1} which arises from the asymmetric C=O stretching band (Ntim and Mitra, 2011). Anchoring of functional groups in LCM-OX is evidenced by the appearance of bands at 1610 and 1536 cm^{-1} corresponding to C=O group and carboxylate anion stretching respectively. Similarly oxidized LCNT exhibited vibrations of C=O and caboxylate groups at 1634 and 1586 cm^{-1} respectively (Daifullahand Girgis, 2003, Davis et al. 1999). All the samples exhibited alkoxy C-O band at 1030 cm^{-1} (Ovejero et al. 2006). G band is related to inplane tangential stretching of C-C bond of sp^2 hybridized carbon atoms of carbon composites. (Saito et al. 2011). The ratio of the intensity of D band to G band (I_D / I_G) depicts the extent of defects in the carbon frame work

The demonstrated that the decolorizing properties of carbons were inherent to the source material and also depended on the thermal processing and the particle size of the finished product. Kayser, (1881) first used the term adsorption to describe the uptake of gases by carbons. Bussy, (1822) The basis for the industrial

production of activated carbon from coal was established in 1900 in order to replace the bone char in the sugar refining process. The first powdered commercial activated carbon, eponite was produced in the Europe in 1909. During First World War (1914), steam activation of coconut shell and almond shell char was developed in the United States for use in gas masks. It has been used subsequently for water treatment, solvent recovery and air purification. This type of activated carbon mainly contains fine pore structures suited for gas phase adsorption applications.

This observation is similar to the earlier reports where sorption of TEX (Su et al. 2010) and xylene (Chin et al. 2007) was found constant in the pH range of 3 to 10 by MWCNT and SWCNT respectively. Study of Yu et al. (2011) illustrated that 60 min was essential for reaching equilibrium of TEX with CNTs and Su et al. (2010) reported 120 min for CNT (NaOCl) to reach equilibrium. Lagergren model (Lagergren, 1898), where q_t (mg/g) represents the adsorption of the TEX at time t , q_e (mg/g) is the adsorption capacity at equilibrium, t (min) is the exposure time and k_1 (min^{-1}) is the pseudo first order rate constant. Kinetics from liquid solutions (Ho, 2006) in eqn (2), k_2 ($\text{g mg}^{-1} \text{min}^{-1}$) is the pseudo second order rate constant of adsorption.

Earlier reports have reported higher sorption capacity for instance Yu et al, (2011) reported a capacity of 112.19 mg/g for m-xylene and nitric acid modified SWCNT has been evaluated for removal of p-xylene (Chin et al. 2007) with an adsorption capacity of 85.5 mg/g. Similar mechanism have been postulated in literature with CNT (NaOCl) (Su et al. 2010) and powdered activated carbon (Daifullah and Girgis, 2003). Additionally, there also exists an electrostatic attraction between TEX molecules and CNT surface. It is reported that TEX

molecules exhibit weak positive charge in the pH range of 3 to 12 (Chen et al. 2007).

Most carbonaceous substances can be converted into activated carbon, final properties of the carbon will depend significantly on the nature of the starting material. A large number of processes for making activated carbons have been developed over the past century. However, most processes consist of the pyrolysis of the starting material, followed by a stage of controlled oxidation or vice versa. The purpose of the oxidation stage is to activate the carbon.

The activated carbon is broadly defined to include a wide range of amorphous carbon based materials prepared in such a way that exhibit a high degree of porosity and an extended surface area. For many centuries the activated carbon was used in the form of carbonized wood. The earliest known use of carbon in the form of wood chars by the Egyptians and Sumerians was in 3750 BC for the reduction of ores in the manufacturing of bronze, domestic smokeless fuel and medicinal application. In 1500 BC, Egyptian papyri was used as adsorbent for odorous vapours from putrefying wounds and from within the abdominal tract. The wrecks of Phoenician trading ships suggest that drinking water was stored in charred wooden barrels. This practise was certainly still in use in the 18th century for extending the use of potable water on long sea voyages. The ancient Hindus in India of the same period (450 B.C) used sand and charcoal filters for purifying drinking water. In 157 AD Claudius Galvanometer referred the use of carbons of both vegetable and animal origin for the treatment of a wide range of diseases.

Activated carbon also called activated charcoal, is a form of carbon that has been processed with oxygen to create millions of tiny pores between the carbon

atoms. Commercial activated carbons have internal surface area ranging from 500 to 1500 m² /g. Activated carbon can be prepared from feed stock with high carbon and low inorganic content. The most common feed stocks used for the production of activated carbon are wood, coconut shell, bituminous coal, peat etc.

The chars obtained from them could be activated easily to produce reasonably high quality activated carbons. During the activation process, the unique internal pore structure is created, which provides the activated carbon its outstanding adsorptive properties. 11 Activated carbons have a number of unique characteristics such as large internal surface area, chemical properties and good accessibility of internal pores. According to IUPAC definitions three groups of pores can be identified. Macropores (above 50nm diameter) Mesopores (2-50 nm diameters) Micropores (Under 2 nm diameter) Micropores generally contribute to a major part of the internal surface area. Macro and micropores can generally be regarded as the highways into the carbon particle, and are crucial for kinetics. The desirous pore structure of an activated carbon product is attained by combining the right raw material and suitable activation procedure.

In this chapter, previous studies on VOC control technologies, factors affecting global era, methods and absorbents are discussed. After critical review of available literature, research gaps and direction for the present study were synthesized. To accomplish the objectives described in Chapter 1, the overall work plan consists of three components: (i) Improving CNT nanotechnology laboratory scale study for reaction kinetics, isotherm, pH, column study and regeneration, (ii) Field application of technology and (iii) characterization adsorbents.

Chapter 3

Materials and Methods

CHAPTER- 3

MATERIAL AND METHODS

3.1. Quality Assurance

In this chapter included the all methods used in the analysis and calculation of results. Reagents and calibration standards for physic-chemical analysis were prepared using milliqui distilled water. Chemicals were used throughout the study analytical grade (AR) chemicals (Merck, Germany) without any further purification or disturbance. The glass-wares were washed with dilute nitric acid (1.15 N) followed by several portions of distilled water.

The quality assurance measures included meticulous infectivity control (stringent washing/cleaning procedures), a solvent for blank, equipment and other materials. The pesticides standards (99.9% purity) were supplied by Sigma-Aldrich, USA. All analyses were carried out in duplicate and the recoveries of individual BTX were determined through the spiked sample method, which was found between 75–98%. A mixture of standard BTX were prepared by combining individual stock solutions to form a working standard. All stock and standard solutions were stored at 4 °C before its use for analysis.

3.1.1. Chemicals

All chemicals used were of analytical reagent grade (AR) unless specified otherwise. High purity gases (Nitrogen, hydrogen, zero air) were purchased from sigma gases, India. De-ionized water obtained from Milli-Q system (Milli-Q, Integral A-10 system, France) was used for all experimental purposes. BTEX standard mix (2000 µg/ml) was purchased from Supleco, USA for calibration purposes. Precursor

chemicals (Purity > 99.5%) used for Solvents viz, Methanol, Ethanol, Acetone were purchased from Merck, Mumbai. Benzene anhydrous (99.8%), Toluene anhydrous (99.8%), Ethyl Benzene (99.8%) and ortho, para, meta-Xylene anhydrous (99.5%) were purchased from Loba Chemicals, Mumbai. Dichloromethane (DCM) (Purity > 99.9%) was purchased from Sigma-Aldrich, USA. Labolene (Qualigens) was used for soap solution. All the glassware's used were of borosilicate type.

3.1.2. Instruments and Accessories

Instruments and accessories used include Gas Chromatograph-flame ionization detector (GC-FID, NUCON Engineers, Model 5765), Ultrasonicator (Enertech, Mumbai) and peristaltic Pump, Chemical vapor deposition (CVD) machine (Mahindra instruments), Reactor (length 10.0 mm and diameter 4.0 mm), Teflon (PTFE) Tape, Oven (Mahindra instruments), testube rotator and (MFC) mass flow controller (Bronkhorst high-tech. Netherlands).

3.2. Preparation of LCNTs using floating catalytic chemical vapor deposition technique

The iron (Fe) metal doped multi walled carbon nanotubes (LCNTs) was prepared using floating catalytic horizontal chemical vapor deposition (CVD) machine (Mahindra instruments) Fig.2 and Fig 3 Showing image of internal CVD machine during reaction The CVD process is based on the catalytic decomposition of liquid hydrocarbons by pyrolysing of the solution. 2% of ferrocene was used with respect to benzene in ferrocene/benzene solutions, to ensure the effect on the formation of the LCNTs. The flow rate of nitrogen gas and ferrocene/benzene solution was controlled using (MFC) mass flow controller (Bronkhorst high-tech. Netherland) and peristaltic pump, respectively. The nitrogen gas has dual roles. First, to produce inert atmosphere within the reactor and second one is to acted as a carrier

during CVD process (to exert the pressure on the ferrocene /benzene solution that regulate the liquid flow directed to the nozzle).

The temperature of the electric furnace was gradually heated up-to 800oC in the presence of nitrogen atmosphere. The flow rate of nitrogen gas and ferrocene/benzene solution was set to 100 sc cm and 1 ml/min respectively. The resulting ferrocene/benzene solution was pumped into the reactor for 30 min at 800oC reactor temperature. The reactor was cooled gradually to room temperature using nitrogen gas. The CNTs deposition occurred in the hot zone of the reactor. The prepared CNTs adhered on the surface of reactor, which was easily removed from the reactor surface.



Figure 2 showing the external image of CVD machine during reaction

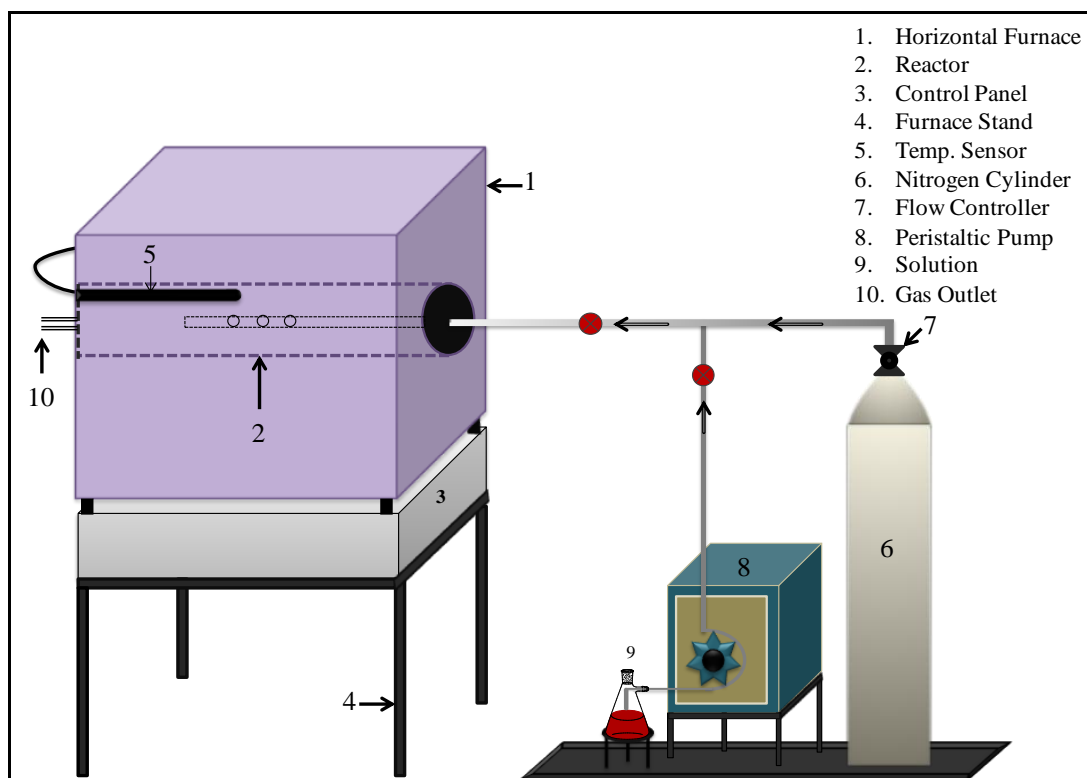


Figure 3 Showing image of internal CVD machine during reaction

3.2.1. Preparation of Oxidized LCNTs (LCNT-OX)

Fig. 4 show the Oxidized LCNTs was prepared by heating 1 gm of as prepared CNTs with 10 ml of nitric acid at 80°C until the acid evaporated completely followed by thorough washing with distilled water until pH of filtrate became neutral. The obtained product was dried in the oven at 70°C for overnight and used for further experiments.

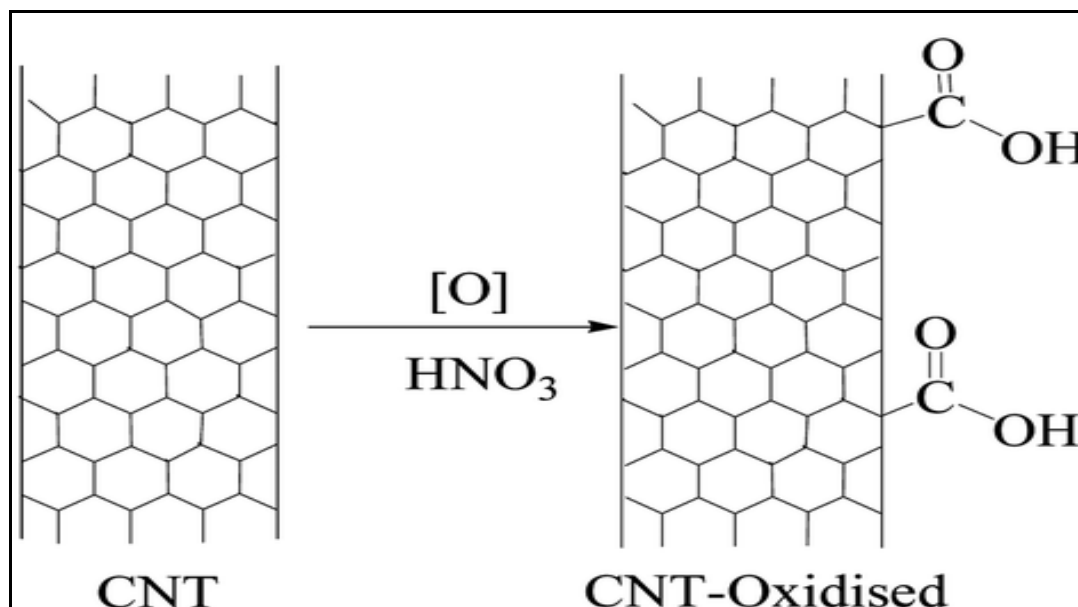


Figure 4 Schematic representation of preparation of CNT-OX

3.3. Preparation of carbon Microspheres (LCM) using floating catalytic chemical vapor deposition (CVD) technique

LCM (carbon microspheres) was also prepared using floating catalytic horizontal CVD (Chemical vapor Deposition) method. The experimental conditions remained similar to the preparation of LCNT except temperature of electric furnace was gradually heated up-to $900^{\circ}C$ in presence of nitrogen atmosphere and 2% ferrocene in benzene solution was pumped for 1 hour into the reactor which was maintained at $900^{\circ}C$ temperature during its preparation both nanotubes and microspheres were prepared using the same set up.

3.3.1. Preparation of Oxidized LCM (LCM-OX)

Fig. 5 show the Oxidized LCM (carbon microspheres) was prepared by heating 1 gm of as prepared carbon microspheres with 10 ml of nitric acid at $80^{\circ}C$ until the acid evaporated completely followed by thorough washing with distilled water until pH of filtrate became neutral. The obtained product was dried in the oven

at 70°C for overnight and used for further experiments.

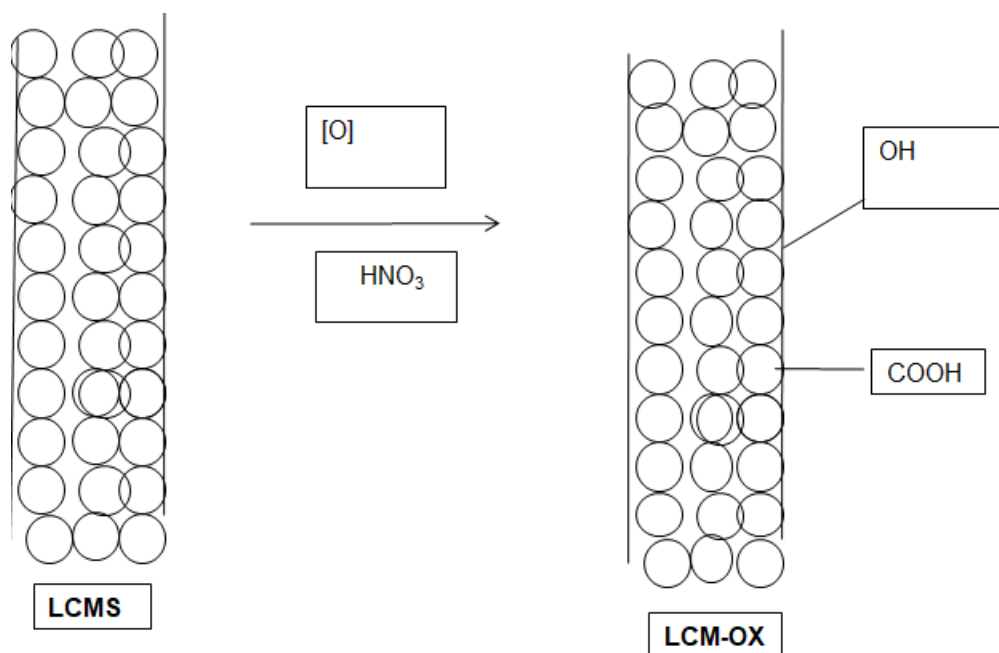


Figure 5 Schematic representation of preparation of LCM-OX

3.4. Preparation of Alkali carbon microsphere (ACM)

As prepared carbon microsphere (1.0 g) and KOH (4.0 g) was put into a perforated boat and then placed in the middle region (heating zone) of a reactor, and nitrogen was introduced into reactor with 100 sc cm flow rate through the entire experiment. The as prepared carbon microsphere and KOH was heated at the rate of 6.67°C/min up to 800°C and this temperature was maintained for 1 h. Finally, the heated material was cooled to room temperature and washed thoroughly with deionized water until pH of filtrate becomes neutral. After that, prepared Alkali carbon microsphere (ACM) was dried in oven at 80°C overnight.

3.5. Field electron scanning electron (FE-SEM) microscopy

The surface morphology of the materials was examined by SEM and EDX analysis using the field emission scanning electron microscope (FE-SEM) (Carl

Zeiss NTS GmbH, Oberkochen (Germany) Model: SUPRA 40VP). The FE-SEM is the simplest microscopic technique due to its simple image elucidation by scanning of sample surface by high energy beam (shaft of light) of electrons which is emitted by electron gun. The focused beam enters the sample surface producing secondary electrons. After hitting a secondary electron the primary electrons will continue on in a new trajectory. This process is called scattering. Emitted secondary electrons are attracted by detector (200 volts potential).

After detection the secondary electron hits the scintillator and produces photons. These emitted photons from scintillator hit the photomultiplier which is used to amplify signals. These signals further analyzed, translated and record into images of the sample (Ma et al.2006). For FE-SEM analysis surface of the sample must be conducting. The sputtering machine is used to make sample conductive using gold sputtering ionized gas molecules of gold tended to melt on sample for approximately 60 sec. The gold sputter coating prevent charging of the samples and also increases the amount of secondary electrons that can be detected from the surface of specimen in the imaging of FE-SEM and therefore increases the signal to noise ratio. Moreover, the analysis must be performed in a sufficient vacuum. Without sufficient vacuum the electron beam cannot be generated and controlled in the SEM.

In the present study, the field emission scanning electron microscope (FE-SEM) was used to examine the surface morphology and fibers diameter of the prepared carbon microspheres and carbon nanotubes. The FE-SEM images of the prepared materials were taken at different locations on the samples and at different magnification with the accelerating voltage of 10 kV and filament current 2.37 A at a working distance of 2-4mm. Prior to the SEM imaging, the sample was mounted on

carbon tape adhere with copper stubs and gold sputtering to obtain better conductivity.

3.5.1. Transmission electron microscopy

Transmission electron microscopy (TEM) is imaging and updated version technique of light microscopy where a shaft of light of electrons is focused onto a specimen sample causing an engorged version to appear on a fluorescent screen or layer of photographic film and get images at increased spatial resolution up to angstroms size and increased the prospect of carrying out diffraction from nano-sized volumes. It uses high energy electrons for penetration though a thin (100 nm) sample. Briefly, the electron gun emits a ray of monochromatic electrons that pass through vacuum in the column of the microscope.

The function of this electron gun is to produce a fine beam or shaft of light of electrons of specifically proscribed energy (Ma et al., 2006). The electromagnetic lens is basically used to focus parallel rays of these electrons into a very emaciated beam which passes through sample and scattered at different angles. These scattered electron signals are exaggerated by an electromagnetic lenses and hit a fluorescent screen, which produces a shadow image of the sample displayed in wide-range of darkness according to the density of the material present.

In the present study, the transmission electron microscopy (TEM) analysis was performed using Technai G2 T-20 (FEI, Eindhoven, Netherland) at 200 kV. Before analyzing samples for TEM, prepared LCNTs dispersed in ethanol using ultra sonication process for approximately 15 min at room temperature. The droplets of LCNTs ethanol dispersed solution were placed on copper grid (3 mm diameter) then grid was incubated in oven at 70°C to remove ethanol, for the TEM analysis.

3.5.2. Raman Spectroscopy

Raman spectroscopy based on inelastic dispersion of a monochromatic excitation source usually from a laser source. Inelastic scattering means that the incidence of photons in monochromatic light changes after interacting with sample. Sample absorbs the photons of the laser light then photon reemitted again. Frequency of the reemitted photons is shifted up or down in comparison with original monochromatic frequency, which is called the Raman Effect. This shift gives information about vibrational, rotational and other transitions in molecules. It can be used to study solid, liquid and gaseous samples and examine the configuration of carbon based materials including CNTs. The number of walls, diameters, and the presence of crystalline and amorphous carbon can be determined with Raman spectroscopic technique. A sample is usually illuminated with a laser beam in the ultraviolet (UV), visible (Vis) or near infrared (NIR) range. Scattered light is collected with a lens and is sent through spectrophotometer to obtain Raman spectrum of a sample.

The Raman spectrum mainly describes the characteristic of each molecular species. The resonance peaks are also observed in the spectrum, which represent the occurrence of particular species, which is intrinsically present. The characteristic spectrum of CNTs includes three main zones such as low (100- 250 cm^{-1}), intermediate (300-1300 cm^{-1}) and high (1500-1600 cm^{-1}) (Colomer et al., 2000). There are two main first order peaks for carbon-based materials. The first one is the D peak; it is observed around 1300 cm^{-1} for excitation He-Ne laser, or at 1350 cm^{-1} for an Ar ion laser. The D peak shows the presence of defects (Ferrari & Basko, 2013). Second one is the G peak and observed at about 1580 cm^{-1} , which is related to the in-plane vibrations of the graphene sheet (Singh et al., 2003, Shanov et al., 2006). A ratio of the D peak to the G peak is significant for CNT characterization

because it gives the amount of disorder within nanotubes (Tans et al., 1997). A small ID/IG ratio, in the range of 0.1-0.2, represents that the defect level in the atomic carbon structure is low and sample has crystalline quality (Singh et al., 2003). In the present study, Raman spectroscopy used to check the graphitic quality of prepared LCNTs.

3.5.3. X-ray diffraction analysis

The X-ray powder diffraction (XRD) is an analytical technique that is usually used to study crystallinity and structure of material (atoms packing in crystalline state, interatomic distance and bond angles, size and shape of unit cells). It is one of the most significant characterization tool used in the field of solid state chemistry and material science. The atomic planes of a crystal cause an incident beam of X-rays to interfere with one another as they leave the crystal. The phenomenon is called X-ray diffraction. When a focused X-ray beam interacts with sample, some part of the beam is transmitted, some parts absorbed by the sample, some part is refracted and scattered, and some is diffracted. These diffracted beams can measure by applying Bragg's Law.

$$\text{Bragg's Law is } \lambda = 2d \sin \theta$$

Where λ is the wavelength of the incident X-ray beam, d is the distance between adjacent planes of atoms, and θ is the angle of incidence of the X-ray beam.

The X-ray diffraction (XRD) patterns of LCNTs were recorded at ambient temperature using Hecus X-Ray Systems GmbH, Graz (Austria) Model: S3 MICRO. The samples were irradiated with mono-chromatized Cu K α Radiation (1.5406 Å) X-ray source and analyzed between 5 to 80°C (2 θ) in case of LCNTs. The operating voltage and current used were 45 kV and 40 mA, respectively. The time constant was maintained at 3.0 s and sweep at 5° min⁻¹. Average particle sizes were calculated

using the Debye–Scherrer equation. JCPDS was used to interpretation of the peaks in the prepared material.

3.5.4. X-ray photoelectron spectroscopy analysis

The X-ray photoelectron spectroscopy (XPS) is based on the photoelectric effect and it was developed by Kai Siegbahn in 1960. It is employed to perform the elemental analysis of a materials surface in terms of its bonding geometry of molecules to the surface, physical topography, chemical composition, chemical structure, atomic structure and electronic state. XPS is based on the principle of photon emission which requires high vacuum conditions (approx 10⁻⁷ mill bar). The x-ray photoelectron spectrum was ascertained using x-ray photoelectron spectrometer (Model/Supplier: PHI 5000 Versa Prob II, FEI Inc). X-ray photoelectron spectroscopy works by irradiating a sample with mono-energetic soft x-rays beam causing electrons to be ejected._ Identification of the elements present in the sample was held directly from the kinetic energies of ejected photo electrons. A typical XPS spectrum is plotted between the number of electrons detected versus the binding energy (eV) of the electrons. The binding energy of electrons (eV) can be determined by using the following equation:

$$E_{\text{binding}} = E_{\text{kinetic}} - E_{\text{photon}}$$

Where, E_{binding} is the minimum energy required to move an inner electron from its orbital to a region away from the nuclear charge, E_{photon} is the energy of the x-ray photons being used and E_{kinetic} is the kinetic energy of the emitted electron as measured by the instrument (Siegbahn, 1981).

In the present study, XPS was used to study the chemical interactions between metal ions and the prepared materials, which provides identification of the sorption sites involved in the accumulation of metals, as well as the forms of

adsorbed metal ion species on the material surface.

3.5.5. Fourier Transform Infrared spectroscopy

Fourier transform infrared spectroscopy (FTIR) technique was performed to analyze the surface functional groups on the metal doped carbon nano tubes and activated carbon nano-fibers. A potassium bromide (KBr) pressed pellet method was used for sample preparation. In this method a gauzily pulverize sample was mixed with potassium bromide (KBr) powder and then it was pressed in a die to form sample pellet. The prepared sample pellet was then analyzed by FTIR in a transmission mode in the range between 400 and 4500 cm^{-1} at room temperature using FT-IR spectrometer. The FT-IR spectrum of a pure KBr pellet was used as a reference. Fourier transform infrared spectroscopy (FTIR) technique is based on the vibrations of the atoms of a molecule. An infrared spectrum is obtained by passing infrared radiation through a sample and determining what fraction of the incident radiation is absorbed by the sample at a particular energy and some of it is passed through sample.

The resulting spectrum represents the molecular absorption and transmission through the sample (Sawant et al., 2011). The sample chamber of the instrument was purged with N_2 gas to reduce the effect of atmospheric carbon dioxide and moisture through out the analysis. The background spectrum was recorded before the experimental measurements were performed. The resolution was set to 4 cm^{-1} and a total of 100 scans were collected for each sample. In present study, FT-IR spectroscopy was used to determine the bonding between iron metal and functional group present in carbon microspheres and carbon nanotubes which may help in adsorption of (BTEX) FT-IR spectroscopy was also used to determine the bonding between functional group present in adsorbent and adsorbate.

3.5.6. BET Surface area and total pore volume analysis

The technique was named BET after its inventor S. Brunauer, P. H. Emmet and E. Teller (BET). It is the first method developed to measure the specific surface area of porous solids. The BET method is based on the adsorption of gas on a surface. The amount of gas adsorbed at a given pressure allows for the determination of surface area. The method is applied in the analysis of pharmaceuticals, catalysts, projectile propellants, medical implants, filters, cements and adsorbents.

The surface area and the porosity of samples were determined by the Quantachome Autosorb-1 BET analyzer. The adsorption/desorption isotherms and pore volumes of the adsorbents were determined by nitrogen adsorption–desorption isotherms. The samples were kept at 200°C under vacuum before starting N₂ adsorption. Total surface area and pore volume were determined using the Brunauer–Emmet–Teller (BET) equation and the single point method, respectively. Micro porosity was determined from t-plot method. Pore size distribution was obtained by Barret–Joyner–Halenda (BJH) method in the adsorption isotherm. Active metal surface area was measured by chemisorption using H₂ gas. 0.1 gm of each sample was loaded into a capillary glass tube and degassed of the samples was carried out at 250°C for 6 h under nitrogen atmosphere. The nitrogen adsorption and desorption spectra were carried out at 77K using Quanta chrome Autosorb-1 BET analyser.

3.6. pH Studies

The pH of a solution has a significant role on adsorption at the liquid-solid interface. The pH will determine whether the ionized or unionized sorbate species will exist in solution as well as ionization of surface charge of functional groups present in adsorbent. Briefly, 0.1 gm of the adsorbent was taken in a series of 50 ml test tube, followed by the addition of 60 mg/l Toluene, ethyl benzene and o-xylene

solution (TEX) to make the final volume 10 ml in each conical.

The initial pH values of solutions were adjusted to 2 to 9 with 0.1M NaOH or 0.1M HCL. The solutions were kept in testube rotator (110 rpm) for 2 h at 25°C and final pH was recorded for each solution. The supernatant was then filtered through a 0.22 μ m membrane and the filtrate was extracted by dichloromethane and analyzed for rest (TEX) by gas chromatograph-flame ionization detector (GC-FID, NUCON Engineers). Removal efficiency of (TEX) was calculated by the difference between the initial and final concentrations of (TEX) in solution divided by the initial concentration.

3.7. Kinetic Studies

Kinetic study would be carried out after optimization of pH (neutral) and dose at specific temperature and speed. For kinetic studies 0.1g of each adsorbent with defenite concentration of VOCs would be placed in testube rotator. With initial pH = 7 at a constant temperature of 25°C for varying equilibration time from 5 min to 2 hrs. and the the count of VOCs adsorbed will be analyzed after extraction.

3.8. Equilibrium isotherm studies

For the equilibrium isotherm studies, Ethyl Benzene, Toluene or o-Xylene solution with initial concentration range 10 to 100 mg/L was prepared by diluting the 1000 mg/L stock solution. A mass of 0.02 g adsorbents such as carbon nanotubes (LCNTs),Oxidized LCNTs (LCNT-OX),carbon Microspheres (LCM),Oxidized LCM (LCM-OX), Alkali carbon microsphere (ACM) and purchased CNT (P-CNT) were purchued from United nanotech, Bangalore, (India) was agitated with 10 ml of aqueous Ethyl Benzene, Toluene or o-Xylene (TEX) solution in a 50 ml testube in a testube rotator at 110 rpm at 25°C for the equilibrium time determined, which was

taken as the contact time that allows the dispersion of adsorbent and Ethyl Benzene, Toluene or o-Xylene (TEX) to reach equilibrium conditions, as found in the equilibrium contact time experiments.

At the end of the equilibrium time, the content was separated by filtration using 0.22 μm pore size filter paper and TEX in solution was extracted by dichloromethane (DCM) and analyzed by gas chromatograph-flame ionization detector (GC-FID, NUCON Engineers). All the experiments were carried out twice. The amount of Ethyl Benzene, Toluene or o-Xylene (TEX) adsorbed (mg) per unit mass (g), q_e , was obtained by mass balance using the following equation:

$$Q_e = \frac{(C_i - C_e)}{m} \times V$$

Where C_i and C_e are initial and equilibrium concentrations of the solution (mg/L), m is dry mass (g) and V is the volume of the solution (L).

3.9. Column or dynamic study for VOCs determination

Fig. 6 represent the schematics of a packed-column (length = 30 cm, I.D. = 1.5 cm) used for the breakthrough analysis. The column contained layers of different packing materials. The middle layer contained the adsorbents carbon nanotube (CNT). The bottom layer and upper layer consisted of glass beads and glass wool, to support the adsorbents. At both ends, a short Perspex-stub was used as an end-cap and was thread-fitted the main column. The SS mesh was fitted to provide the structural support. Neoprene O-rings were fixed between the side-walls of the main column and the stub to prevent any leakage of the test solution.

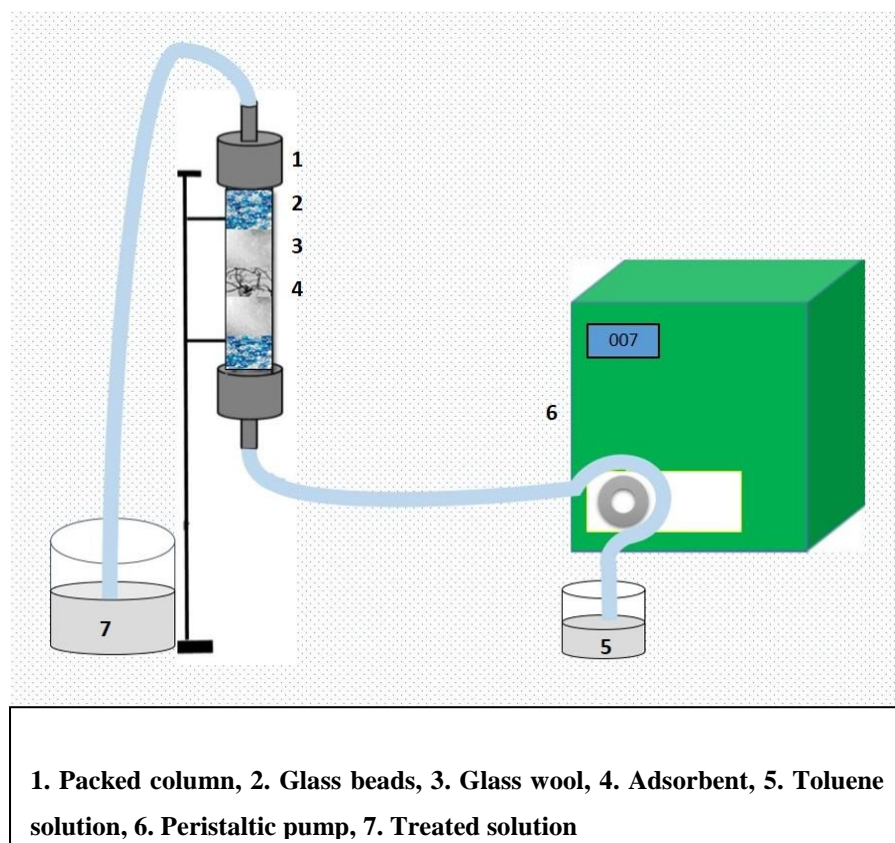


Figure 6 Column Study

3.10. Gas Chromatography

All the VOCs samples were analyzed by using Gas chromatography model Nucon GC 5765 equipped with flame ionization detector (FID) detector (Fig. 7). The column used in this experiment was capillary silica column (Column EC-5) with specifications 30-meter length, 0.53 mm internal diameter with the film thickness of 1.2 μm . Oven temperature was programmed as initial temperature 40 $^{\circ}\text{C}$ and then increased up to 185 $^{\circ}\text{C}$ by increasing rate of 35 $^{\circ}\text{C}/\text{min}$ and hold for 1 min. injector port temperature was set at 230 $^{\circ}\text{C}$. Detector temperature was maintained at 240 $^{\circ}\text{C}$, nitrogen was used as carrier gas with flow rate 1.0 ml/min and 1.0 μL of sample was injected in GC system. All the VOCs sample was extracted by dichloromethane and analyzed by gas chromatograph.

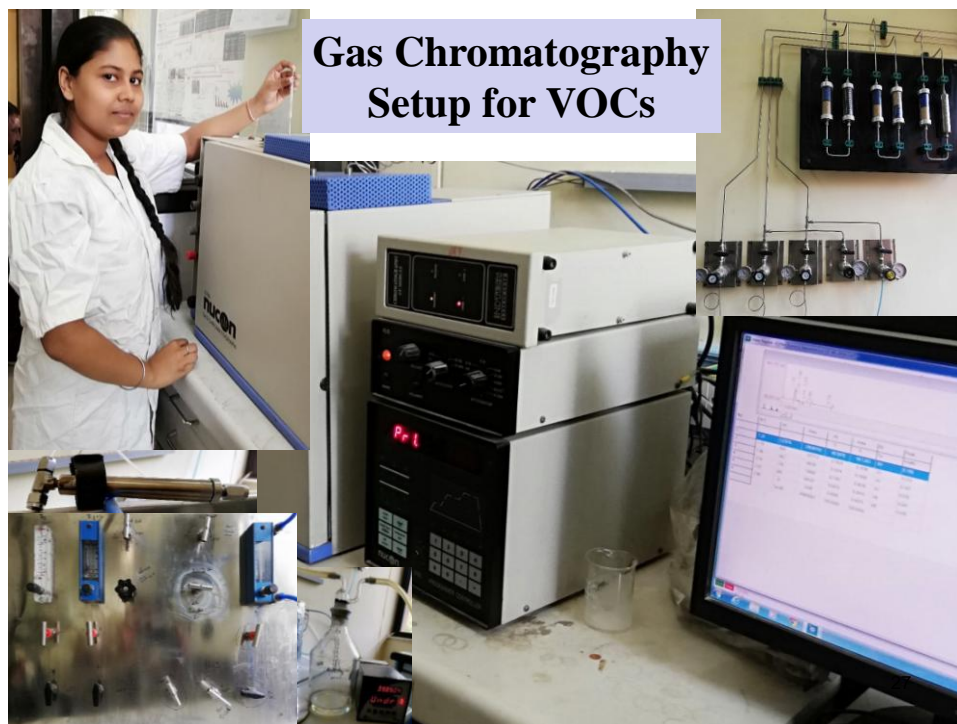


Figure 7 Gas Chromatography external image with all accessories

3.11. Model for VOCs adsorption

Rotameters were used to control the flow rates of various gas streams in the system. Rotameters (R1) (10-100 ml/min) was used for controlling the air flow rate through the VOC bottle which was made of glass, R2 (50-500 ml/min) was used for controlling the of makeup air flow rate of nitrogen, above mentioned rotameters (R1 and R2) were made of Pyrex. However, a special glass rotameter, mass flow controller (MFC) was used at the outlet section of the reactor to control the flow rate in the automated Gas sampling valve of the GC. This was done to avoid any possible chemical reaction between the VOCs in the gas stream and the rotameter material. Whenever required, the same rotameter was used to control the inlet feed rate to the reactor by making slight changes to the piping connections.

Five needle valves were provided respectively for controlling the gas flow rate, as per requirement. one toggle valves were used to prevent the backflow of

gases into the bottles in the reverse direction, while they are cut off from the flow circuit. All the rotameters and the other accessories such as needle valves and toggle valves were mounted on a common console for the convenience of operation as shown in Figure8.

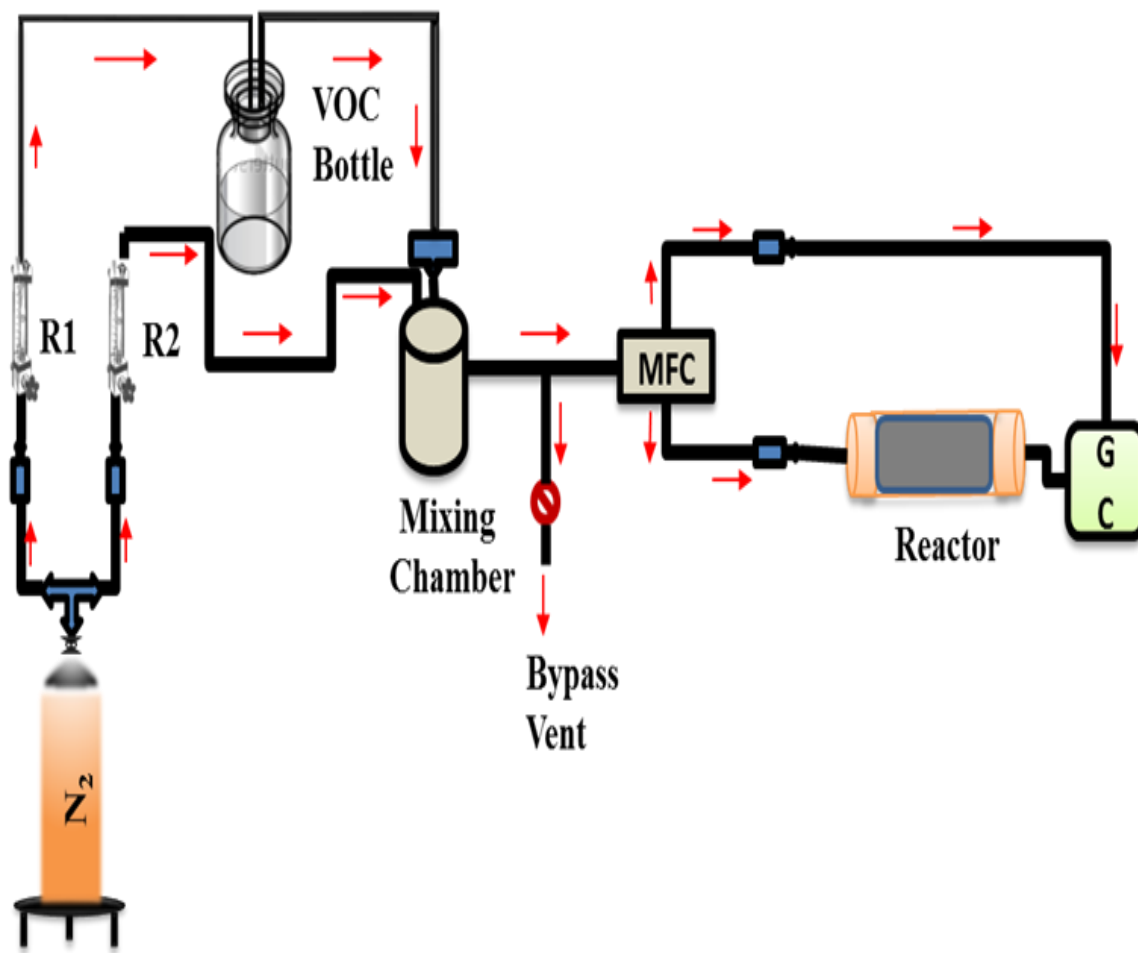


Figure 8 Experimental model for VOCs adsorption from air contamination

Chapter 4

Results

CHAPTER- 4

RESULTS

4.1. Introduction

In the result chapter covered the portion of analyzing results of water and air experiment study to removal of VOCs through different CNTx and modified CNTS. In the water objective cover “Fast and efficient removal of Toluene, Ethylbenzene and O-Xylene from aqueous phase by functionalized carbon micro/nano composites”. Volatile organic compounds namely toluene (T), ethylbenzene (E) and o-xylene (X) are widely used in various industrial processes. Huge amounts of TEX contaminated wastewater discharged into surrounding water bodies from these industries.

Various carbon composites thus prepared namely, LCNT, LCNT-OX, LCM and LCM-OX were characterized using various spectroscopic techniques including Scanning electron microscopy (SEM), transmission electron microscopy (TEM), Brunauer-Emmett-Teller (BET) Surface Area measurements, X-ray diffraction (XRD), Fourier transform infra red spectroscopy (FTIR), Raman, X-ray photoelectron spectroscopy (XPS) and systematically evaluated for the removal of TEX from both distilled water and ground water. Column studies were conducted to demonstrate the applicability of prepared carbon composite under dynamic conditions. Static adsorption experiments were also carried out to evaluate the uptake capacity of vapour phase of TEX by various prepared carbon composites. The results obtained were compared with the commercially available CNT (P-CNT) acquired from United nanotech, Bangalore, India.

4.2. Characterization of carbon composites SEM images of -

(a) LCNT, (b) LCNT-OX,

(c) and (d) TEM images of LCNT,

(e) SEM Image of LCM

(f) TEM image of LCM

4.2.1. SEM and TEM Analysis

The SEM images of LCNT, LCNT-OX and LCM are depicted in Fig. 9(a), 9(b), and 9(e) respectively. It is evident from the figure that there are no appreciable changes observed in the surface morphology of oxidized CNTs (CNT-OX) image as compare to virgin CNTs. The TEM image revealed the presence of nanotubes and iron particles located both at the tip as well as inside the nanotubes Fig. 9(c), 9(d) and 9(f).

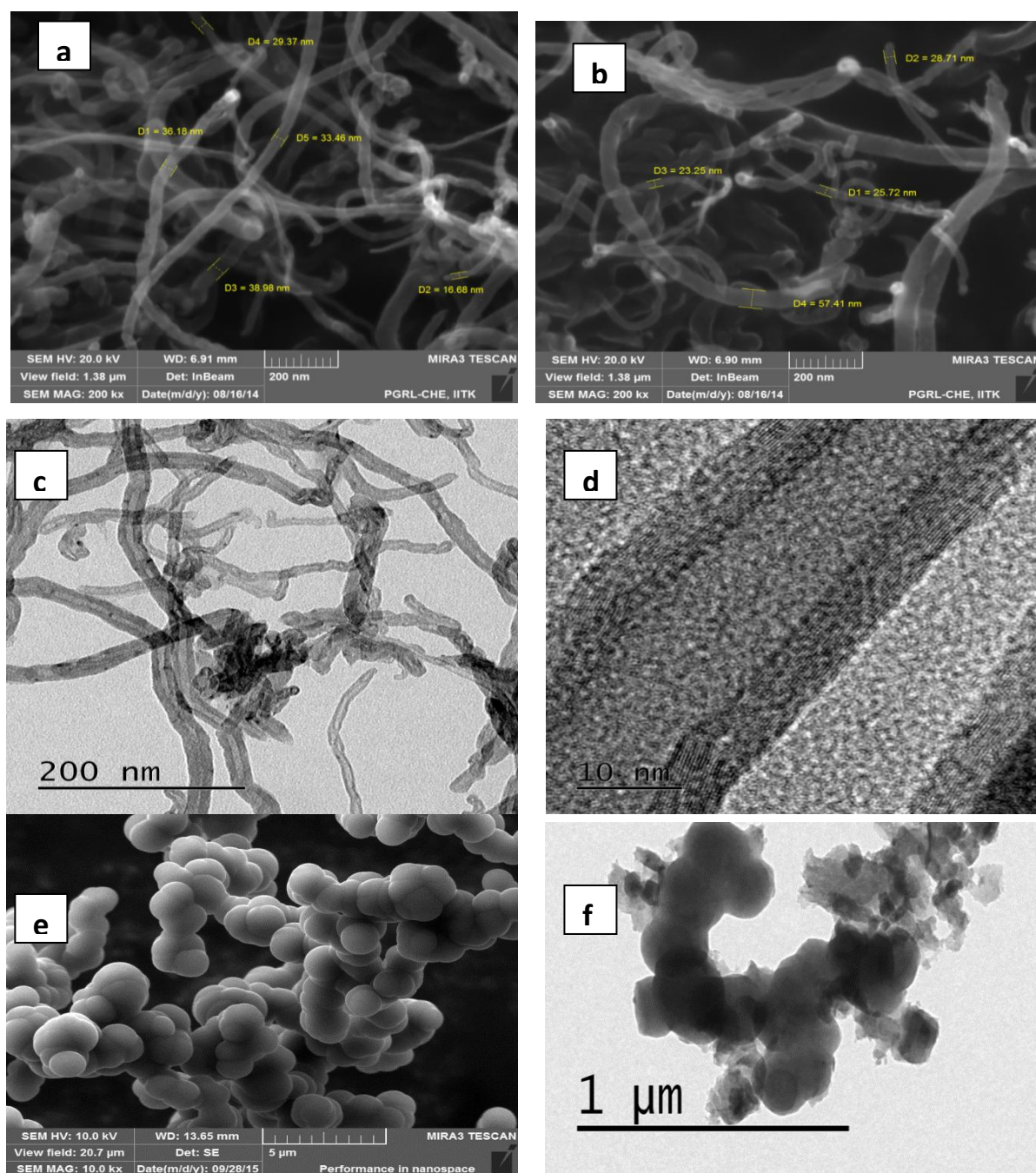


Figure 9 SEM images of (a) LCNT, (b) LCNT-OX, (c) and (d) TEM images of LCNT, (e) SEM Image of LCM (f) TEM image of LCM

4.2.2.BET analysis

BET analysis provides precise specific surface area evaluation of materials by nitrogen multilayer adsorption measured as a function of relative pressure using a fully automated analyzer. Table 3 show the specific surface area (SSA) and pore-size characterization of L-CNT, L-CNT-OX, L-CM, L-CM-OX and P-CNT were performed by nitrogen (77.4 K) adsorption/ desorption experiments. The results obtained are presented in Table 3. The increased surface area of the CNT-OX might be attributed to the increased defects on the surface owing to the heat treatment and oxidation processes.

Table 3 Specific surface area and pore volumes of various carbon composites

Sample	Specific Surface Area (m ² /g)	Total pore (cc/g)	Average pore Diameter (nm)	Micropores (%)	Mesopores (%)	Macropores (%)
L-CNT	99.81	0.3661	7.33	26.25	16.68	57.07
L-CNT-OX	121.68	0.2943	5.26	0.45	45.99	53.56
L-CM	7.22	0.0126	16.33	6.34	67.44	26.22
L-CM-OX	12.706	0.0134	4.106	22.35	64.95	12.70
P-CNT	199.01	1.3710	27.56	0.60	54.55	44.85

4.2.3. XRD Analysis

The X-ray powder diffraction (XRD) is an analytical technique that is usually used to study crystallinity and structure of material Fig. 10 and Fig.11 revealed that the carbon composites possessed one broad diffraction peak at 2θ values around 26.4.

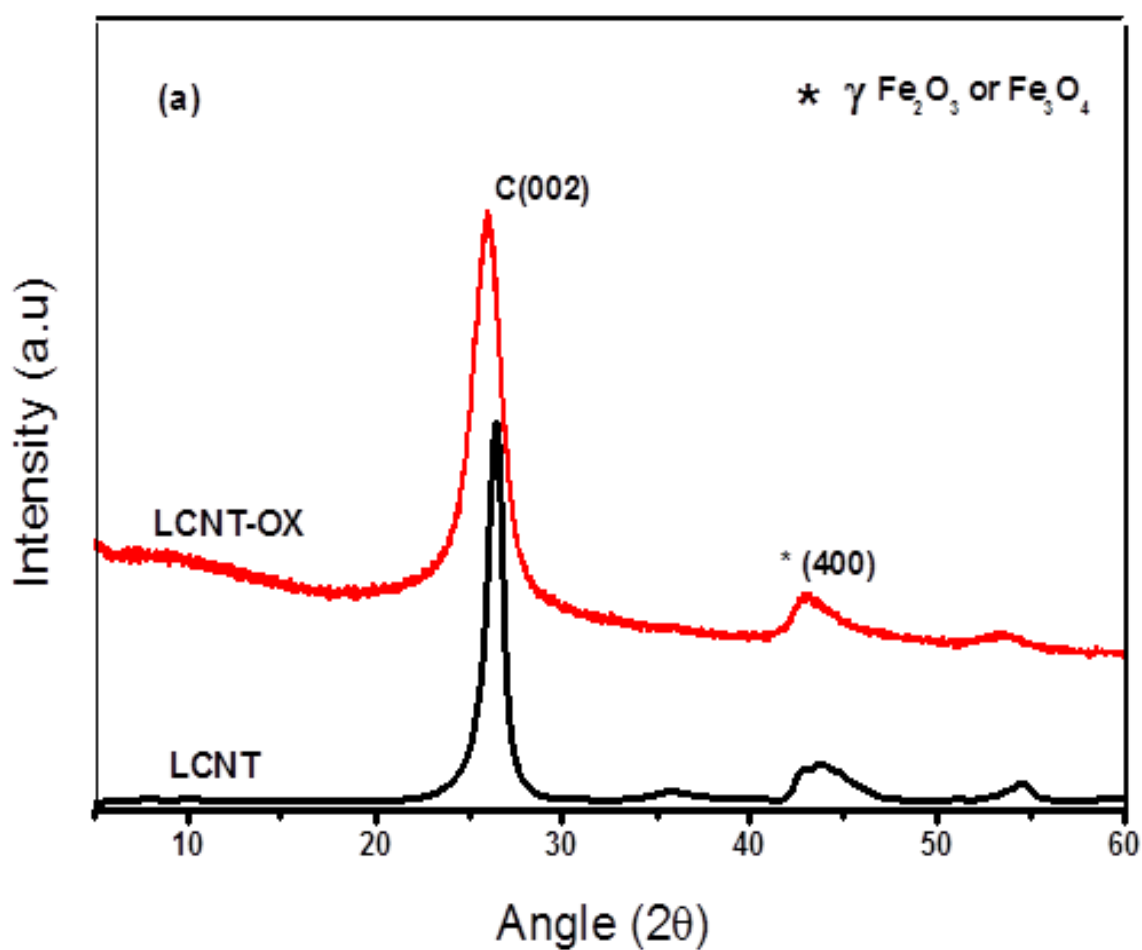


Figure10 X-ray diffraction pattern of LCNT and LCNT-OX

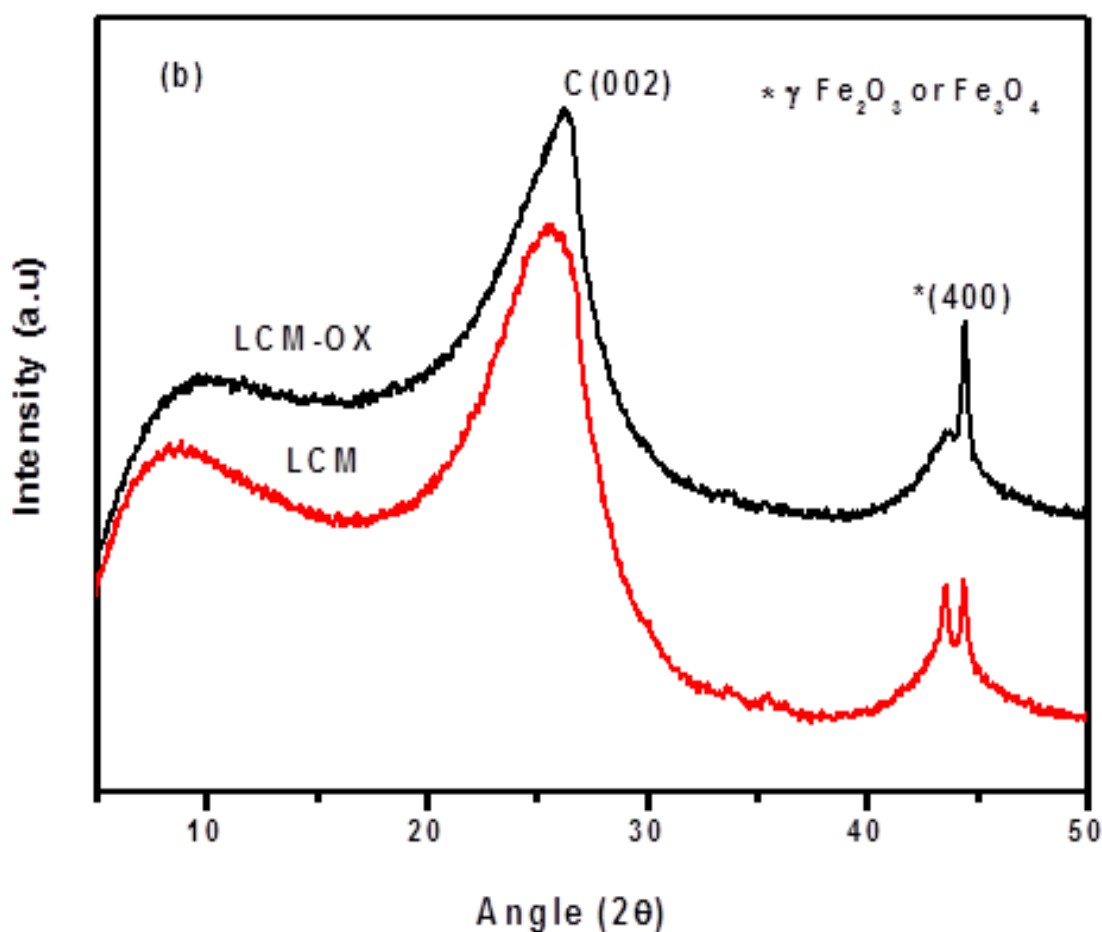


Figure 11 X-ray diffraction pattern of LCM and LCM-OX

4.2.4. FTIR analysis

FTIR is an effective analytical instrument for detecting functional groups and characterizing covalent bonding information. FT-IR spectra of in LCNT, LCNT-OX, LCM and LCM-OX Fig. 12 After oxidation by concentrated (HNO_3) LCNT-OX, and LCM-OX the peaks at 1720 cm^{-1} and appeared clearly in the spectra which are associated with the asymmetric C=O stretching band of the carboxylic acid ($-\text{COOH}$) group.

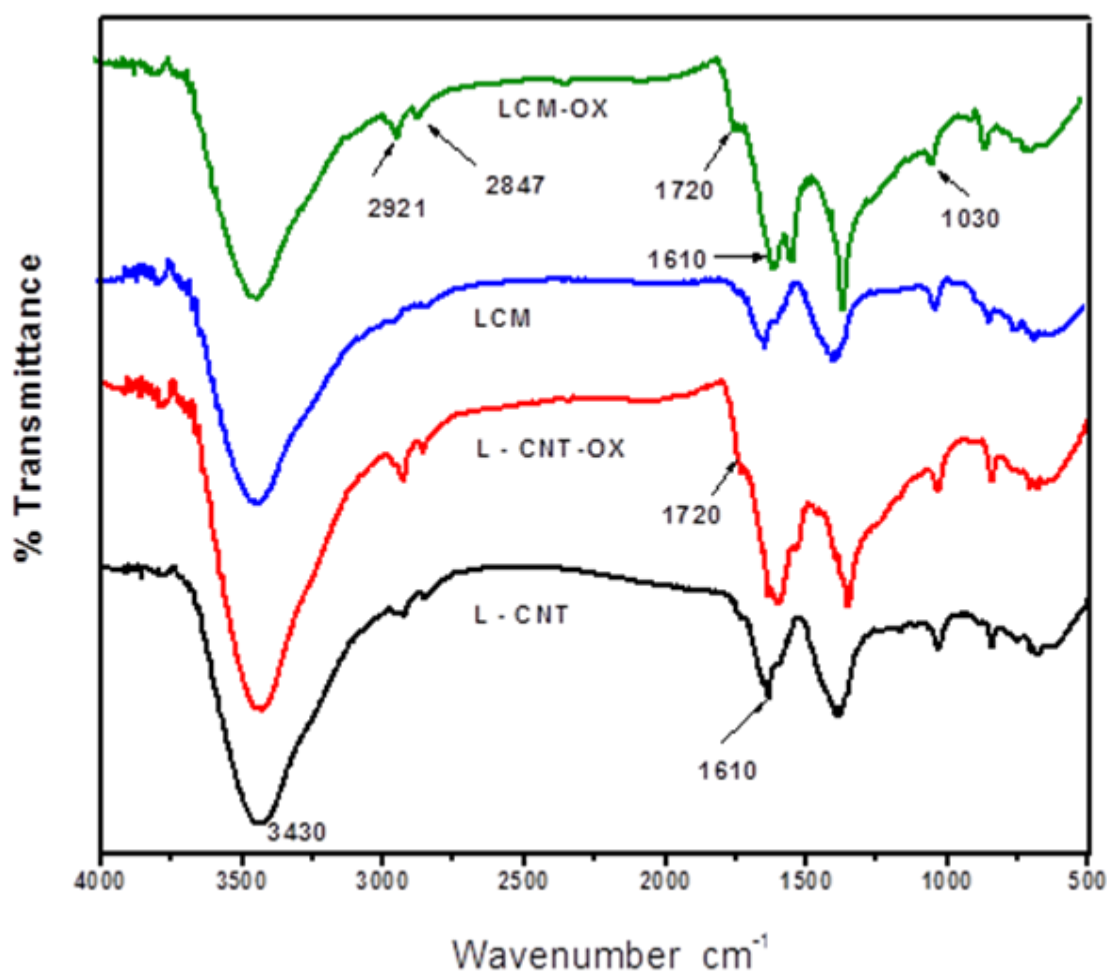


Figure 12 FTIR spectra of LCNT, LCNT-OX, LCM and LCM-OX

4.2.5. Raman Analysis

Raman spectroscopy provides information about molecular vibrations that can be used for sample identification and quantitation. The Raman spectra of LCNT, LCNT-OX, LCM, and LCM-OX Figure 13 and Table 4 show the ratio increased LCNT-OX and LCM-OX compared to plain CNT and LCM forms indicating the presence of imperfections on oxidized composites surfaces.

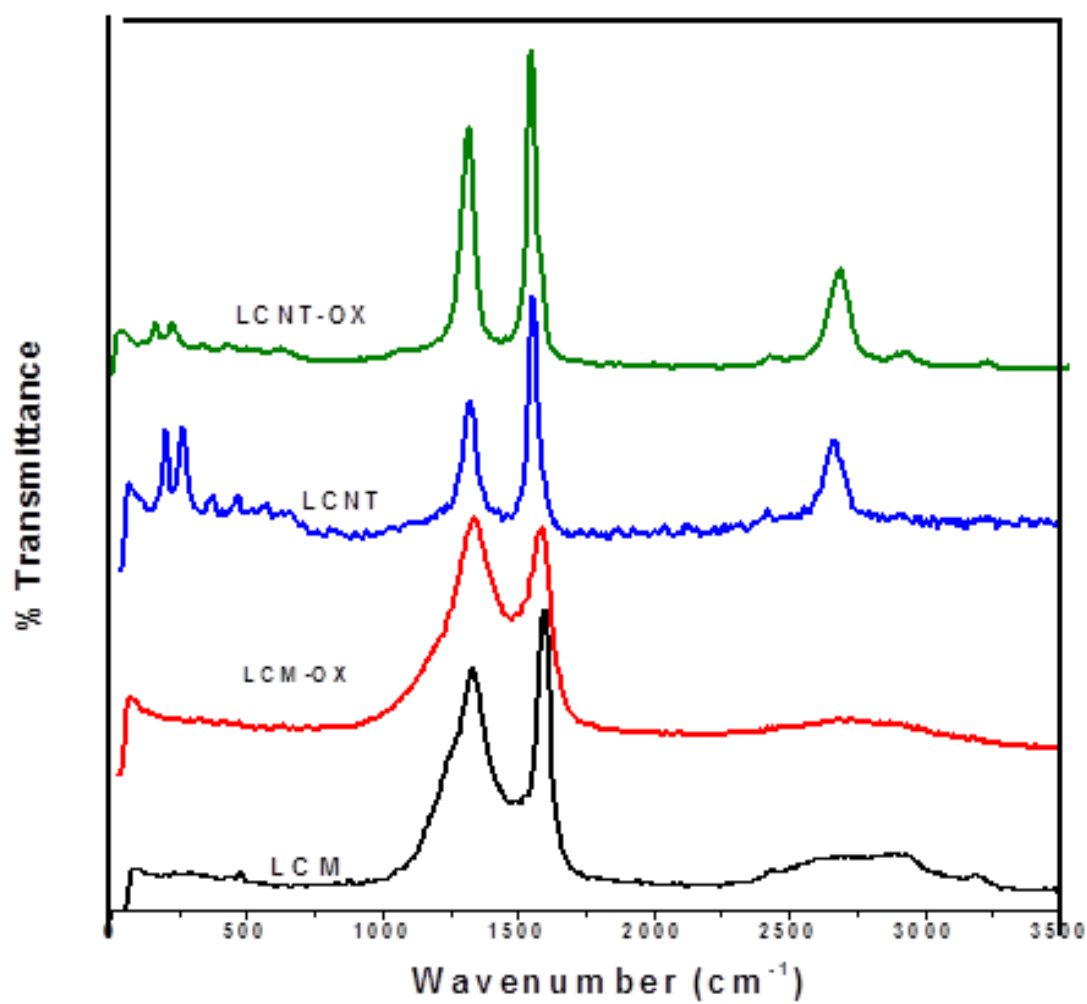


Figure 13 Raman Spectra of LCNT, LCNT-OX, LCM and LCM-OX

Table 4 Raman spectra of LCNT, LCNT-OX, LCM and LCM-OX

Adsorbent	D-Bandcm^{-1}	G-Bandcm^{-1}	I_D/I_G
LCNT	1318	1558	0.976
LCNT-OX	1319	1548	0.847
LCM	1350	1588	1.013
LCM-OX	1337	1587	0.943

4.2.6. XPS Analysis

XPS was used to study the chemical interactions between metal ions and the prepared materials, XPS survey spectra of LCNT, LCNT-OX, LCM and LCM-OX. Figure 14 show the major peak of the graphitic carbon present in all carbon composites and it was also increased the atomic percentage of oxygen.

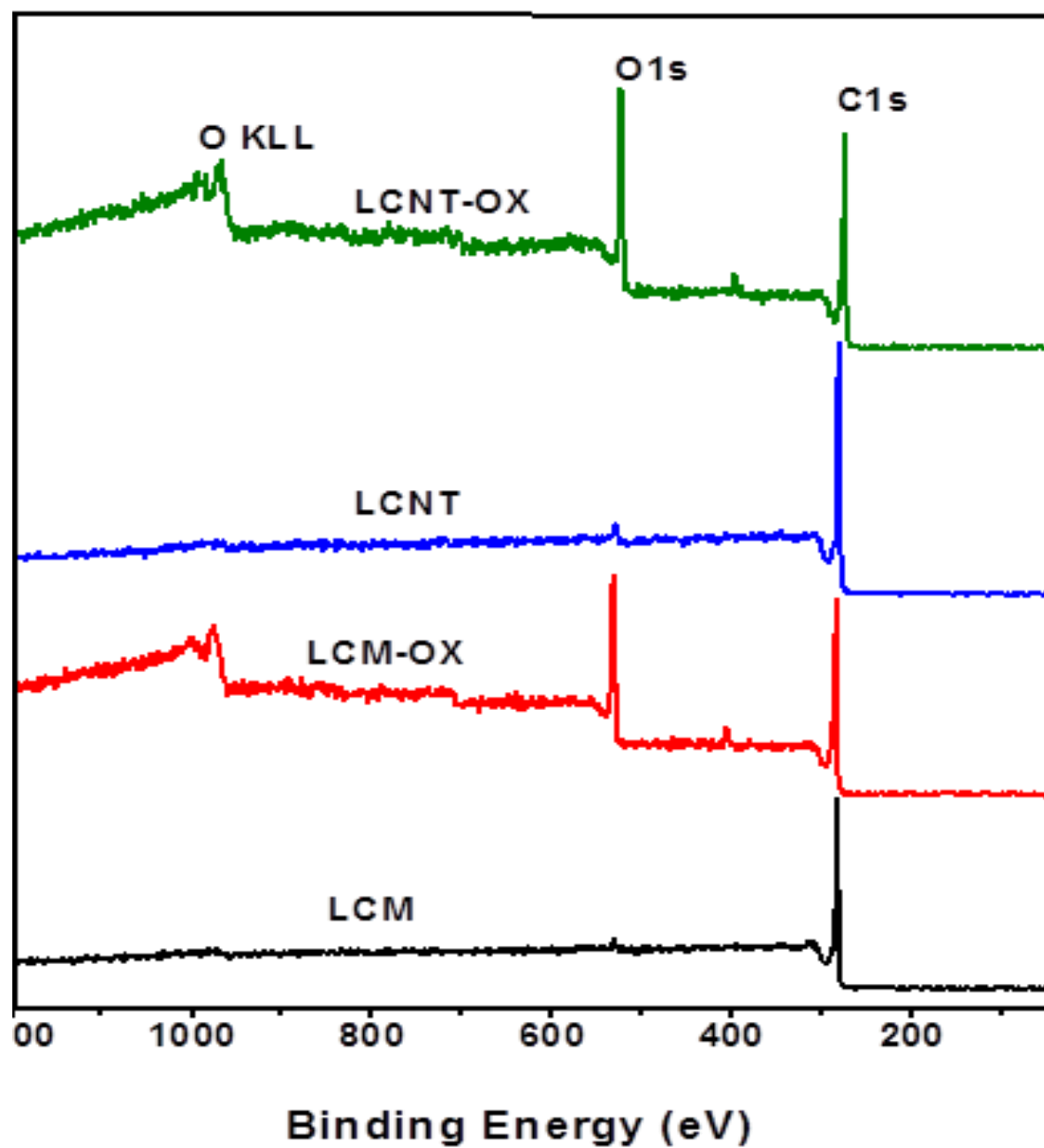


Figure 14 XPS Survey spectra of LCNT, LCNT-OX, LCM and LCM-OX

4.2.6.1. Studies on (TEX) removal

4.2.6.2. Effect of initial pH

Fig. 15 show that The pattern of initial pH is almost same and values are more or less constant for TEX. Therefore in this research we considered the neutral pH for further analyses.

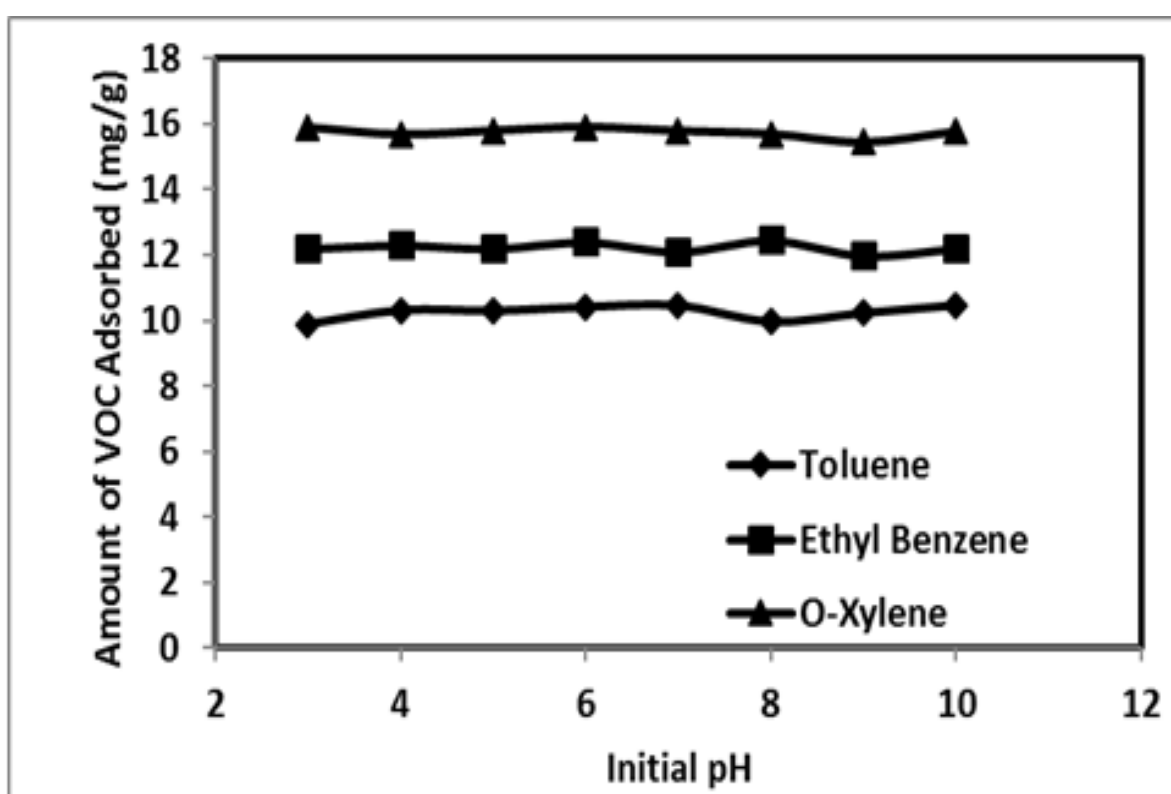


Figure 15 Effect of initial pH on the sorption behavior of TEX using LCNT

4.2.6.3. Effect of kinetics

Kinetics analyses was compared for all carbon composites and results revealed that L-CM-OX and followed by L-CNT-OX attained equilibrium at earliest. show in Fig.16 (a) (b) and (c) and Table 5.

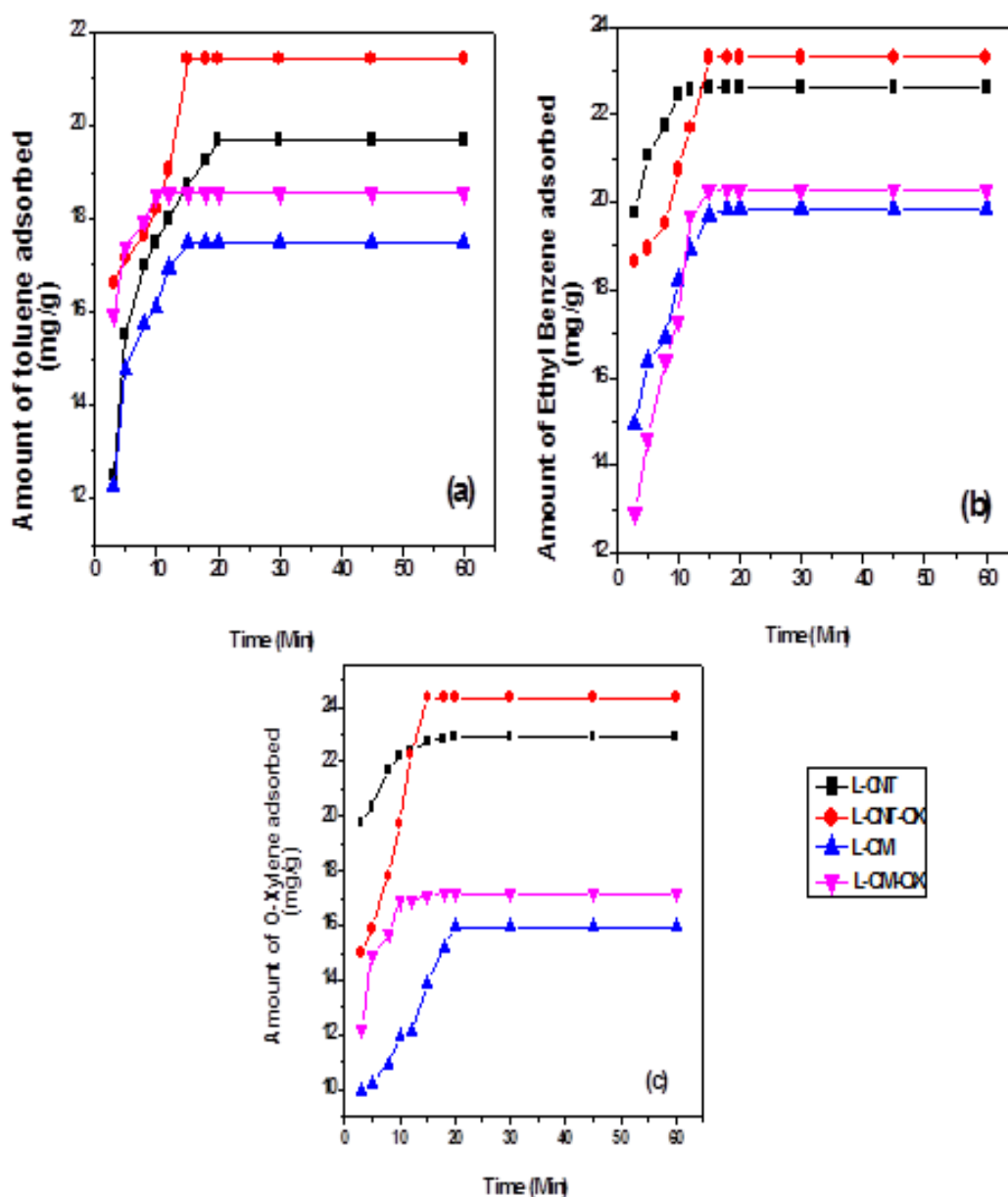


Figure 16 Kinetics of adsorption of LCNT, LCNT-OX, LCM and LCM-OX with

(a) Toluene, (b) Ethyl Benzene and (c) O-Xylene

Table 5 Kinetic parameters for TEX sorption using LCNT, LCNT-OX, LCM and LCM-OX

Adsorbent	VOC	Pseudo First Order		Pseudo Second Order		Web Morris Model	
		K_t (min^{-1})	R^2	k_2' (mg/g/min)	R^2	k_{in}	R^2
LCNT	Toluene	0.170	0.983	0.048	0.999	2.354	0.924
	Ethyl Benzene	0.407	0.946	0.276	0.999	1.620	0.964
	o-Xylene	0.223	0.985	0.276	0.999	1.321	0.935
LCNT-OX	Toluene	0.585	0.985	0.044	0.999	1.965	0.846
	Ethyl Benzene	1.151	0.940	0.056	0.999	2.123	0.940
	o-Xylene	0.154	0.904	0.026	0.999	4.448	0.967
LCM	Toluene	0.225	0.945	0.071	0.999	2.038	0.971
	Ethyl Benzene	0.112	0.928	0.054	0.999	2.281	0.934
	o-Xylene	0.080	0.871	0.054	0.999	2.268	0.923
LCM-OX	Toluene	0.059	0.938	0.255	0.999	1.468	0.922
	Ethyl Benzene	0.128	0.990	0.032	0.998	3.567	0.975
	o-Xylene	0.350	0.961	0.984	0.999	2.630	0.930

4.2.6.4. Adsorption Isotherm

The order of sorption capacity of adsorbents followed the order: CNT-OX > P-CNT > L-CNT, LCM-OX > LCM. Fig. 17 (a), (b), and (c) show that the Maximum adsorption capacity of CNT-OX could be recognized to larger surface area and presence of various functional groups like carboxyl, hydroxyl and carbonyl groups.

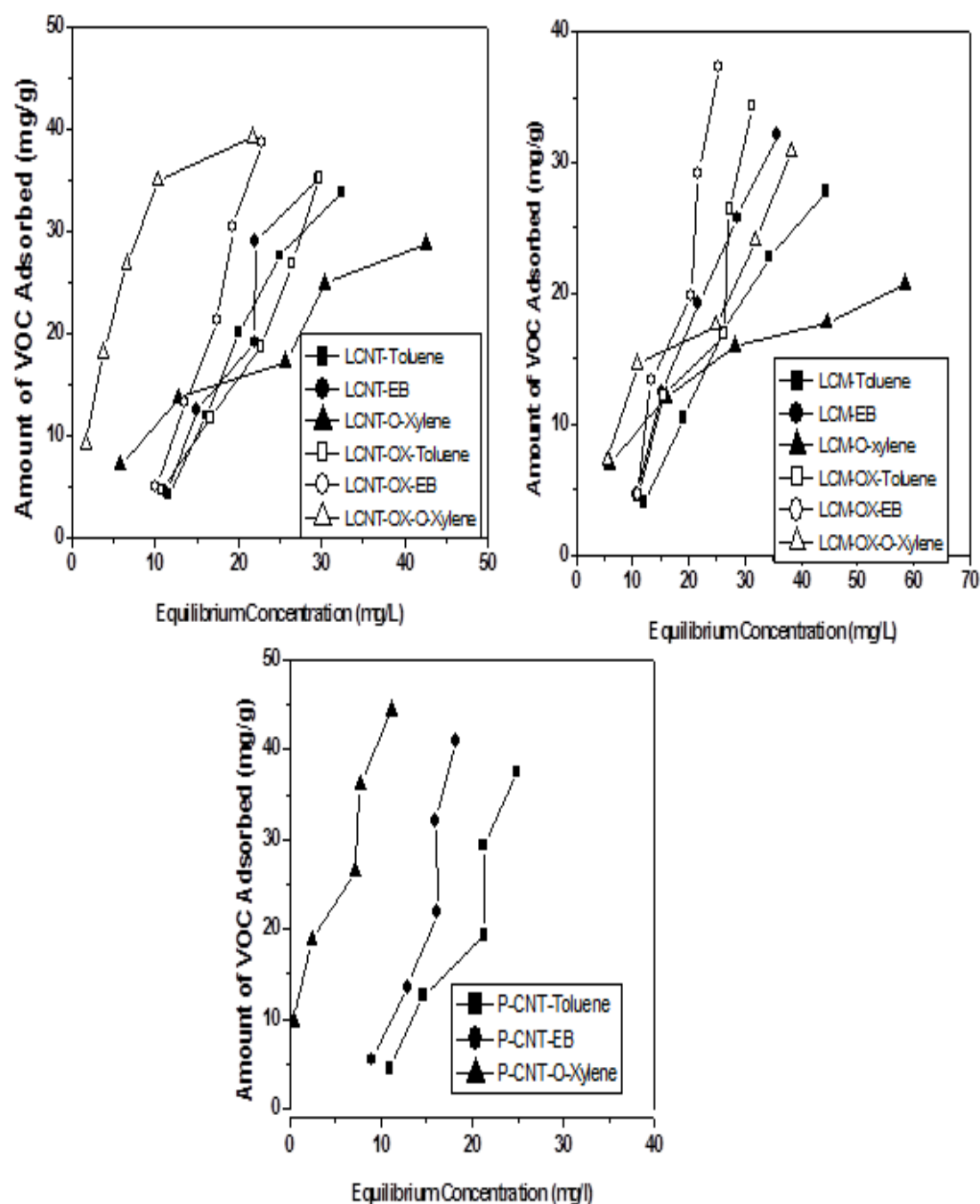


Figure 17 Equilibrium Isotherms of (a) LCNT and LCNT-OX, (b) LCM and LCM-OX and (c) P-CNT with TEX

Table 6, 7 and 8 As per the comparative analyses for amount of VOCs adsorbed the results showed that oxidized CNTs/CMs is performing significantly well. However the pattern was as same as in purchased CNTs .Fig. 18 (a), (b), and

(c). Table 9 show that the Comparative studies of carbon composites reported in the literature.

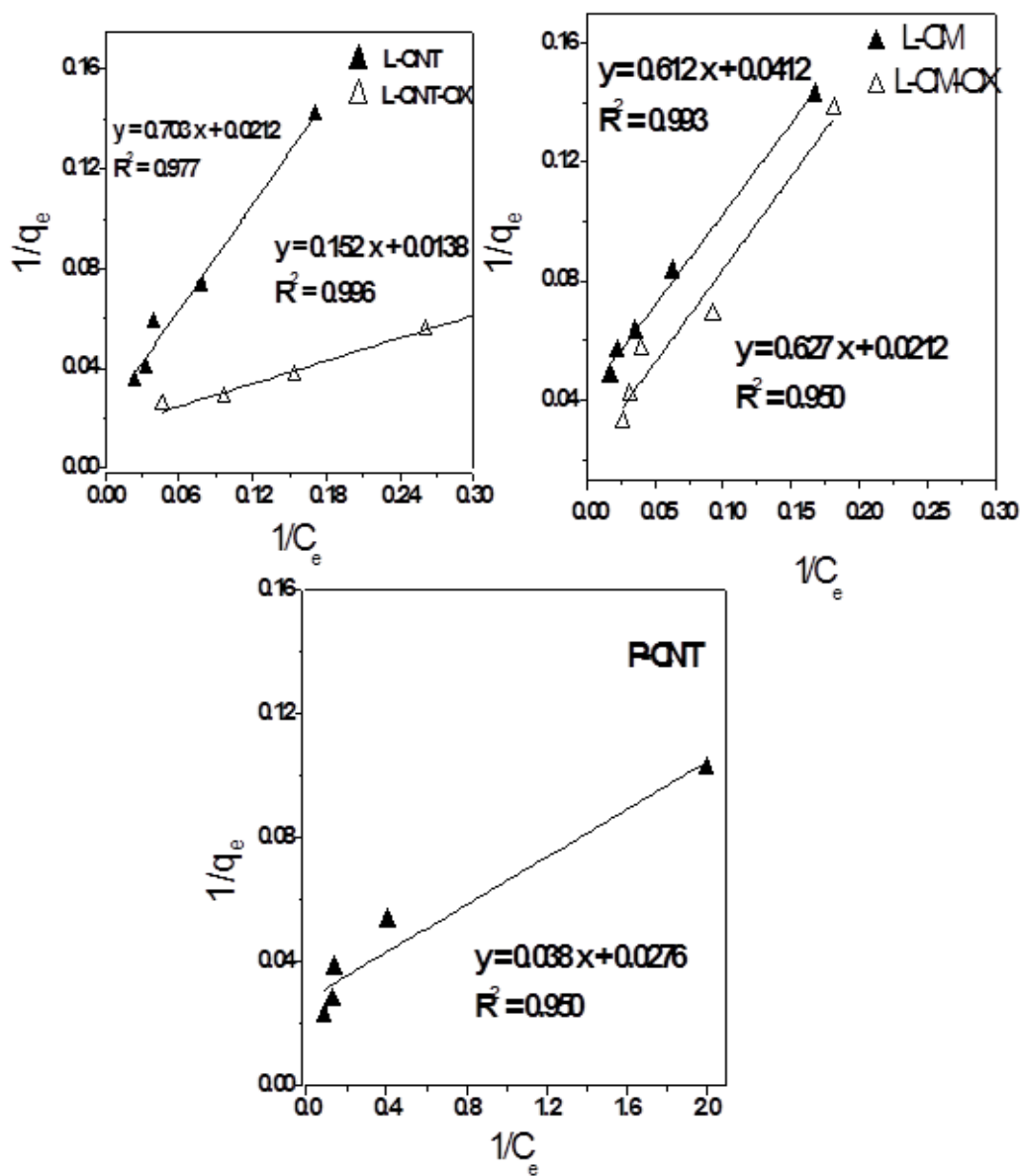


Figure 18 Linearised Langmuir isotherm plots of (a) LCNT and LCNT-OX; (b) LCM and LCM-OX and (c) P-CNT with o-Xylene

Table 6 Langmuir Isotherm Constants for o-Xylene

Adsorbent	Langmuir Model constants		
	q_{\max} (mg/g)	b (ml/mg)	R^2
L- CNT	47.17	0.030	0.977
L -CNT-OX	72.46	0.055	0.980
L-CM	24.27	0.067	0.993
L-CM-OX	47.16	0.338	0.950
P-CNT	52.63	0.220	0.978

Table 7 Freundlich Isotherm Constants

Adsorbent	VOC	Freundlich Model		
		k_f	$1/n$	R^2
L-CNT	Toluene	0.007	6.055	0.930
	Ethyl Benzene	3.758	0.606	0.960
	O-Xylene	0.545	1.456	0.961
L -CNT-OX	Toluene	0.638	2.306	0.990
	Ethyl Benzene	0.016	2.512	0.981
	O-Xylene	7.850	0.581	0.935
L-CM	Toluene	0.113	1.492	0.962
	Ethyl Benzene	0.144	1.549	0.938
	O-Xylene	3.169	0.466	0.986
L -CM-OX	Toluene	0.0883	1.702	0.921
	Ethyl Benzene	0.0311	2.199	0.910
	O-Xylene	2.735	0.618	0.863
P-CNT	Toluene	0.635	2.780	0.937
	Ethyl Benzene	0.012	2.782	0.961
	O-Xylene	12.820	0.454	0.961

TABLE 8 Langmuir Isotherm Constants for o-Xylene

Adsorbent	Langmuir Model constants		
	q_{\max} (mg/g)	b (ml/mg)	R^2
L- CNT	47.17	0.030	0.977
L -CNT-OX	72.46	0.055	0.980
L-CM	24.27	0.067	0.993
L-CM-OX	47.16	0.338	0.950
P-CNT	52.63	0.220	0.978

Table 9 Comparative studies of carbon composites reported in the literature for the removal of o-xylene from aqueous phase

Adsorbent	Adsorption capacity (mg/g)	Equilibration time	Reference
CNT – 2.0% O	62.82	10 h	Yu et al. 2011
CNT- 3.2% O	112.19		
CNT- 4.1% O	100.45		
CNT- 5.9% O	48.73		
CNTs NaOCl	413.7	2 h	Su et al. 2010
SWCNT	77.5	24h	Chin et al. 2007
SWCNT-HNO ₃	85.5		
Magnetic CNT	138.04	24 h	Yu et al. 2016
Magnetic SWCNT	50.0	20 min	Pourzamani et al. 2017
LCNT	47.17	20 min	Present work
LCNT-OX	72.46		
LCM	24.27		
LCM-OX	47.16		

4.2.6.5. Static sorption

It is evident from table 10 the sorption capacity follows the order o-xylene > ethyl benzene > toluene. According to five adsorbents namely LCNT, LCNT-OX, LCM, LCM-OX and PCNT.

Table 10 Static sorption test of carbon composites			
Sorbent	Amount Adsorbed (mg/g)		
	Toluene	Ethyl Benzene	o-Xylene
LCNT	229.4	184.8	248.4
LCNT-OX	280.4	226.2	315.8
LCM	195.6	175.2	205.6
LCM-OX	242.8	200.2	260.5
PCNT	240.8	196.6	255.5

4.2.6.6. Column Study

It is demonstrate the amount of toluene adsorbed was found to be 40.19 mg/g and 71.2% of Toluene was removed from aqueous solution. The breakthrough curve of LCNT-OX with Toluene suggests the applicability for separation with following the Langmuir model. it is evident Fig.19.

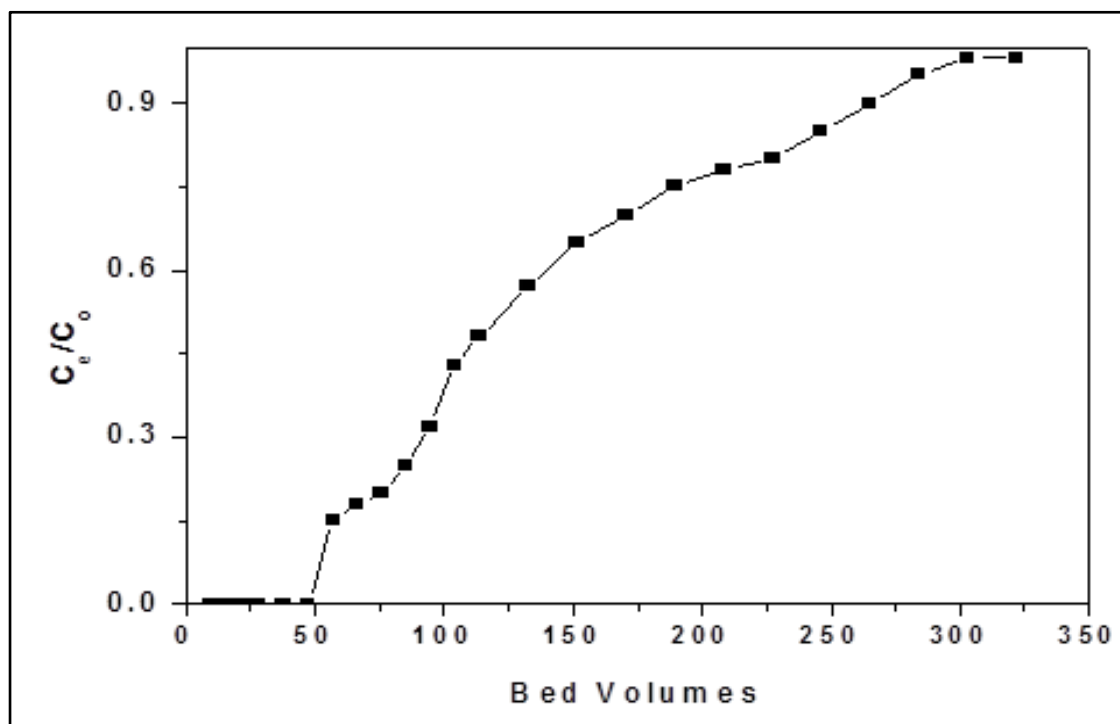


Figure 19 Breakthrough curve of LCNT-OX with Toluene

4.2.6.7. Recyclability Studies

This table 11 and Fig 20 show that there was no appreciable change in sorption behavior even after 5 cycles and the data revealed significant recyclability of LCNT-OX and LCM-OX for VOCs removal.

Table 11 Recyclability Studies

Cycles	Amount of VOC Adsorbed (mg/g)					
	LCNT-OX			LCM-OX		
	Toluene	Ethyl Benzene	O-Xylene	Toluene	Ethyl Benzene	O-Xylene
1	18.67	21.27	26.74	16.87	17.82	19.54
2	18.58	21.26	26.75	16.85	17.88	19.56
3	18.55	21.23	26.74	16.82	17.90	19.55
4	18.60	21.25	26.79	16.86	17.91	19.52
5	18.65	21.28	26.72	16.83	17.86	19.53

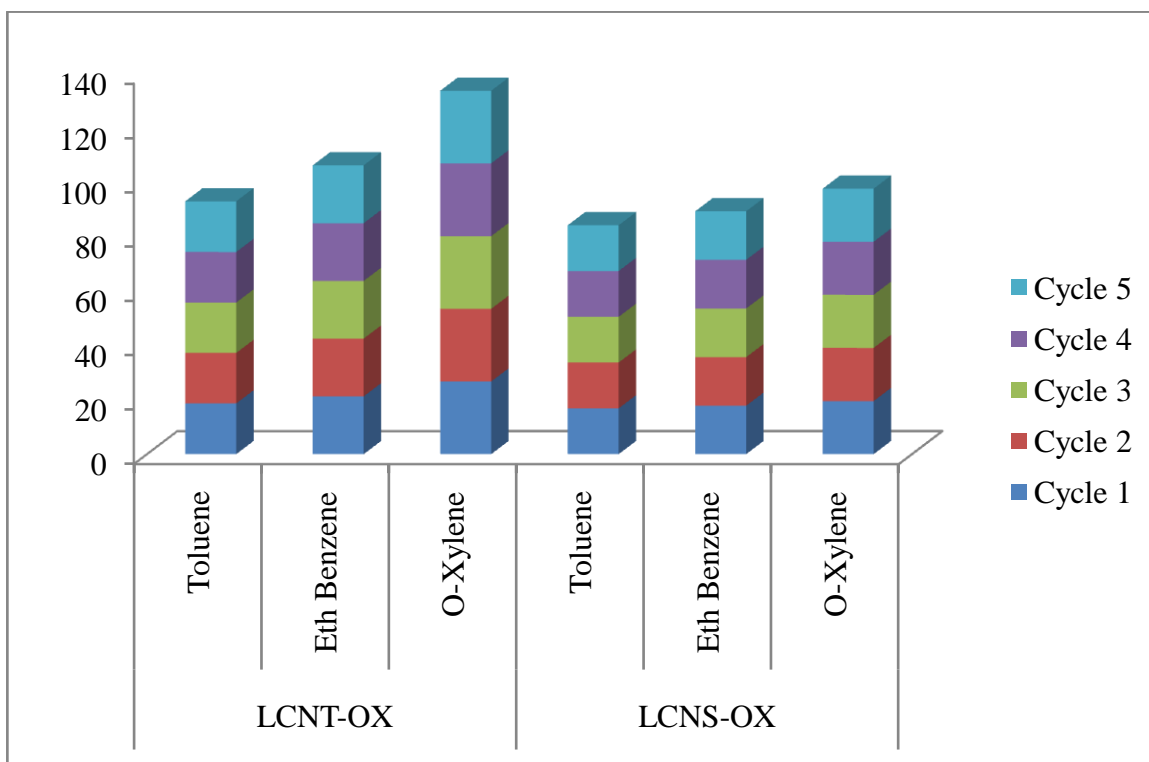


Figure 20 Recyclability Studies

4.2.6.8. Applicability to Ground water

This table 12 and Fig. 21 define that the data amount of TEX adsorbed remained more or less same in both distilled water and ground water. so the applicability of adsorbents in ground water and distilled water are same.

Table 12 Applicability to Ground water

Sorbent	Amount of VOC Adsorbed (mg/g)					
	Toluene		Ethyl Benzene		O-Xylene	
	DW	GW	DW	GW	DW	GW
LCNT-OX	13.90	14.08	15.57	15.72	17.15	18.08
LCM-OX	12.22	12.12	13.35	13.27	14.59	14.63

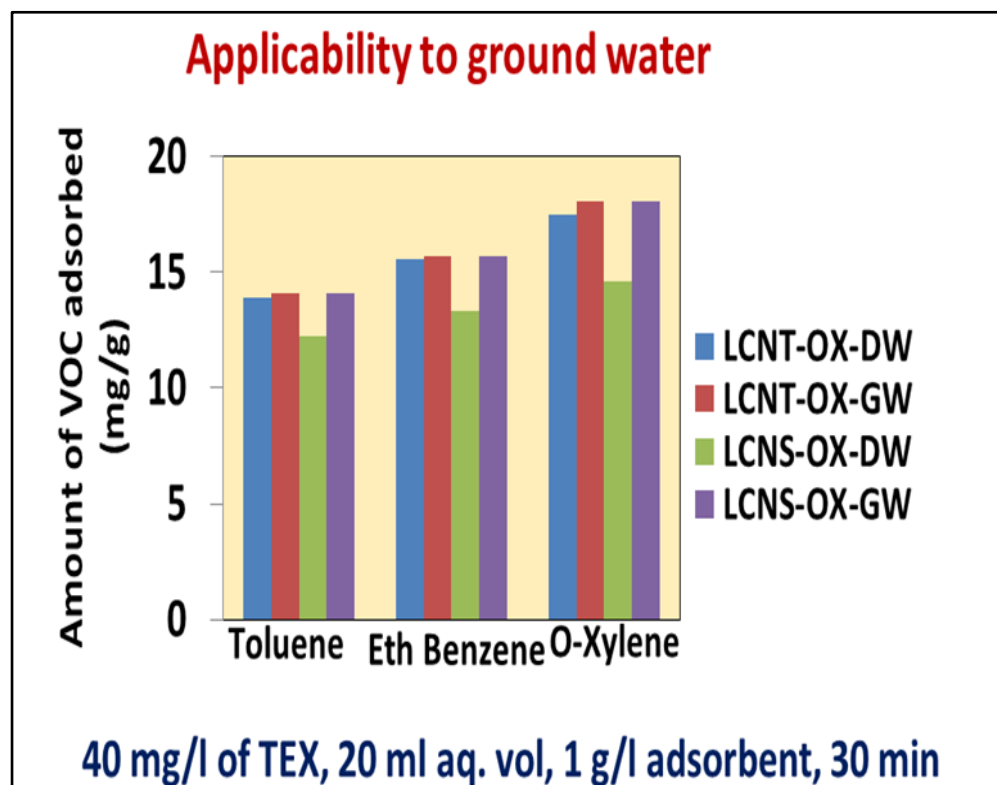


Figure 21 Applicability to Ground water

4.3. TEX Analysis in Air Experiment

4.3.1. Introduction

4.3.2. Characterization of mesoporous carbon microspheres

5.3.2.1. BET Isotherm and BET Isotherm

It is demonstrate that the maximum pore size existed in the range of 4.6 to 4.8 nm in all the samples except LCM. Furthermore average pore diameter ranged from 10.80 to 18.45 nm. According to the Nitrogen adsorption and desorption isotherms of LCM, LCM-Alk, LCNT, LCNT-OX. Fig. 22 and Fig. 23.

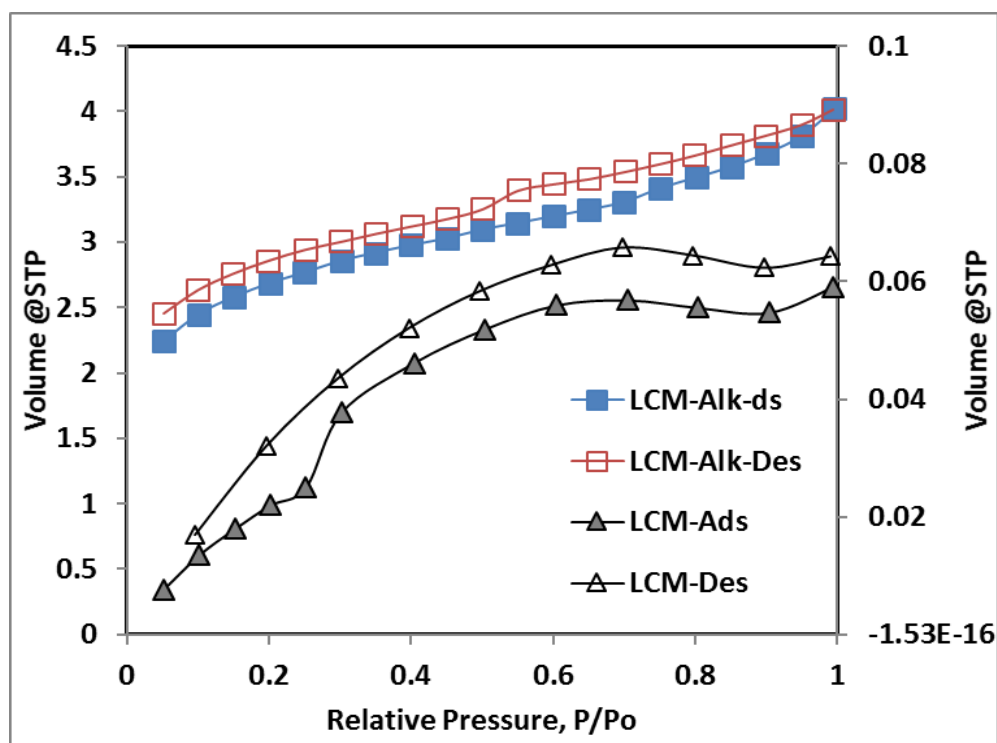


Figure 22 BET Isotherm (a) Adsorption and Desorption

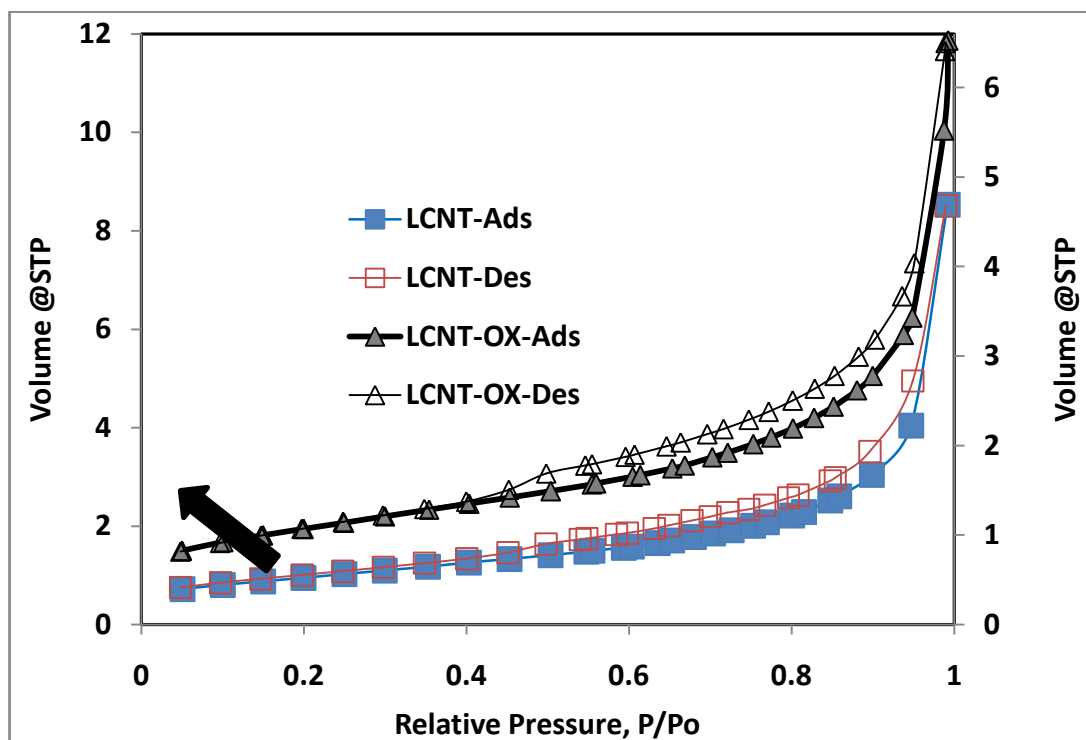


Figure 23 BET Isotherm (b) Adsorption and Desorption

4.3.2.2. Calibration curve for TEX

Calibration graph define the straight lines. It was obtained with a correlation factor (R^2) of 0.999, 0.991, and 0.980 for ethyl benzene, toluene and o-xylene respectively. It is evident that show in Fig 24, 25, and 26.

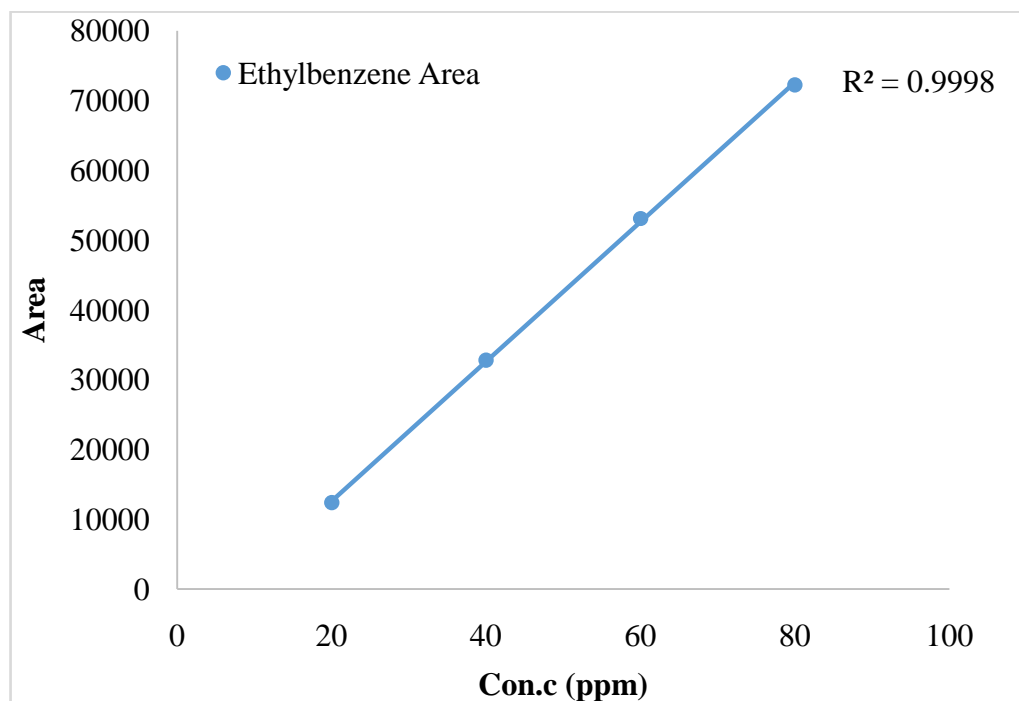


Figure 24 Calibration curve for Ethylbenzene

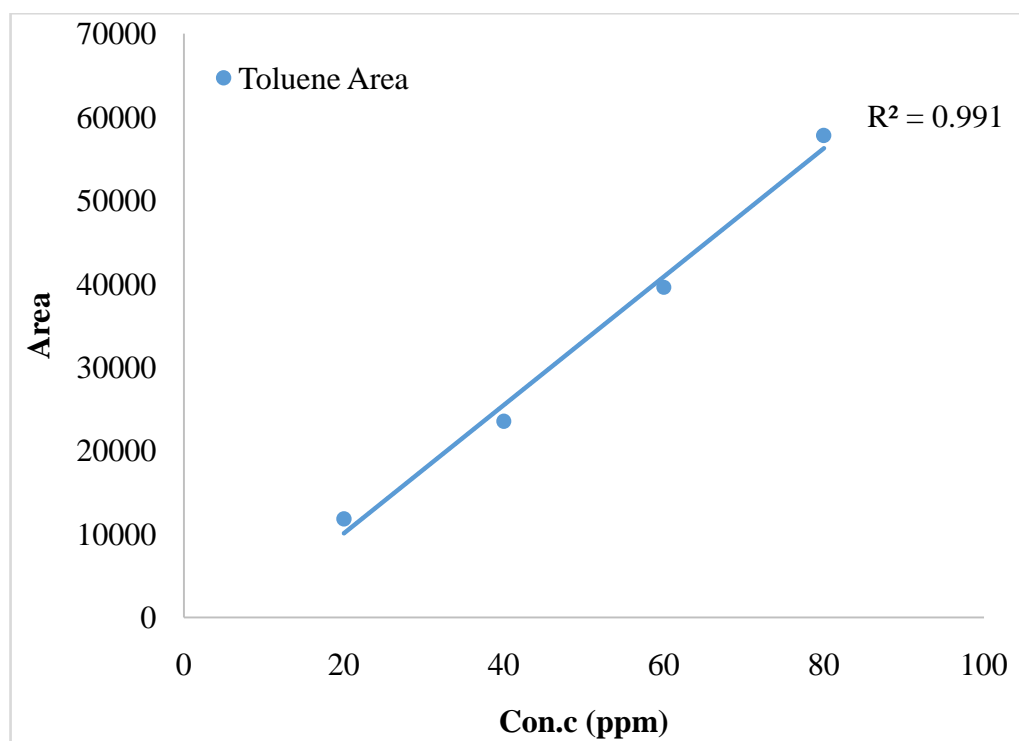


Figure 25 Calibration curve for Toluene

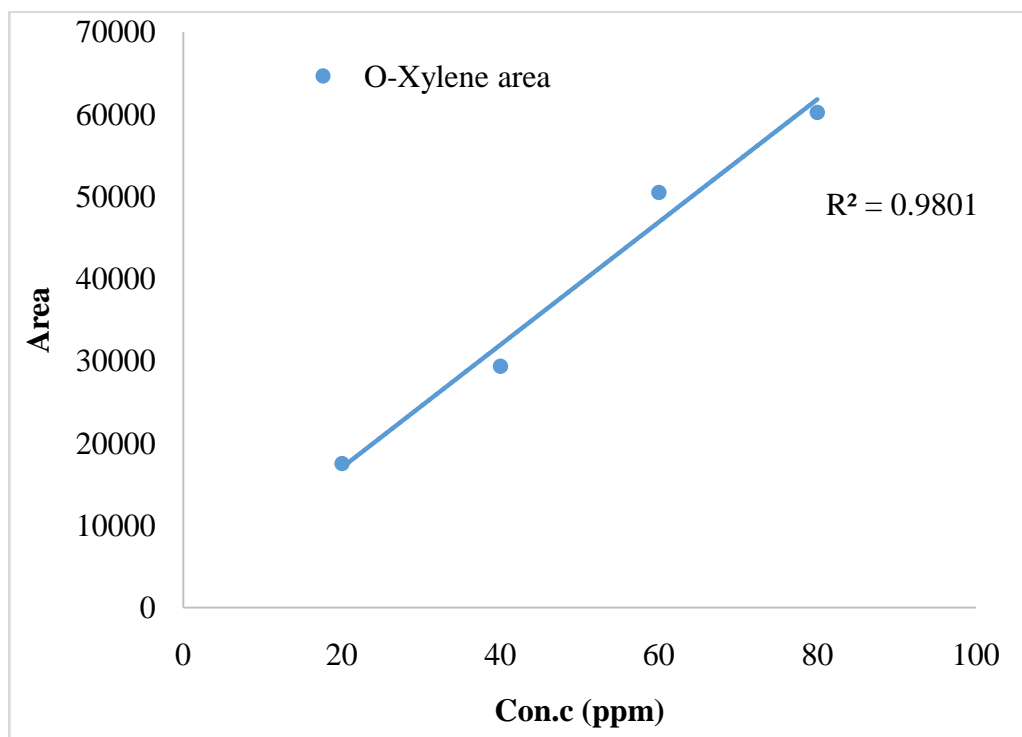


Figure 26 Calibration curve for O-Xylene

4.3.2.3. Breakthrough curves

Table 13 shows that the breakthrough curves define the adsorbent capacity according to carbon composite and also depict the percentage of removal of TEX.

Table 13 Effect of contact time in Breakthrough curves

Adsorbent ^a	VOC	t _e (min)	Uptake (mg/g)	% Removal
CNT-Plain	Ethyl Benzene	36	7.47	38.94
	O-Xylene	40	10.55	49.45
	Toluene	16	4.93	57.76
CNT-OX	Ethyl Benzene	164	58.89	67.33
	O-Xylene	164	66.80	76.39
	Toluene	100	39.85	74.72

CMS	Ethyl Benzene	32	7.86	46.02
	O-Xylene	32	7.09	41.56
	Toluene	20	5.48	51.37

4.3.2.4. Breakthrough curves CMS, CNT-Plain, and CNT-OX with Toluene low concentration:

It is evident fig.(27) that the maximum adsorption capacity CNT-OX and a very few min show the adsorption CNT-plain and CMS.

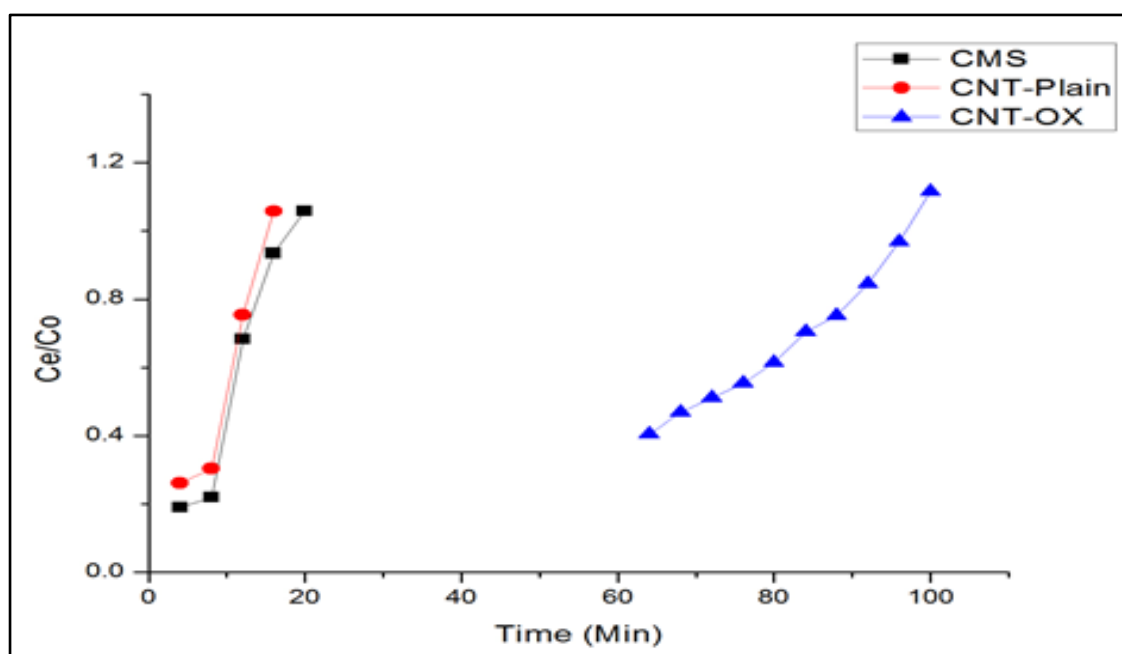


Figure 27 Breakthrough curve of CMS, CNT-Plain, and CNT-OX with Toluene, (100ppm)

4.3.2.5. Breakthrough curves CMS, CNT-Plain, and CNT-OX with Ethylbenzene low concentration:

It is evident fig.(28)that the maximum adsorption capacity CNT-OX and a very few min show the adsorption CNT-plain and CMS.

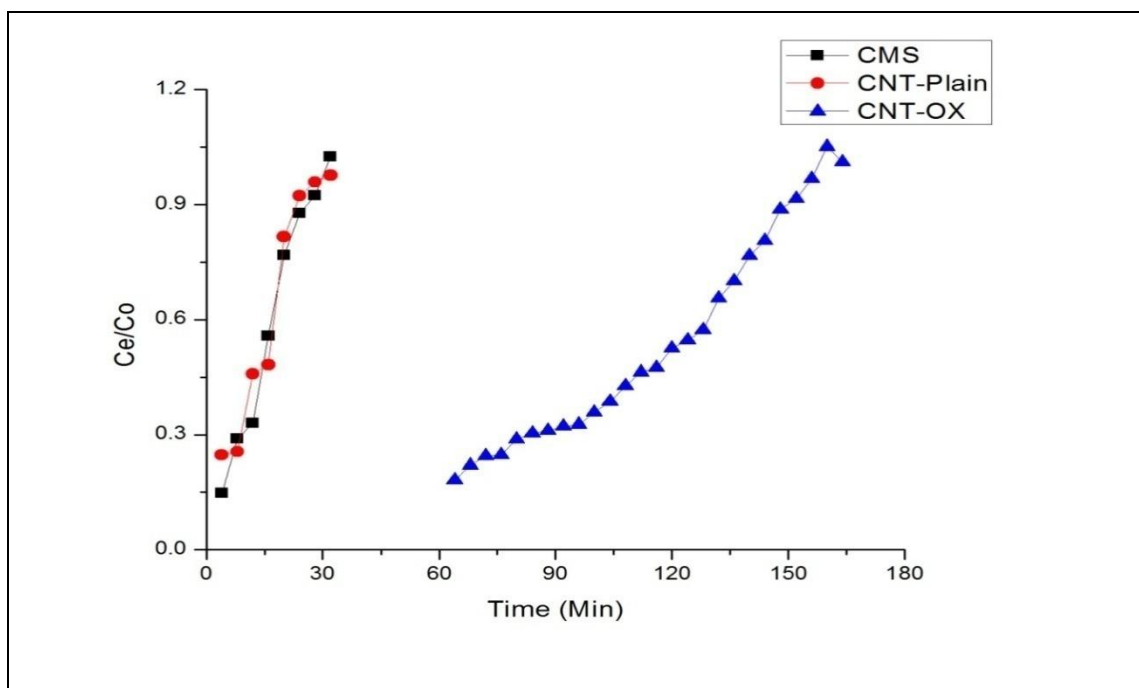


Figure 28 Breakthrough curve of CMS, CNT-Plain, and CNT-OX with (b) Ethylbenzene, (100 ppm)

4.3.2.6. Breakthrough curves CMS, CNT-Plain, and CNT-OX with o-xylene low concentration:

It is evident fig.(29) That the maximum adsorption capacity CNT-OX and a very few min show the adsorption CNT-plain and CMS.

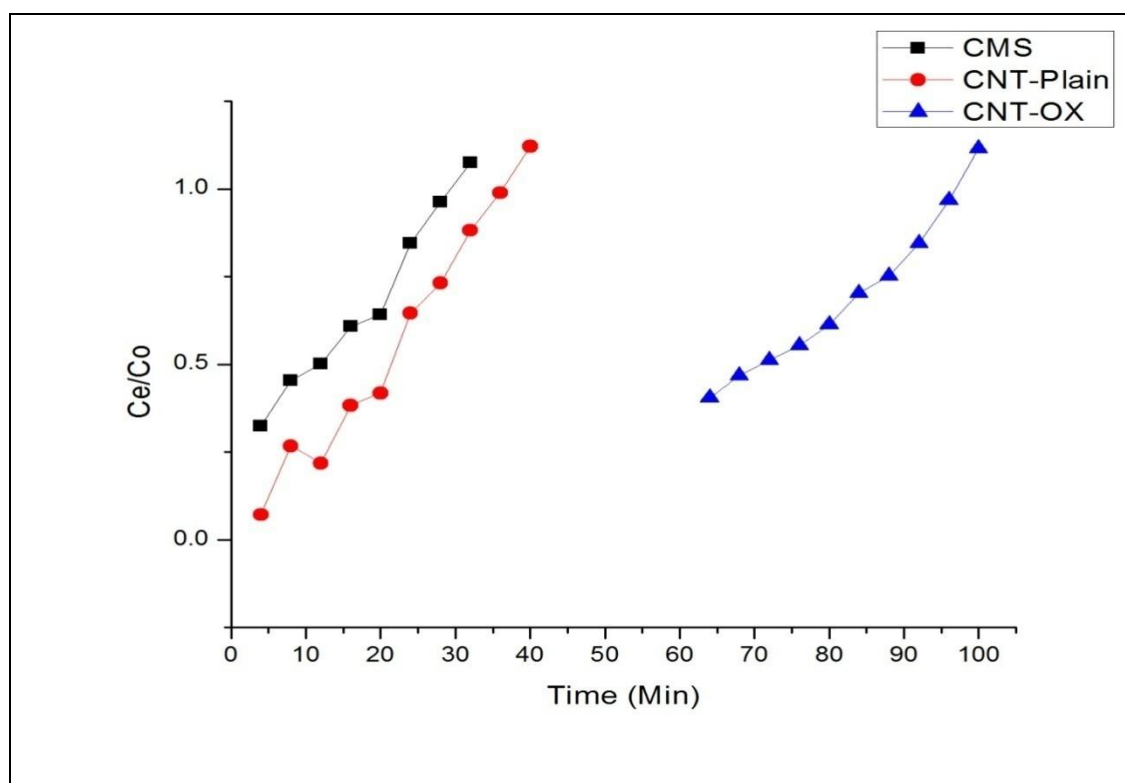


Figure 29 Breakthrough curve of CMS, CNT-Plain, and CNT-OX with (b) O-Xylene, (100 ppm)

4.3.2.7. Breakthrough curves CMS, CNT-Plain, and CNT-OX with toluene medium concentration:

It is evident fig.(30) that the maximum adsorption capacity CNT-OX and a very few min show the adsorption CNT-plain and CMS.

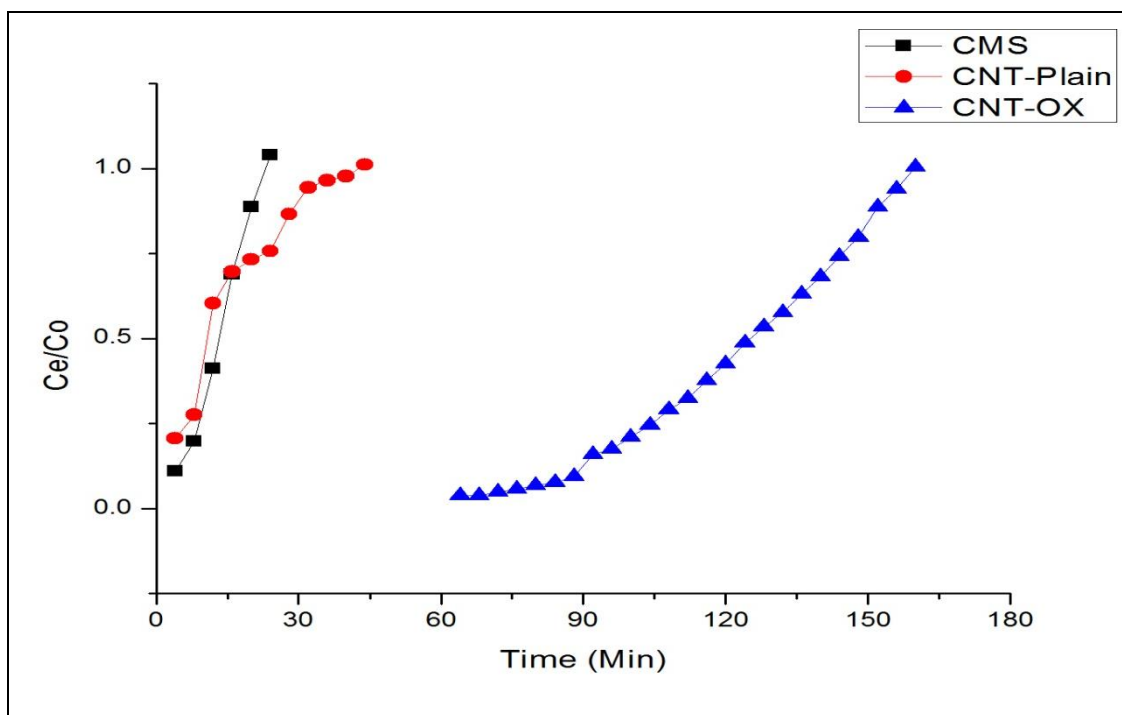
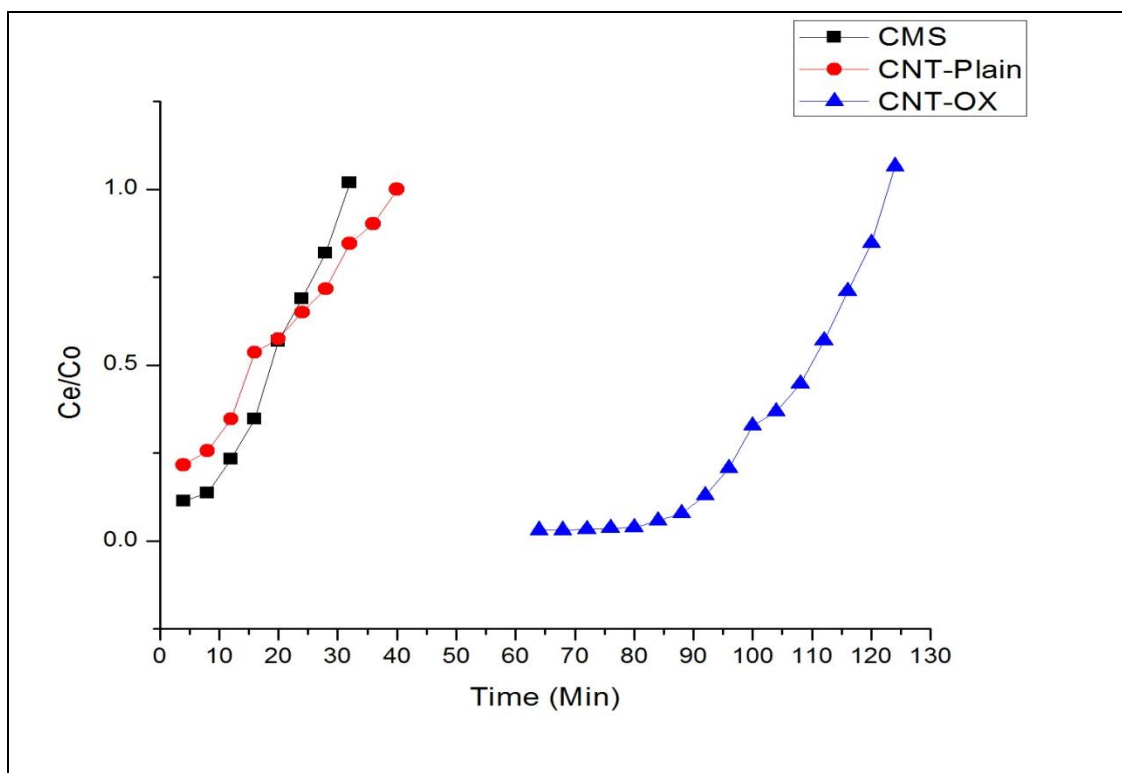


Figure 30 Breakthrough curve of CMS, CNT-Plain, and CNT-OX with (b)

Toluene, (300 ppm)

4.3.2.8. Breakthrough curves CMS, CNT-Plain, and CNT-OX with Ethylbenzene medium concentration:

It is evident fig.(31) that the maximum adsorption capacity CNT-OX and a very few min show the adsorption CNT-plain and CMS.



**Figure 31 Breakthrough curve of CMS, CNT-Plain, and CNT-OX with (b)
Ethylbenzene, (300 ppm)**

4.3.2.9. Breakthrough curves CMS, CNT-Plain, and CNT-OX with 0-xylene medium concentration:

It is evident fig.(32) that the maximum adsorption capacity CNT-OX and a very few min show the adsorption CNT-plain and CMS.

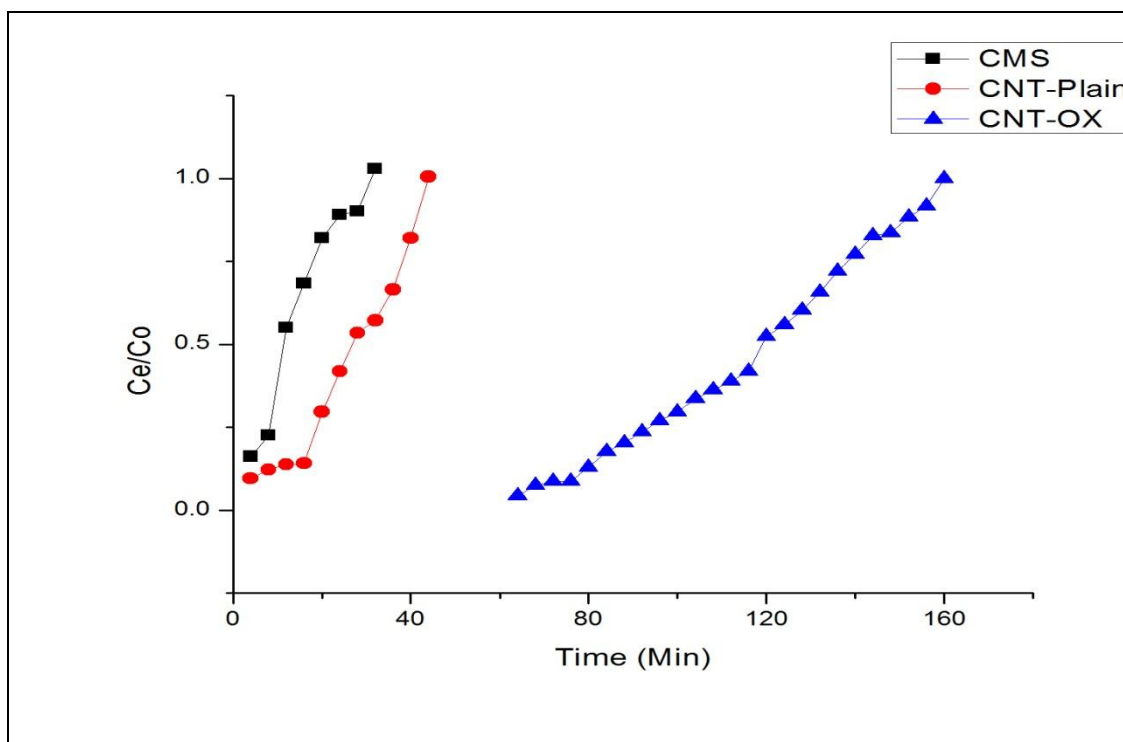


Figure 32 Breakthrough curve of CMS, CNT-Plain, and CNT-OX with (b) O-Xylene, (300 ppm)

4.3.2.10. Breakthrough curves CMS, CNT-Plain, and CNT-OX with toluene high concentration:

It is evident fig.(33) that the maximum adsorption capacity CNT-OX and a very few min show the adsorption CNT-plain and CMS.

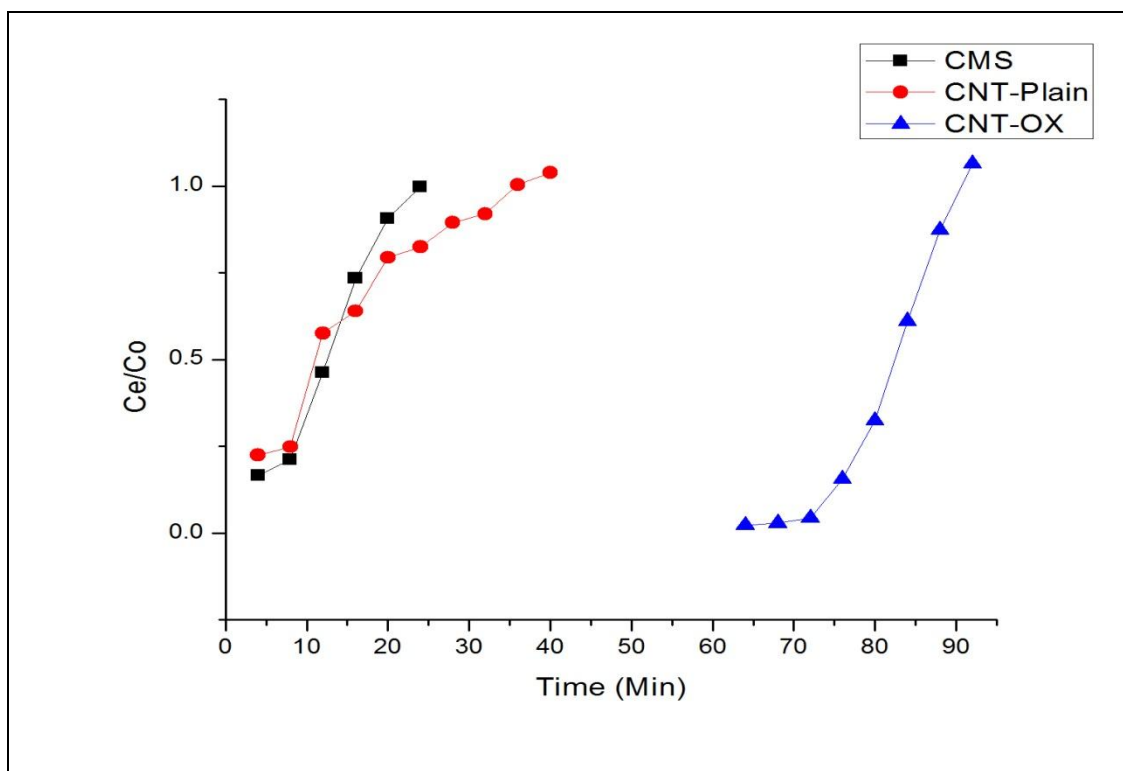


Figure 33 Breakthrough curve of CMS, CNT-Plain, and CNT-OX with (b) Toluene, (700 ppm)

4.3.2.11. Breakthrough curves CMS, CNT-Plain, and CNT-OX with Ethylbenzene high concentration:

It is evident fig.(34) that the maximum adsorption capacity CNT-OX and a very few min show the adsorption CNT-plain and CMS.

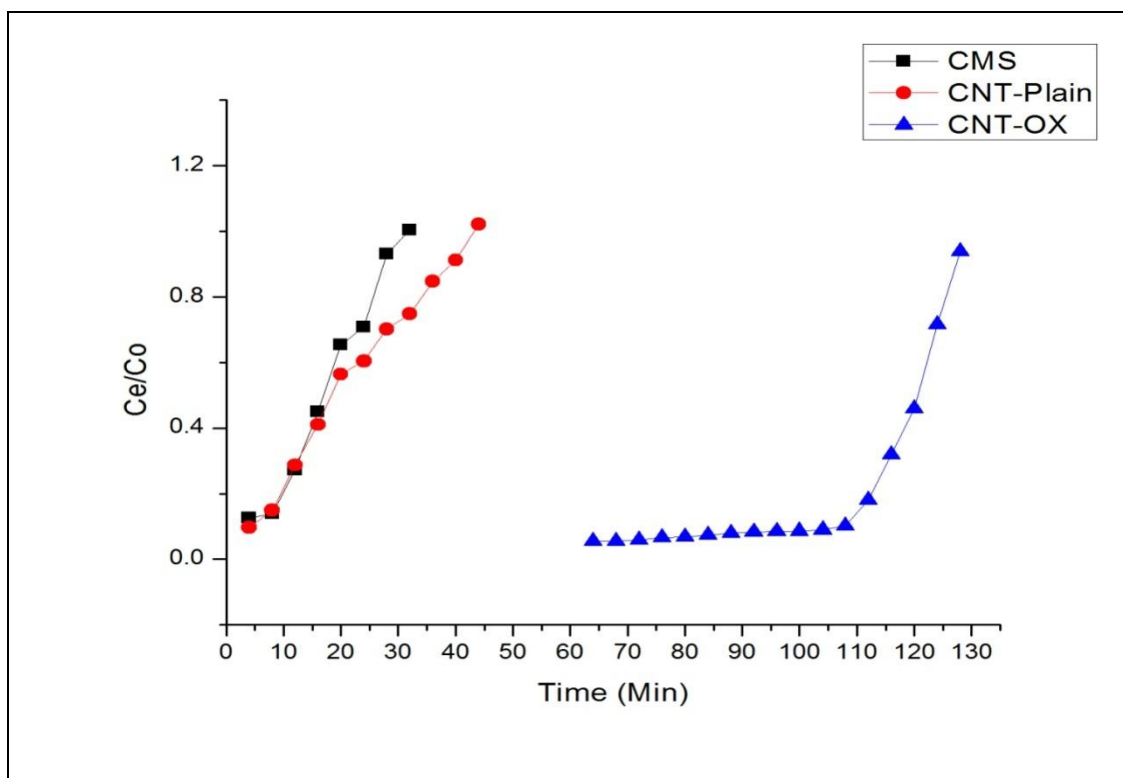


Figure 34 Breakthrough curve of CMS, CNT-Plain, and CNT-OX with (b) Ethylbenzene, (700 ppm)

4.3.2.12. Breakthrough curves CMS, CNT-Plain, and CNT-OX with o-xylene high concentration:

It is evident fig.(35) that the maximum adsorption capacity CNT-OX and a very few min show the adsorption CNT-plain and CMS.

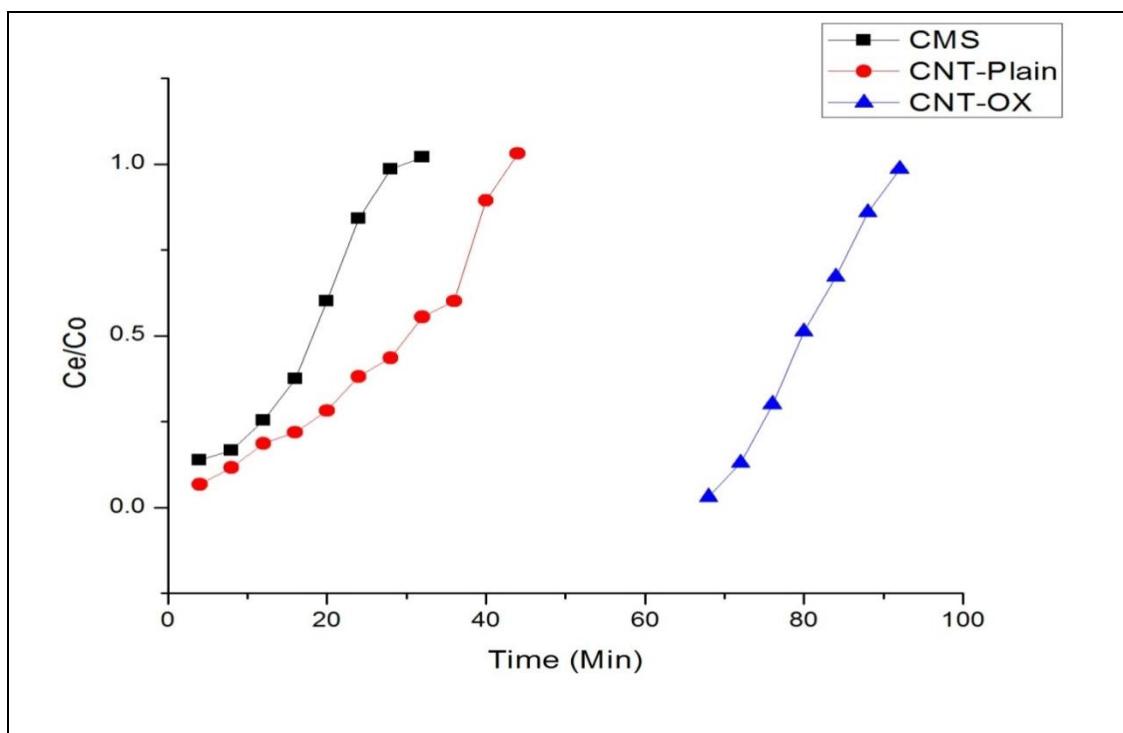


Figure 35 Breakthrough curve of CMS, CNT-Plain, and CNT-OX with (b) O-Xylene, (700 ppm)

Chapter 5

Discussion

CHAPTER - 5

DISCUSSION

5.1. Introduction

Volatile organic compounds namely toluene (T), ethylbenzene (E) and o-xylene (X) are widely used in various industrial processes. Huge amounts of TEX contaminated Waste water is discharged into surrounding water bodies from these industries. TEX are carcinogenic, toxic, and flammable substances, presence of greater amounts of these carcinogenic solvents in water bodies may affect water quality and thus endanger both public health and wellbeing (Purdom, 1980).

Thus it is imperative that cost effective and sustainable wastewater treatment is required for TEX contamination. Conventionally activated carbon is the most widely used adsorbent (Daifullah and Girgis, 2003, Lillo-Rodenas et al. 2005, Wibowo et al. 2007). In recent years carbon nano tubes (CNTs) have been found useful in removing various pollutants owing to their large surface area, greater chemical stability, thermal resistance, unique hollow structure and hydrophobic surface.

Carbon based nanocomposites have been found useful in removing many organic pollutants including volatile organic compounds (Agnihotri et al. 2005, Hsu and Lu, 2007) from air streams, 1,2 dichlorobenzene (Fagan et al. 2004, Chen et al. 2007), xylene (Chin et al. 2007, Su et al. 2010), TEX (Yu et al. 2011, 2016), trihalomethanes (Lu et al. 2005, 2006), triazine based pollutant (Engel and Chefetz, 2017), pharmaceuticals (Shan et al. 2016) etc. from various aqueous solutions.

It is evident from literature that a very few studies have been carried out in the removal of TEX from aqueous solutions using carbon nano composites. Therefore in this study, carbon nanotubes (LCNT) and carbon microspheres (LCM) were prepared indigenously using horizontal floating catalytic chemical vapor deposition technique. A solution containing 2% ferrocene in benzene served as hydrocarbon source.

Use of ferrocene served a dual purpose as the source of hydrocarbon as well as floating catalyst towards growth of nanotubes and microspheres. With slight modification in temperature during its preparation both nanotubes and microspheres were prepared using the same set up. Prepared materials were oxidized with nitric acid to produce LCNT-OX and LCM-OX.

Various carbon composites thus prepared namely, LCNT, LCNT-OX, LCM and LCM-OX were characterized using various spectroscopic techniques including Scanning electron microscopy (SEM), transmission electron microscopy (TEM), Brunauer-Emmett-Teller (BET) Surface Area measurements, X-ray diffraction (XRD), Fourier transform infra red spectroscopy (FTIR), Raman, X-ray photoelectron spectroscopy (XPS) and systematically evaluated for the removal of TEX from both distilled water and ground water. Column studies were conducted to demonstrate the applicability of prepared carbon composite under dynamic conditions. Static adsorption experiments were also carried out to evaluate the uptake capacity of vapour phase of TEX by various prepared carbon composites. The results obtained were compared with the commercially available CNT (P-CNT) acquired from United nanotech, Bangalore, India.

5.2. Characterization of carbon composites

5.2.1. SEM and TEM Analysis

SEM images of LCNT and LCNT-OX is shown Figures 9(a) and (b), respectively. The width of nano tube varied from 20 to 60 nm and length ran to few micrometers. It is evident that after oxidation no appreciable change in surface morphology was observed. Figure 9(c) and 1(d) reveals the TEM images of LCNT where the hollow structure and multiwalled tubular structure is evident. SEM and TEM images of LCM are shown in figures 9(e) and 1(f), respectively. It is evident that the microspheres are agglomerated and it is not hollow inside. The size of microspheres varied from 100 – 300 nm.

5.2.2. BET analysis

The specific surface area of the L-CNT, L-CNT-OX, L-CM, L-CM-OX and P-CNT were obtained over the relative pressure range from 0.05 to 0.35 using the standard BET method. The total pore volume, mesopore, macropore and micropore volumes were calculated using the instrument's software supplied by Quantachome using Barrett–Joyner–Halenda (BJH) and density functional theory (DFT) methods. Table 3 summarizes data for specific surface area (SSA) and pore volume. Salient features are: (a) BET total surface area and total pore volume of LCM samples were smaller than those obtained for LCNT. (b) Smallest BET total surface area and total pore volume were observed for LCM. (c) Contribution of mesopores to the total pore volume was larger than that of the micropores for all carbon composites except LCNT which had a larger contribution from the macropores. It is evident that total

surface area increased after oxidation. Higher surface area obtained after oxidation could be attributed to the opening of pores.

5.2.3. XRD Analysis

The XRD diffraction patterns of carbon composites are shown in Fig 10 and 11. Most intense peak at $2\theta = 26.4$ was observed in the diffraction spectra of both LCNT and LCM which is due to the (002) reflection of sp^2 carbon of carbon composites (Sankararamakrishnan et al. 2016). Additionally, diffraction peaks at 43.5 (400) corresponding to γ Fe_2O_3 or Fe_3O_4 phase (matched with JCPDS Card No. (79 - 0417) was also observed. Iron oxide arises due to the use of ferrocene during composite preparation.

5.2.4. FTIR analysis

FT-IR spectra of LCNT, LCNT-OX and LCM and LCM-OX are shown in Fig. 12. For all four samples, the peaks around 1610 cm^{-1} could be assigned to the C=C stretching vibration. Further, absorption bands at 2847 cm^{-1} and 2921 cm^{-1} could be attributed to symmetric and asymmetric stretching vibrations of $-CH_2$ which could be due to the presence of amorphous carbon. Oxidized carbon composites (LCNT-OX and LCM-OX), exhibited the peaks around 1720 cm^{-1} which arises from the asymmetric C=O stretching band (Ntim and Mitra, 2011).

Anchoring of functional groups in LCM-OX is evidenced by the appearance of bands at 1610 and 1536 cm^{-1} corresponding to C=O group and carboxylate anion stretching respectively. Similarly oxidized LCNT exhibited vibrations of C=O and caboxylate groups at 1634 and 1586 cm^{-1} respectively (Daifullahand Girgis, 2003,

Davis et al. 1999). All the samples exhibited alkoxy C-O band at 1030 cm^{-1} (Ovejero et al. 2006). Intramolecular hydrogen bonding arising due to the presence of -OH groups are observed at 3430 cm^{-1} and OH bending vibration is also observed at 1375 cm^{-1} in all the samples.

5.2.5. Raman Analysis

Figure 13 shows the Raman spectra of LCM, LCM-OX, LCNT and LCNT-OX. It is evident from the spectra that two sharp and intense peaks $\sim 1300\text{ cm}^{-1}$ and $\sim 1550\text{ cm}^{-1}$ are observed which corresponds to D- band and G-bands respectively. D-band arises due to the imperfections/ disorderliness in carbon framework which could be attributed to impurities, vacancies, symmetry breaking defects etc. G band is related to in plane tangential stretching of C-C bond of Sp^2 hybridized carbon atoms of the carbon composites. The ratio of the intensity of D band to G band (I_D/I_G) depicts the extent of defects in the carbon frame work (Saito et al. 2011). In the present case, the ratio increased in both the oxidized form (LCNT-OX and LCM-OX) compared to plain forms (Table 4) indicating the presence of defects on oxidized composites surfaces, which introduced more oxygen containing functional groups like carbonyl, carboxyl, hydroxyl as shown in FTIR and XPS spectra.

5.2.6. XPS Analysis

Figure 14 shows the XPS survey spectra of LCNT, LCNT-OX, LCM and LCM-OX. The major peak which is C 1s peaks arises due the graphitic carbon present in carbon composites. It is evident from the spectra that after oxidation with nitric acid, intense peaks corresponding to O1s appeared and it was also evident that atomic percentage of oxygen increased from 4.3 to 26.5%. Which confirm the

introduction of various functional groups like hydroxyl, carbonyl and carboxyl groups.

5.2.6.1. Studies on (TEX) removal

5.2.6.2. Effect of initial pH

Effect of initial pH on the sorption behavior of TEX by LCNT is shown in Fig 13 . Sorption of TEX is almost constant irrespective of initial pH (Fig.15). This confirms the possibility that molecular forms of TEX are adsorbed and sorption of TEX by ion exchange plays an insignificant. This observation is similar to the earlier reports where sorption of TEX (Su et al. 2010) and xylene (Chin et al. 2007) was found constant in the pH range of 3 to 10 by MWCNT and SWCNT respectively. Experiments with other prepared carbon composites including LCNT-OX, LCM, LCM-OX, CNT-P revealed similar results with respect to initial pH (Figure not shown).

5.2.6.3. Effect of kinetics

Adsorption kinetic plays a significant role in the solute uptake and also represents the sorption efficiency of the sorbent. Figure 16(a-c) reveals the rate of sorption of TEX with various sorbents. It is observed that sorption is very fast and equilibrium is attained within 20 min with all the carbon composites prepared. It is to be noted that oxidized forms of LCNT and LCM attains equilibrium within 15 min.

This is one of the major advantage of these adsorbents compared to the one reported in literature. Study of Yu et al. (2011) illustrated that 60 min was essential for reaching equilibrium of TEX with CNTs and Su et al. (2010) reported 120 min for

CNT (NaOCl) to reach equilibrium. The kinetic data was modelled by Pseudo First order and Pseudo second order model given in equations 1 and 2 respectively.

$$\log(q_e - q_t) = \log q_e - \frac{k_1}{2.303} t \quad (1)$$

$$\frac{t}{q_t} = \frac{1}{k_2' q_e^2} + \frac{t}{q_e} \quad (2)$$

Equation (1) is commonly referred as Lagergren model (Lagregren, 1898), where q_t (mg/g) represents the adsorption of the TEX at time t , q_e (mg/g) is the adsorption capacity at equilibrium, t (min) is the exposure time and k_1 (min^{-1}) is the pseudo first order rate constant. Equation (2) represents pseudo second order where the adsorption rate is directly proportional to the square of the number of unoccupied sites and used to analyze the chemisorption kinetics from liquid solutions (Ho, 2006). In eqn (2), k_2' ($\text{g mg}^{-1} \text{min}^{-1}$) is the pseudo second order rate constant of adsorption. The kinetic parameters evaluated for these two models for TEX is shown in Table 3. It is to be observed that all the adsorbents namely LCNT, LCNT-OX, LCM and LCM –OX followed pseudo second order kinetics with regression coefficients greater than 0.99. Thus, it could be concluded that adsorption of TEX upon various carbon composites prepared is governed by chemical interactions.

Adsorption of TEX upon prepared adsorbents could involve surface diffusion (where TEX is transported from the aqueous solution to the surface of the carbon composites) or intraparticle/pore diffusion (where TEX molecules move into the carbon composites interior pores). The intraparticle diffusion model by Weber-Morris has been used to determine whether the rate determining step is caused by intraparticle diffusion or surface diffusion (Wu et al., 2009). Thus, the obtained

kinetic data was modelled using Web-Morris intraparticle diffusion model given in eqn(3).

$$q_t = k_{\text{int}} \sqrt{t} + C \quad (3)$$

Where k_{int} represents the intraparticle diffusion rate constant ($\text{mg g}^{-1} \text{min}^{0.5}$) and C represents the intercept. According to Web Morris model, a plot of amount adsorbed at a given time (q_t) versus $t^{0.5}$ should be linear plot without intercept if intraparticle diffusion is the sole process governing the rate determining step and a linear plot with intercept confirms that one of the process in adsorption process is intraparticle diffusion. Thus, a plot of amount of TEX adsorbed over prepared adsorbents yielded a straight line with an intercept C which gives the information about the thickness of the boundary layer. The constants obtained using this model is detailed in Table 5. Thus, results indicate apart from diffusion mechanism other boundary layer mechanisms could also be present in the adsorption of TEX onto prepared composites.

5.2.6.4. Adsorption Isotherm

Adsorption isotherm experiments were conducted on TEX using LCNT, LCNT-OX, LCM, LCM-OX and P-CNT. Concentration range between 0 to 100 ppm was studied and higher concentrations were not simulated due to low solubility of VOCs in water. The equilibrium adsorption isotherm obtained for various VOCs are shown in Figs.17 (a) – (c).

Further data obtained was modelled with linearised Langmuir and Freundlich isotherm shown in equations 4 and 5, respectively.

$$\frac{1}{q_e} = \frac{1}{q_{\max}} + \frac{1}{C_e q_{\max} \cdot b} \quad (4)$$

$$\log q_e = \log K_f + \frac{1}{n} \log C_e \quad (5)$$

Where q_e (mg/g) is amount of TEX adsorbed per unit mass of carbon composite and C_e (mg/l) is concentration of TEX at equilibrium. q_{\max} is maximum amount of TEX per unit mass of carbon composite to form a complete monolayer on surface of sorbent and b is Langmuir constant (L/mg). K_f (mg/g) and n are constants representing Freundlich adsorption capacity and intensity of TEX sorption.

Langmuir model is postulated on the assumption that monolayer adsorption occurs on a homogenous sorbent surface and a limited amount of sorbent sites are available for sorption is postulated by Langmuir isotherm model. Furthermore, Langmuir model also predicts that there exists a negligible interaction between adsorbed solute molecules. Freundlich isotherm model works on the assumption that TEX adsorbs on heterogeneous surface of prepared carbon composites.

Equilibrium data obtained was modelled by both Langmuir and Freundlich isotherm. It was observed that only O-Xylene followed Langmuir model (Fig 16 (a) – (c); Table 6 - 8) with regression coefficients > 0.95 , however, toluene and ethyl benzene did not followed this model.

The order of sorption capacity of adsorbents followed the order: CNT-OX $>$ P-CNT $>$ L-CNT, LCM-OX $>$ LCM. Higher adsorption capacity of CNT-OX could be attributed to larger surface area and presence of various functional groups like carboxyl, hydroxyl and carbonyl groups. A very few reports are available in

literature on removal of xylene from aqueous phase using modified CNTs. A comparison of the prepared adsorbents with those reported in literature is depicted in Table 9.

It is evident from table 9 that earlier reports have reported higher sorption capacity for instance Yu et al, (2011) reported a capacity of 112.19 mg/g for m-xylene and nitric acid modified SWCNT has been evaluated for removal of p-xylene (Chin et al. 2007) with an adsorption capacity of 85.5 mg/g. Though the sorbent prepared in this study exhibited a slightly lower capacity, it is noteworthy that sorption kinetics was very fast and equilibration was attained within 20 min as compared to 24h and 10 h as reported in earlier reports.

5.2.6.5. Static Adsorption Test and mechanism of adsorption

Adsorption capacity depends on various factors including surface area, porosity, and presence of functional groups as well as chemical properties of TEX. Static adsorption tests for TEX were conducted with all five adsorbents namely LCNT, LCNT-OX, LCM, LCM-OX and PCNT and results obtained are shown in Table 10.

It is evident from table that LCNT-OX exhibited highest sorption capacity for TEX though surface area of P-CNT ($199.01 \text{ m}^2/\text{g}$) was higher than LCNT-OX ($121.68 \text{ m}^2/\text{g}$). This could be attributed to presence of functional groups like hydroxyl and carboxyl groups introduced during oxidation. Further it is observed that sorption capacity follows the order o-xylene > ethyl benzene > toluene. In addition, even though LCM-OX surface area ($12.7 \text{ m}^2/\text{g}$) is much lower than LCNT and

PCNT, its adsorption capacity towards TEX is comparable with LCNT and PCNT (Table 7).

Furthermore, it is clear from Table 7 that oxidized forms of carbon composites performed better sorption of TEX as compared with the as prepared composites. This could be attributed to electron donor acceptor mechanism involving $\pi - \pi$ interaction. In this case, oxygen atom of various functional groups like carboxyl, carbonyl and hydroxyl acts as electron donor and TEX molecules aromatic ring acts as electron acceptor.

Similar mechanisms have been postulated in literature with CNT (NaOCl) (Su et al. 2010) and powdered activated carbon (Daifullah and Girgis, 2003). Additionally, there also exists an electrostatic attraction between TEX molecules and CNT surface. It is reported that TEX molecules exhibit weak positive charge in the pH range of 3 to 12 (Chen et al. 2007). Hence, adsorption of TEX is more favored with oxidized LCNT and LCM as they possess higher electronegative surface charge due to presence of surface oxygen atoms which results in strong electrostatic attraction leading to higher sorption of TEX. Higher sorption of O-Xylene compared to Toluene can be attributed to lower solubility in water (T 515 mg/L > O-X, 180 mg/L) resulting due to its higher hydrophobicity.

5.2.6.6. Column Studies

Dynamic equilibration studies were conducted using a column reactor in an upflow mode. The flow rate was maintained at 3ml/min. Performance of packed column reactor is described through the breakthrough curves obtained for that particular set up. Breakthrough curve is normally depicted in terms of either effluent

VOC concentration (C_e) or the ratio of effluent VOC concentration to inlet VOC concentration (C_e/C_o) as a function of flow time (t) or volume of effluent (V_{eff}) or bed volumes (BV) for a particular bed height. Effluent volume (V_{eff}) calculated from Eq. (6):

$$V_{eff} = F \cdot t_{total} \quad (6)$$

Where F and t_{total} are the volumetric flow rate and total flow time respectively.

The quantity of VOC retained in the packed column reactor is represented by area above breakthrough curve (C_{eff} Vs t), which is obtained through numerical integration. The uptake capacity (Q) of carbon composite is obtained by dividing VOC mass adsorbed (VOC_{ad}) by carbon composite mass (M).

Amount of VOC sent to packed column reactor (VOC_{total}) can be obtained from Eq. (7):

$$VOC_{total} = C_o \cdot F \cdot t_e \quad (7)$$

Where, t_e is bed exhaustion time (t_e , time at which C_{eff} exceeded 9.7 mg/ L)

Finally, VOC percent removal can be obtained from the following from Eqn.

$$Total\ VOC\ Percent\ removal(\%) = \frac{VOC_{ad}}{VOC_{total}} \times 100 \quad (8)$$

The breakthrough curve of toluene using lab CNT is shown in Fig 10.

It is evident (Fig. 19) that around 50 bed volumes of (950 ml) 30 ppm toluene containing water could be treated reducing concentration from 30 ppm to below

detection limit using 3g of LCNT. Furthermore, amount of toluene adsorbed was found to be 40.19 mg/g and 71.2% of Toluene was removed from aqueous solution using 3mg of adsorbent with a flow rate 3ml/min. Thus, it is evident that CNTs could be used as micro trapping devices or solid phase extraction cartridges for concentrating VOC.

5.2.6.7. Recyclability Studies

Recyclability tests were conducted for LCNT-OX and LCM-OX using 60 ppm of TEX as analytes. After adsorption, adsorbent was filtered and heated in oven at 100 °C for 60 min and subsequently adsorbents were used for adsorption. This process was repeated for 5 cycles and results obtained are shown in Table 11 and Fig. 20. It is evident from the data that there was no appreciable change in sorption behavior even after 5 cycles which proves recyclability of sorbent.

5.2.6.8. Applicability in ground water matrix

To test applicability of adsorbents in ground water, similar to distilled water, adsorption experiments were conducted with LCNT-OX and LCM-OX in TEX spiked ground water. Groundwater was acquired from IIT Kanpur. Characteristics of water included: pH 7.7, total dissolved solids 608 mg/l, hardness 140 mg/l, alkalinity 280 mg/l, chloride 160 mg/l, sulfate 34.9 mg/l and iron 0.12 mg/l. Acquired ground water was spiked with 40 ppm of TEX and equilibrated with 0.02 g of LCNT-OX and LCM-OX for 30 min and the amount adsorbed was evaluated using GC. Results obtained are shown in Table 12 and Fig. 21. It is evident from the data amount of TEX adsorbed remained more or less same in both distilled water and ground water. Hence, adsorbent can find applicability in TEX contaminated aqueous streams.

DW-(Distilled Water)

GW-(Ground Water)

5.3. TEX Analysis in Air

5.3.1. Introduction

During the past two decades, volatile organic compounds (VOCs), are one of the major source of air pollution, have widely attracted legislators and scientists. VOCs are a sub-branch of anthropogenic or biogenic compounds and categorized as hazardous air pollutant materials. VOCs can not only cause serious harm to human health and irreversible defects during long-lasting exposure, but also can deplete ozone layer and lead to greenhouse effect. Thus, VOCs removal from both indoor and outdoor environment has become indispensable.

For abatement of VOCs from atmosphere, various removal technologies have been developed, including membrane separation (Zhang, L. and Weng et al.,2002) condensation, (Patoulis, D., and Fountoukis, C. et al., 2015) catalytic oxidation, (Kamal, M. S. and Razzak, S. A. et al., 2016) absorption (Rahbar, M. S., & Kaghazchi, T. et al., 2005). photocatalytic reaction (Cao, J., & Lee, S. et al., 2016). and adsorption. (Gaur, V., & Verma, N. et al.,2004). Although each technique has its own advantage and disadvantage, adsorption has been considered as the most energy efficient, economical, and versatile and sustainable technique. Though various commercial adsorbents, including zeolites, (Chung, T. W., & Wu, H. et al., 2004). Silica gels and activated carbons, have been widely used for adsorptive removal of VOCs.

However, these adsorbents suffer from high energy demand, low regeneration efficiency and poor adsorption capacity. Hence, in recent years, a great amount of research is focused on novel carbon-based adsorbents like grapheme, (Ahn, H., & Kim, D. J. et al., 2015). Porous carbon materials (Nichols, M. et al., 2013). , multi-walled nanotube (Saridara, C., & Mitra, S. et al., 2010) metal organic framework (ref) and biochar, (Zhang, X., Gao, et al., 2017) in search of better alternative to commercial adsorbents. Furthermore, mesoporous materials are preferred over microporous carbon materials owing to clogging of micropores by competitive sorption of water vapor molecules along with VOCs leading to decreased adsorption performace (Zhao, X. S., Ma, Q., & Lu, G. Q. 1998). It is also well known that a mesoporous material possesses good mass transfer ability of pollutant molecules compared micropores (Qi et al, CEJ, 2017).

Thus in this work efforts were made to synthesize mesoporous carbon microspheres (LCNS) and nano tubes (LCNT) in floating catalytic chemical vapor deposition method using ferrocene in benzene as the hydrocarbon source. Both LCM and LCNT were synthesized using the same set up by altering the temperature of the horizontal furnace. Further, to increase the surface area, chemical activation was carried out using nitric acid and potassium hydroxide. The prepared materials were characterized and applied for the removal of VOCs in air using horizontal reactor.

5.3.2. Characterization of mesoporous carbon microspheres

5.3.2.1. BET Isotherm and BET Isotherm

The Nitrogen adsorption and desorption isotherms of LCM, LCM-Alk, LCNT, LCNT-OX are presented in Fig.22 and 23 respectively. The isotherms are

Type-IV which is characteristic of mesoporous material. The hysteresis loop of LCM-Alk is Type –H1 which confirms uniform and regular pore structure. However, the hysteresis loop of LCM, LCNT and LCNT-OX is Type –H3 combining the pore diameter distribution (Fig 1), which indicates that the sizes are not uniform and its channels are narrow, and the shapes are irregular. It is also evident from the Fig.22 and 23 that maximum pore size existed in the range of 4.6 to 4.8 nm in all the samples except LCM. Furthermore average pore diameter ranged from 10.80 to 18.45 nm.

5.3.2.2. Calibration curve for TEX

Different TEX solutions with different concentration were prepared. The samples were analyzed using Gas Chromatography. Calibration curve were constructed by plotting the value of area under the Area Vs. concentration of standard TEX as shown in Fig. (24 -26). A straight lines was obtained with a correlation factor (R^2) of 0.999, 0.991, and 0.980 for ethyl benzene, toluene and o-xylene respectively.

5.3.2.3. Breakthrough curves

The equilibrium dynamic adsorption capacity of the carbon composite was evaluated from the breakthrough curves. The experiments were repeated for three different initial concentrations of 100, 300 and 700 ppm of TEX using CNT-Plain, CNT-OX and CMS as adsorbents.

5.3.2.4. Breakthrough curves CMS, CNT-Plain, and CNT-OX with Toluene low concentration:

The effect of contact time on the adsorption of Toluene by CMS, CNT-Plain, and CNT-OX and there was studied in the range of 4-100 min. The results are shown in Fig. (27) The Figure shows that Toluene adsorption has been slowly increased then the adsorption capacity increases rapidly until it reached equilibrium. The experiments were carried out for VOC inlet concentrations: 100 ppm. For each run, 3 g adsorbent was taken. The bed temperature was set at the optimum temperature of 25° C and the flow rate at 16ml/min. Fig. 27 describes the experimentally obtained breakthrough curves for toluene under the VOC gas inlet concentrations for CMS, CNT-Plain and CNT-OX. As observed from Fig. 27, the breakthrough times are less than 20 min for CMS and CNT-Plain, and for CNT-OX equilibrium time 100 min.

5.3.2.5. Breakthrough curves CMS, CNT-Plain, and CNT-OX with Ethylbenzene low concentration:

The effect of contact time on the adsorption of Ethylbenzene by CMS, CNT-Plain, and CNT-OX and there was studied in the range of 4-164 min. The results are shown in Fig. (28) The Figure shows that Ethylbenzene adsorption has been slowly increased then the adsorption capacity increases rapidly until it reached equilibrium. The experiments were carried out for VOC inlet concentrations: 100 ppm. For each run, 3 g adsorbent was taken. The bed temperature was set at the optimum temperature of 25o C and the flow rate at 16ml/min. Fig. 28 describes the experimentally obtained breakthrough curves for Ethylbenzene under the VOC gas inlet concentrations for CMS, CNT-Plain and CNT-OX. As observed from Fig. 28, the breakthrough times are less than 32 min for CMS and CNT-Plain, and for CNT-OX equilibrium time 164 min.

5.3.2.6. Breakthrough curves CMS, CNT-Plain, and CNT-OX with o-xylene low concentration:

The effect of contact time on the adsorption of o-xylene by CMS, CNT-Plain, and CNT-OX and there was studied in the range of 4-100 min. The results are shown in Fig. (29) The Figure shows that o-xylene adsorption has been slowly increased then the adsorption capacity increases rapidly until it reached equilibrium. The experiments were carried out for VOC inlet concentrations: 100 ppm. For each run, 3 g adsorbent was taken. The bed temperature was set at the optimum temperature of 25° C and the flow rate at 16ml/min. Fig. 29 describes the experimentally obtained breakthrough curves for o-xylene under the VOC gas inlet concentrations for CMS, CNT-Plain and CNT-OX. As observed from Fig. 29, the breakthrough times are less than 40 min for CMS and CNT-Plain, and for CNT-OX equilibrium time 100 min.

5.3.2.7. Breakthrough curves CMS, CNT-Plain, and CNT-OX with toluene medium concentration:

The effect of contact time on the adsorption of Toluene by CMS, CNT-Plain, and CNT-OX and there was studied in the range of 4-160 min. The results are shown in Fig. (30) The Figure shows that Toluene adsorption has been slowly increased then the adsorption capacity increases rapidly until it reached equilibrium. The experiments were carried out for VOC inlet concentrations: 300 ppm. For each run, 3 g adsorbent was taken. The bed temperature was set at the optimum temperature of 25o C and the flow rate at 16ml/min. Fig. 30 describes the experimentally obtained breakthrough curves for toluene under the VOC gas inlet concentrations for CMS, CNT-Plain and CNT-OX. As observed from Fig. 30, the breakthrough times are less

than 40 min for CMS and CNT-Plain, and for CNT-OX equilibrium time 160 min.

5.3.2.8. Breakthrough curves CMS, CNT-Plain, and CNT-OX with Ethylbenzene medium concentration:

The effect of contact time on the adsorption of ethylbenzene by CMS, CNT-Plain, and CNT-OX and there was studied in the range of 4-124 min. The results are shown in Fig. (31) The Figure shows that ethylbenzene adsorption has been slowly increased then the adsorption capacity increases rapidly until it reached equilibrium. The experiments were carried out for VOC inlet concentrations: 300 ppm. For each run, 3 g adsorbent was taken. The bed temperature was set at the optimum temperature of 25o C and the flow rate at 16ml/min. Fig. 31 describes the experimentally obtained breakthrough curves for ethylbenzene under the VOC gas inlet concentrations for CMS, CNT-Plain and CNT-OX . As observed from Fig. 31, the breakthrough times are less than 40 min for CMS and CNT-Plain, and for CNT-OX equilibrium time 124 min.

5.3.2.9. Breakthrough curves CMS, CNT-Plain, and CNT-OX with 0-xylene medium concentration:

The effect of contact time on the adsorption of 0-xylene Toluene by CMS, CNT-Plain, and CNT-OX and there was studied in the range of 4-160 min. The results are shown in Fig. (32) The Figure shows that 0-xylene Toluene adsorption has been slowly increased then the adsorption capacity increases rapidly until it reached equilibrium. The experiments were carried out for VOC inlet concentrations: 300 ppm. For each run, 3 g adsorbent was taken. The bed temperature was set at the optimum temperature of 25o C and the flow rate at 16ml/min. Fig. 32 describes the

experimentally obtained breakthrough curves for 0-xylene toluene under the VOC gas inlet concentrations for CMS, CNT-Plain and CNT-0X . As observed from Fig. 32, the breakthrough times are less than 40 min for CMS and CNT-Plain, and for CNT-0X equilibrium time 160 min.

5.3.2.10. Breakthrough curves CMS, CNT-Plain, and CNT-0X with toluene high concentration:

The effect of contact time on the adsorption of Toluene by CMS, CNT-Plain, and CNT-0X and there was studied in the range of 4 - 92 min. The results are shown in Fig. (33) The Figure shows that Toluene adsorption has been slowly increased then the adsorption capacity increases rapidly until it reached equilibrium. The experiments were carried out for VOC inlet concentrations: 700 ppm. For each run, 3 g adsorbent was taken. The bed temperature was set at the optimum temperature of 25o C and the flow rate at 16ml/min. Fig. 33 describes the experimentally obtained breakthrough curves for toluene under the VOC gas inlet concentrations for CMS, CNT-Plain and CNT-0X . As observed from Fig. 33, the breakthrough times are less than 40 min for CMS and CNT-Plain, and for CNT-0X equilibrium time 92 min.

5.3.2.11. Breakthrough curves CMS, CNT-Plain, and CNT-0X with Ethylbenzene high concentration:

The effect of contact time on the adsorption of ethylbenzene Toluene by CMS, CNT-Plain, and CNT-0X and there was studied in the range of 4-128 min. The results are shown in Fig. 34 The Figure shows that ethylbenzene Toluene adsorption has been slowly increased Then the adsorption capacity increases rapidly until it reached equilibrium. the experiments were carried out for VOC inlet

concentrations: 700 ppm. For each run, 3 g adsorbent was taken. The bed temperature was set at the optimum temperature of 25o C and the flow rate at 16ml/min. Fig. 34 describes the experimentally obtained breakthrough curves for ethylbenzene toluene under the VOC gas inlet concentrations for CMS, CNT-Plain and CNT-0X . As observed from Fig. 34, the breakthrough times are less than 40 min for CMS and CNT-Plain, and for CNT-0X equilibrium time 128 min.

5.3.2.12. Breakthrough curves CMS, CNT-Plain, and CNT-0X with o-xylene high concentration:

The effect of contact time on the adsorption of o-xylene by CMS, CNT-Plain, and CNT-0X and there was studied in the range of 4-92 min. The results are shown in Fig. 35 The Figure shows that o-xylene Toluene adsorption has been slowly increased Then the adsorption capacity increases rapidly until it reached equilibrium. the experiments were carried out for VOC inlet concentrations: 700 ppm. For each run, 3 g adsorbent was taken. The bed temperature was set at the optimum temperature of 25o C and the flow rate at 16ml/min. Fig. 35 describes the experimentally obtained breakthrough curves for o-xylene toluene under the VOC gas inlet concentrations for CMS, CNT-Plain and CNT-0X. As observed from Fig. 35, the breakthrough times are less than 40 min for CMS and CNT-Plain, and for CNT-0X equilibrium time 92 min.

Chapter 6

Summary and Conclusion

CHAPTER - 6

SUMMARY AND CONCLUSIONS

The floating catalytic chemical vapor deposition method was applied to prepare carbon nanotubes (LCNT) and carbon microspheres (LCM). A solution containing 2% ferrocene in benzene was used as the hydrocarbon source. Ferrocene being a heterocyclic aromatic compound served as both hydrocarbon source and the heteroatom “Fe” acted as the floating catalyst. Carbon nanotubes (LCNT) and carbon microspheres (LCM) were prepared indigenously and subsequently oxidised to obtain the corresponding oxidised nanotubes (LCNT-OX) and microspheres (LCM-OX). Surface morphology of the prepared composites was studied using SEM, TEM and BET measurements.

FTIR and XPS spectroscopy revealed the anchoring of functional groups during oxidation. The prepared carbon composites were evaluated for TEX removal in water/air phase. In aqueous phase, it was found that irrespective of initial pH, sorption remained constant and adsorption of these VOCs attained equilibrium within 20 min. Adsorption of TEX upon various carbon composites followed pseudo second order kinetics with regression coefficients >0.99 . Langmuir and Freundlich isotherms were used to model the obtained equilibrium data and various isotherm constants were evaluated. Maximum adsorption capacity of LCNT, LCNT-OX, LCM and LCM-OX towards o-xylene was found to be 47.17, 72.46, 24.27 and 47.16 mg/g, respectively. Static adsorption tests of the prepared carbon composites revealed adsorption capacity in the order o-xylene $>$ toluene $>$ ethylbenzene.

Furthermore, sorption capacity of oxidized composites was found to be higher in both phases (air and water) compared to as prepared carbon composites.

This could be attributed to the introduction of surface functional groups, increased surface area and the increased percentage of mesopores. Further the prepared composites revealed the recyclability without depreciation in adsorption capacity. Application of the prepared composites to TEX spiked ground water was also carried out. The results evidenced that the adsorption capacity was same irrespective of the matrix. Column studies revealed that 50 bed volumes of (950 ml) of 30 ppm of toluene containing distilled water could be treated reducing the concentration from 30 ppm to below detection limit using 3 mg of LCNT.

Indigenous set up was constructed to evaluate the adsorption capacity of various composites towards the removal of TEX from air. Experiments were conducted with three different initial concentrations of TEX were studied namely 100, 300, and 700 ppm at a flow rate of 16ml/min. Nitrogen was used as the diluant gas. The concentration of various VOCs was monitored using GC. Using the concentration of TEX before and after passing through the adsorbent with time, breakthrough curves were constructed. Weight of the adsorbent for this method was maintained at 3g. The results obtained from break through revealed that similar to water experiments, higher uptake capacity of LCNT-OX compared to other adsorbents.

Further uptake capacity of O-Xylene was high compared to ethyl benzene and toluene. The uptake capacity of TEX at an initial concentration of 300 ppm using CNT-OX as adsorbent was found to be 39.85, 58.89 and 66.80 mg/g respectively. Furthermore, the percentage removal of TEX from air using the carbon composites ranged from 38.9 to 76.4%.

Finally, removal TEX from air and water matrix without depreciation in sorption capacity, faster kinetics, dynamic equilibrium and recyclability studies demonstrate

the applicability of prepared carbon composites in filter cartridges, air scrubbers and wastewater treatment units.

References

REFERENCES

1. Dhaouadi, A., Monser, L. and Adhoum, N., 2010. Removal of rotenone insecticide by adsorption onto chemically modified activated carbons. *Journal of Hazardous Material*, Vol. 181, pp. 692-699.
2. Gaur, A. and Shim, M., 2008. Substrate-enhanced O₂ adsorption and complexity in the Raman G-band spectra of individual metallic carbon nanotubes. *Physical Review B*, Vol. 78, pp. 125-422.
3. Silvestre-Albero, A., Ramos-Fernández, J., MartínezEscandell, M. A., Sepúlveda-Escribano, J., Silvestre-Albero, F. and Rodríguez- E., 2010. High saturation capacity of activated carbons prepared from mesophase pitch in the removal of volatile organic compounds. *Carbon*, Vol. 48, pp. 548-556.
4. Daifullah, A. A. M. and Girgis, B.S., 2003. Impact of surface characteristics of activated carbon on adsorption of BTEX. *Colloids and Surfaces A*, Vol. 214, pp. 181–193.
5. Allabaksh, M.B., Mandal, B.K., Kesarla, M.K., Kumar, K. S. and Reddy, P. S., 2010. Preparation of stable zerovalent iron nanoparticles using different chelating agents. *Journal of Chemical and Pharmaceutical Research*, Vol. 2, pp. 67-74.
6. Berenjian, A., Chan, N. and Malmiri, H. J., 2012. Volatile Organic Compounds Removal Methods: A Review. *American Journal of Biochemistry and Biotechnology*, Vol. 8, Issue 4, pp. 220-229.

7. Pan, B. and Xing, B., 2008. Adsorption mechanisms of organic chemicals on carbon nanotubes. *Environmental Science & Technology*, Vol. 42, pp. 9005-9013.
8. Barbieri, C. and Mshenga, P., 2008. The role of firm and owner characteristics on the performance of agritourism farms. *Sociologia Ruralis*, Vol. 48, Issue 2, pp. 166–183.
9. Bautista, L., Martínez, M. and José A., 2003. Adsorption of α -amylase in a fixed bed: Operating efficiency and kinetic modeling, *AIChE Journal*, Vol. 49, pp. 2631- 2641.
10. Blocki, S. W., 1993. Hydrophobic zeolite adsorbent: a proven advancement in solvent separation technology. *Environmental Progress*, Vol. 12, pp. 226–230.
11. Borba, C., Guirardello R., Edson, S., Veit, M.T. and Célia, T., 2006. Removal of nickel(II) ions from aqueous solution by biosorption in a fixed bed column: Experimental and theoretical breakthrough curves. *Biochemical Engineering Journal*, Vol. 30, pp. 184-191.
12. Brown, S. K., Sim, M. R., Abramson, M. J. and Gray, C. N., 1994. Concentrations of volatile organic compounds in indoor air—a review. *Indoor Air*, Vol. 4, pp. 123–134.
13. Brunauer, S., Emmett, P. H. and Teller, E., 1938. Adsorption of gases in multimolecular layer. *Journal of the American Chemical Society*, Vol. 60, pp. 309-319.
14. Burstyn, I., You, X., Cherry, N. and Senthilselvan, A., 2007. Determinants of airborne benzene concentrations in rural areas of western Canada. *Atmospheric Environment*, Vol. 41, pp. 7778–7787.

15. Lu, C., Chung, Y. L. and Chang, K.F., 2005. Adsorption of trihalomethanes from water with carbon nanotubes. *Water Research*, Vol. 39, pp. 1183.
16. Lu, C., Chung, Y.L. and Chang, K.F., 2006. Adsorption thermodynamic and kinetic studies of trihalomethanes on multiwalled carbon nanotubes. *Journal of Hazardous Materials*, Vol. 138, pp. 304–310.
17. Chen, C., Hu, J., Shao, D., Li, J. and Wang, X., 2009a. Adsorption behavior of multiwall carbon nanotube/iron oxide magnetic composites for Ni(II) and Sr(II). *Journal of Hazardous Materials*, Vol. 164, pp. 923-928.
18. Chen, C., Hu, J., Xu, D., Tan, X., Meng, Y. and Wang, X., 2008. Surface complexation modeling of Sr (II) and Eu (III) adsorption onto oxidized multiwall carbon nanotubes. *Journal of Colloid and Interface Science*, Vol. 323, pp. 33-41.
19. Chen, C., Wang, X. and Nagatsu, M., 2009. Europium adsorption on multiwall carbon nanotube/iron oxide magnetic composite in the presence of polyacrylic acid. *Environ. Science and Technology*, Vol. 43, pp. 2362-2367.
20. Chin, C. J., Shih, L. C., Tsai, H. J. and Liu, T.K., 2007. Adsorption of o-xylene and p-xylene from water by SWCNTs. *Carbon*, Vol. 45, pp. 1254–1260.
21. Hussain, C. M., Saridara, C. and Mitra, S., 2008. Microtrapping characteristics of single and multi-walled carbon nanotubes. *Journal of Chromatography A*, Vol. 1185, pp. 161-166.
22. Carp, O., Huisman, C. L. and Reller, A., 2004. Photoinduced reactivity of titanium dioxide. *Progress in Solid State Chemistry*, Vol. 32, pp. 33-177.

23. Cheng, M., Li, C., Zhou, L. and Xie, S. C., 2015. Mo marine geochemistry and reconstruction of ancient ocean redox states. *Science China: Earth Sciences*. Vol. 58.
24. Cheng, T., Jiang, Y., Zhang, Y. and Liu, S., 2004. Prediction of Breakthrough Curves for Adsorption on Activated Carbon Fibers in a Fixed Bed. *Article in Carbon*, Vol. 42, pp. 3081-3085.
25. Choi, N. C., Choi, J. W., Kim, S. B., Park, S. J. and Kim, D. J., 2009. Two-dimensional modelling of benzene transport and biodegradation in a laboratory-scale aquifer. *Environmental Technology*, Vol. 30, pp. 53–62.
26. Chuang, Y. H., Tzou, Y. M., Wang, M. K., Liu, C. H. and Chiang, P. N., 2008. Removal of 2-chlorophenol from aqueous solution by Mg/Al layered double hydroxide (LDH) and modified LDH. *Industrial and Engineering Chemistry Research*, Vol. 47, pp. 3813–3819.
27. Colomer, C., Stephen, S., Lefrant, G., Tendeloo, V., Willems, I. and Konya, Z., 2000. Large-scale synthesis of single-wall carbon nano tubes by catalytic chemical vapour deposition (CCVD) method. *Chemical Physics Letters*, Vol. 317, pp. 83-89.
28. Shan, D., Deng, S., Zhao, T., Yu, G., Winglee, J. and Wiesner, M.R., 2016. Preparation of regenerable granular carbon nanotubes by a simple heating-filtration method for efficient removal of typical pharmaceuticals. *Chemical Engineering Journal*, Vol. 294, pp. 353-361.
29. Das, D., Gaur, V. and Verma, N., 2004. Removal of volatile organic compound by activated carbon fiber. *Carbon*, Vol. 42, Issue 14, pp. 2949-2962.

30. Davis, W.M., Erickson, C.L. and Johnston, C.T., 1999. Quantitative Fourier transform infrared spectroscopic investigation of humic substance functional group composition. *Chemosphere*, Vol. 38, pp. 2913–2928.
31. De Bortoli, M., Knoppel, H., Pecchio, E., Peil, A., Rogora, L., Schauenburg, H., Schlitt, H. and Vissers, H., 1986. Concentrations of selected organic pollutants in indoor and outdoor air in northern Italy. *Environment International*, Vol. 12, pp. 343 - 350.
32. Deshusses, M.A. and Johnson, C. T., 2000. Development and validation of a simple protocol to rapidly determine the performance of biofilters for VOC treatment. *Environmental Science & Technology*, Vol. 34, Issue 3, pp. 461-467.
33. Dhada, I., Nagar, P. and Sharma, M., 2015. T1 - Photo-catalytic oxidation of individual and mixture of benzene, toluene and p-xylene. *International Journal of Environmental Science and Technology*, Vol. 13.
34. Dutta, C., Som, D., Chatterjee, A., Mukherjee, A. K., Jana, T. K. and Sen, S., 2009. Mixing ratios of carbonyls and BTEX in ambient air of Kolkata, India and their associated health risk. *Environmental Monitoring and Assessment*, Vol. 148, pp. 97–107.
35. ECA-IAQ. European concerted action indoor air quality & its impact on man (formerly COST Project 61 3) environment and quality of life. Effects of indoor air pollution on human health. Report No 10. Luxembourg: European Union; EUR 14086 EN, 1991.
36. Edgerton, S. A., Holdren, M. W., Smith, D.I. and Shah, J., 1989. Inter urban comparison of ambient volatile organic compound concentration. *Journal of the Air & Waste Management Association*, Vol. 39, pp. 729–732.

37. EPA, 2012. Volatile Organic Compounds (VOCs). Finlayson-Pitts, B.J. and J.N. Pitts, 1986. Atmospheric Chemistry: Fundamentals and Experimental Techniques. John Wiley and Sons, New York, ISBN-10: 0471882275, pp. 1098.
38. European chlorinated solvent associations (ECSA), 1999. <http://www.chlorinated-solvents.eu/index.php/regulatory-compliance/voc-regulation-ied>
39. Su, F., Lu, C. and Hu, S., Adsorption of benzene, toluene, ethylbenzene and p-xylene by NaOCl- oxidized carbon nanotubes, Colloids and Surfaces A: Physicochem. Eng. Aspects, Vol. 353, pp. 83–91.
40. Yu, F., Ma, J., Wang, J., Zhang, M. and Zheng, J., 2016. Magnetic iron oxide nanoparticles functionalized multi-walled carbon nanotubes for toluene, ethylbenzene and xylene removal from aqueous solution. Chemosphere, Vol. 146, pp. 162 – 172.
41. Fu, F. and Wang, Q., 2011. Removal of heavy metal ions from wastewaters: a review. Journal of Environmental Management., Vol. 92, pp. 407-418.
42. Carlos- Wallace, F. M., Zhang, L., Smith, M.T., Rader, G. and Steinmaus, C., 2016. Parental, in utero, and early-life exposure to benzene and the risk of childhood leukemia: a meta-analysis. Am Journal of Epidemiology., Vol. 183, pp. 1-14.
43. Fan, X., Sokorai, K. J., Engemann, J., Gurtler, J. B. and Li,u Y., 2012. Inactivation of *Listeria innocua*, *Salmonella Typhimurium*, and *Escherichia coli* O157:H7 on surface and stem scar areas of tomatoes using in- package ozonation. Journal of Food Protection, Vol. 75, Issue 9, pp. 1611-1618.

44. Ferrari, A. C. and Basko, D.M., 2013. Raman spectroscopy as a versatile tool for studying the properties of grapheme. *Nat. Nanotechnol*, Vol. 8, pp. 235-246.
45. Ovejero, G., Sotelo, J.L., Romero, M.D., Rodriguez, A., Ocana, M.A., Rodriguez, G. and García, J., 2006. Multiwalled carbon nanotubes for liquid-phase oxidation. Functionalization, characterization, and catalytic activity. *Industrial & Engineering Chemistry Research* , Vol. 45, pp. 2206–2212.
46. Gariazzo, C., Pelliccioni, A., Di Filippo, P., Sallusti, F. and Cecinato, A., 2005. Monitoring and analysis of volatile organic compounds around an oil refinery. *Water Air Soil Pollution*, Vol. 167, pp. 17–38.
47. Gupta, V. and Verma, N., 2002. Removal of volatile organic compounds by cryogenic condensation followed by adsorption. *Chemical Engineering Science*, Vol. 57, Issue 14, pp. 97-114.
48. Nourmoradi, H., Nikaeen, M. and Khiadani, M., 2012. Removal of benzene, toluene, ethylbenzene and xylene (BTEX) from aqueous solutions by montmorillonite modified with non-ionic surfactant: Equilibrium, kinetic and thermodynamic study. *Chemical Engineering Journal* Vol. 191, pp. 341 – 348.
49. Hyung, H. and Kim, J. H., 2008. Natural organic matter (NOM) adsorption to multi-walled carbon nanotubes: effect of NOM characteristics and water quality parameters. *Environmental Science & Technology*., Vol. 42, pp. 4416-4421.
50. Sone, H., Fugetsu, B., Tsukada, T. and Endo, M., 2008. Affinity-based elimination of aromatic VOCs by highly crystalline multi-walled carbon nanotubes. *Talanta*, Vol. 74, pp. 1265-1270.

51. Ho, Y.S., 2006. Review of second-order models for adsorption systems. *Journal of Hazardous Materials* Vol. 136, pp. 681-689.
52. Hosseini, A., David, N., Kwong, Y. Z., Harish, S., Xu, X. and Ray, T. C., 2011. Multimode Interference Beam Splitter Design Techniques for on-chip optical Interconnections. *IEEE Journal of Selected topics In Quantum Electronics*, VOL. 17, NO. 3.
53. Hsieh, C. C., Babcock, R. W. and Stenstrom, M. K., 1993b. Estimating Emissions of Twenty VOCs: Diffused Aeration *Journal of Environmental Engineering. Div., American Society of Civil Engineers: New York*, Vol. 119, pp. 1099–1118.
54. Hsieh, C. C., Ro. K. S. and Stenstrom, M. K., 1993a. Estimating Emissions of Twenty VOCs: Surface Aeration. *American Society of Civil Engineers: New York Journal of Environmental Engineering Div., Vol. 119*, pp. 1077– 1098.
55. Huang, Y., Ho, S. S. H., Lu, Y., Niu, R., Xu, L., Cao, J. and Lee, S., 2016. Removal of indoor volatile organic compounds via photocatalytic oxidation: a short review and prospect. *Molecules*, Vol. 21, Issue 1, pp. 56.
56. Hussain, C. M., Saridara, C. and Mitra, S., 2010. Microtrapping of volatile organic compounds with carbon nanotubes Sonklanakaran. *Journal of Science and Technology*, Vol. 32, Issue 5, pp. 505.
57. ISO- 16000, 1989. Indoor air — Part 10: Determination of the emission of volatile organic compounds from building products and furnishing — Emission test cell method, <https://www.iso.org/obp/ui/#iso:std:iso:16000:-10:ed-1:v2:en>
58. Goering, J., Kadossov, E. and Burghaus, U., 2008. Adsorption kinetics of alcohols on single-wall carbon nanotubes: an ultrahigh vacuum surface

- chemistry study. *Journal of Physical Chemistry. C*, Vol. 112, pp. 10114-10124.
59. Jahangiri, F., Hirschfeld-Cytron, J., Goldman, K., Pavone, M. E., Gerber, S. and Klock, S.C., 2011. Correlation between depression, anxiety, and nausea and vomiting during pregnancy in an in vitro fertilization population-a pilot study *Journal of Psychosomatic Obstetrics & Gynecology* , Vol. 32, pp. 113–118.
60. Jaynes, W. E. and Vance, G.E., 1999. Sorption of benzene, toluene, ethylbenzene and xylene (BTEX) compounds by hectorite clays exchanged with aromatic organic cations. *Clays Clay Miner*, Vol. 47, Issue 3, pp. 358 – 365.
61. Jeong, J., Sekiguchi, K., Lee, W. and Sakamoto, K., 2005. Photodegradation of gaseous volatile organic compounds (VOCs) using TiO₂ photoirradiated by an ozone-producing UV lamp: decomposition characteristics, identification of by-products and water-soluble organic intermediates. *Journal of Photochemistry and Photobiology*, Vol. 169, pp. 279–287.
62. Agnès, J. and Alain, P., 2009. Linear driving force models for dynamic adsorption of volatile organic compound traces by porous adsorbent beds. *Mathematics and Computers in Simulation*, Vol. 79, pp. 3492-3499.
63. Takeuchi, K., Hayashi, T., Kim, Y. A., Fujisawa, K. and Endo, M., 2014. "The state-of-the-art science and applications of carbon nanotubes". Vol. 5, Issue 1, pp 15.
64. Kamal, M. S., Razzak, S. A. and Hossain, M. M., 2016. Catalytic oxidation of volatile organic compounds (VOCs)—A review. *Atmospheric Environment*, Vol. 140, pp. 117-134.

65. Krause, C., Mailahn, W., Nagel, R., Schulz, C., Seifert, B. and Ullrich, D., 1987. Occurrence of volatile organic compounds in the air of 500 homes in the Federal Republic of Germany. In: B. Seifert, H. Esdorn, M. Fischer, H. Riiden and J. Wegner (eds.), *Indoor Air '87. Proceedings of the 4th International Conference on Indoor Air Quality and Climate*. Berlin, 17 - 21 August 1987, Vol. 1, pp. 102 - 106.
66. Wang, L., Zhu, D., Duan, L. and Chen, W., 2010. Adsorption of single-ringed N-and S-heterocyclic aromatics on carbon nanotubes. *Carbon*, Vol. 48, pp. 3906-3915.
67. Lagergren, S., 1898. About the Theory of So-Called Adsorption of Soluble Substances. *Kungliga Svenska Vetenskapsakademiens*, Vol. 24, pp. 1-39.
68. Lau, W. L. and Chan, L. Y., 2003. Commuter exposure to aromatic VOCs in public transportation modes in Hong Kong. *Science of the Total Environment*, Vol. 308, pp. 143-155.
69. Levin, A. T., Onatski, A., Williams, J. C. and Williams, N., 2006. "Monetary Policy under Uncertainty in Micro-founded Macroeconomic Models". *NBER Macroeconomics Annual 2005*, MIT Press, pp. 229-287.
70. Lillo-Rodenas, M.A., Cazorla-Amoros, D. and Linares-Solano, A., 2011. Benzene and toluene adsorption at low concentration on activated carbon fibres. *Adsorption*. Vol. 17, Issue 3, pp. 473-481.
71. Lin, K.-Y., Chang, J.-K., Chen, C.-Y. and Tsai, W.-T., 2009. Effects of heat treatment on materials characteristics and hydrogen storage capability of multi-wall carbon nanotubes. *Diamond and Related Materials*., Vol. 18, pp. 553-556.

72. Lu, H., Wen, S., Feng, Y., Wang, X., Bi, X., Sheng, G. and Fu, J., 2006. Indoor and outdoor carbonyl compounds and BTEX in the hospitals of Guangzhou, China. *Science of The Total Environment*, Vol. 368, pp. 574–584.
73. Engel, M. and Chefetz, B., Removal of triazine-based pollutants from water by carbon nanotubes: Impact of dissolved organic matter (DOM) and solution chemistry. *Water Research* Vol. 106, pp. 146 - 154.
74. Ahmaruzzaman, M., 2008. Adsorption of phenolic compounds on low-cost adsorbents: a review. *Advances in Colloid and Interface Science* Vol. 143, pp. 48-67.
75. Seredych, M. and Badosz, T.J., 2010. Adsorption of ammonia on graphite oxide/Al₁₃ composites, *Colloids Surf. A Physicochemical and Engineering Aspects*, Vol. 353, pp. 30-36.
76. Ma, H., Shieh, K-J. and Qiao, T., 2006. Study of transmission electron microscopy (TEM) and Scanning Electron Microscopy (SEM). *Nature Science*, Vol. 4, pp. 14-22.
77. Manahan, S. E., 1994. *Environmental Chemistry*, 6th ed. Lewis Publisher, USA.
78. Mohammed, M., Adamu, A. A. M. and Borkoma, M. B., 2015. Determination of air pollution tolerance index of selected trees in selected locations in Maiduguri. Vol.1, Issue 7, pp.378-383.
79. Molhave, L., 1992. Controlled experiments for studies of the sick building syndrome. In: G. Tucker, B.P. Leaderer, L. Mprlhave, and W.S. Cain (eds.), *Sources of indoor air contaminants - characterizing emissions and health*

- impact. Special issue of Annals of the New York Academy of Science, Vol. 641, pp. 46-55.
80. Ott, M. G., Townsend, J. C., Fishback, W. A. and Langner, R. A., 1978. 'Mortality among individuals occupationally exposed to benzene' Archives of Environmental Health, Vol. 33, pp. 3–10.
81. Park, H., Lee, E., Chung, Y., Lee, S., Ahn, H. and Kim, D. J., 2015. VOC gas sensors fabricated with graphene oxide composites for food safety and quality. ECS Transactions, Vol. 69, Issue 38, pp. 41-45.
82. Park, K.-H. and Jo, W.-K., 2004. 'Personal volatile organic compound (VOC) exposure of children attending elementary schools adjacent to industrial complex'. Atmospheric Environment, Vol. 38, pp. 1303–1312.
83. Patoulias, D., Fountoukis, C., Riipinen, I. and Pandis, S. N., 2015. The role of organic condensation on ultrafine particle growth during nucleation events. Atmospheric Chemistry and Physics, Vol. 15, Issue 11, pp. 6337-6350.
84. Pearce, W., Brown, B., Nerlich, B. and Koteyko, N., 2015. Communicating climate change: conduits, content, and consensus. Wiley Interdiscip. Reviews: Climate Change; Vol. 6, pp. 613–626.
85. Popov, V. N., 2004. Carbon nanotubes: properties and application. Materials Science and Engineering, Vol. 43, pp. 61–102.
86. Pourfayaz, F., Jafari, S. H., Mortazavi, Y. K., Abbas, A. and Khonakdar, H. A., 2015. Combination of Plasma Functionalization and Phase Inversion Process Techniques for Efficient Dispersion of MWCNTs in Polyamide 6: Assessment through Morphological, Electrical, Rheological and Thermal Properties, Journal, Vol. 54, Issue 6.

87. Profumo, A., Fagnoni, M., Merli, D., Quartarone, E., Protti, S., Dondi, D. and Albini, A., 2006. Multiwalled carbon nanotube chemically modified gold electrode for inorganic As speciation and Bi(III) Determination, *Analytical Chemistry* Vol. 78, pp. 4194-4199.
88. Purdom, P.W., 1980. *Environmental Health*, Academic Press, New York.
89. Rahbar, M. S. and Kaghazchi, T., 2005. Modeling of packed absorption tower for volatile organic compounds emission control. *International Journal of Environmental Science & Technology*, Vol. 2, Issue 3, pp. 207-215.
90. Ren X., Chen, C., Nagatsu, M. and Wang, X., 2011. Carbon nanotubes as adsorbents in environmental pollution management: a review *Chemical Engineering Journal* Vol. 170, pp. 395-410.
91. Rene, E. R., Murthy, D. V. S. and Swaminathan, T., 2005. Performance evaluation of a compost biofilter treating toluene vapours. *Process Biochem.*, Vol. 40, Issue 8, pp. 2771–2779.
92. Kayser, R., 1881. GBIF Backbone Taxonomy. Checklist dataset <https://doi.org/10.15468/39omei> accessed via GBIF.org on 2018-06-25.
93. Roberts, I. M., Robinson, D. J. and Harrison, B. D., 1984. Serological relationships and genome homologies among gemini viruses *Journal of General Virology.*, Vol. 65, pp. 1723-1730.
94. Rodenas Lillo, M.A., Cazorla-Amoros, D. and Linares-Solano, A., 2006. Behaviour of activated carbons with different pore size distributions and surface oxygen groups for benzene and toluene adsorption at low concentrations. *Carbon*, Vol. 43, issue 8, pp. 1758–1767.

95. Romero-Anaya, A., Lillo-Ródenas, M., De Lecea, Salinas-Martínez, Linares-Solano, A., 2012. Hydrothermal and conventional H₃PO₄ activation of two natural bio-fibers, Vol. 50.
96. Rothweiler, H., Wager, P.A. and Schlatter, C., 1992. Volatile organic compounds and some very volatile organic compounds in new and recently renovated buildings in Switzerland. *Atmospheric Environment*, Vol. 26, Issue 12, pp. 2219 - 2225.
97. Agnihotri, S., Rood, M.J. and Rostam-Abadi, M., 2005. Adsorption equilibrium of organic vapors on single-walled carbon nanotubes. *Carbon*, Vol. 43, pp. 2379–2388.
98. Hsu, S. and Lu, C., 2007. Modification of single-walled carbon nanotubes for enhancing isopropyl alcohol vapor adsorption from air stream, *Separation Science and Technology*, Vol. 42, pp. 2751–2766.
99. Sharmasarkar, S., Jaynes, W.F. and Vance, G.F., 2000. BTEX sorption by montmorillonite Organoclays: TMPA, ADAM, HDTMA. *Water, Air & Soil Pollution*, Vol. 119, pp. 257 – 273.
100. Agnihotri, S., Rood, M.J. and Rostam-Abadi, M., 2005. Adsorption equilibrium of organic vapors on single-walled carbon nanotubes. *Carbon*, Vol. 43, pp. 2379-2388.
101. Ntim, S. A. and Mitra, S., 2011. Removal of Trace Arsenic To Meet Drinking Water Standards Using Iron Oxide Coated Multiwall Carbon Nanotubes, *Journal of Chemical & Engineering . Data*, Vol. 56, 2077–2083.
102. Fagan, S. B., Souza, A. G., Lima, J. O. G., Mendes, J., Ferreira, O.P., Mazali, I.O., Alves, O.L. and Dresselhaus, M.S., 2004. 1,2-Dichlorobenzene interacting with carbon nanotubes. *Nano Letters*, Vol. 4, pp. 1285–1288.

103. Saito, R. and Kataura, H., 2011. Optical properties and Raman spectroscopy of carbon nanotubes, in: Carbon Nanotubes: Synthesis Structure and Applications. Springer, Berlin/Heidelberg, Vol. 19, pp. 213–247.
104. San, J.-Y., Hsu, Y.-C. and Wu, L.-J., 1998. Adsorption of toluene on activated carbon in a packed bed. International Journal of Heat and Mass Transfer, Vol. 41, Issue 21, pp. 3229-3238.
105. Sankararamakrishnan, N., Chauhan, D. and Dwivedi, J., 2016. Synthesis of functionalized carbon nanotubes by floating catalytic chemical vapor deposition method and their sorption behavior toward arsenic. Chemical Engineering Journal, Vol. 284, pp. 599-608.
106. Sawant, S.D., Baravkar, A. A. and Kale, R.N., 2011. FT-IR spectroscopy: principle, techniques and mathematics. International Journal of Pharma and Bio Sciences, Vol. 2, pp. 513-519.
107. Schierz, A. and Zanker, H., 2009. Aqueous suspensions of carbon nanotubes: Surface oxidation, colloidal stability and uranium sorption. Environmental Pollution, Vol. 157, pp. 1088–1094.
108. Seifert, B., 1990. Regulating indoor air. In: Walkinshaw, D.S. (ed.), Indoor Air '90, Proceedings of the 5th International Conference on Indoor Air Quality and Climate, Toronto, Canada, July 29 -August 3, Vol. 5, pp. 35-49.
109. Shanov, V., Yun, Y. H. and Schulz, M.J., 2006. Synthesis and characterization of carbon nanotube materials. Journal of Chemical Technology and Metallurgy, Vol. 41, pp. 377-390.
110. Shim, W.-G., Jae, W. L. and Hee, M., 2006. Adsorption equilibrium and column dynamics of VOCs on MCM-48 depending on pelletizing pressure. Microporous and Mesoporous Materials, Vol. 88, pp. 112-125.

111. Siahpoosh, M., Fatemi, S. and Vatani, A., 2009. Mathematical modeling of single and multi-component adsorption fixed beds to rigorously predict the mass transfer zone and breakthrough curves. *Iranian Journal of Chemistry and Chemical Engineering*, Vol. 28, pp. 25–44.
112. Siegbahn, K.M., 1981. X-Ray photoelectron spectroscopy (XPS), electron spectroscopy for chemical analysis (ESCA), Chang Gung University. *Advanced Photonics Laboratory*, Vol. 6, pp. 1-55.
113. Singh, C., Shaffer, M.S. P. and Windle, H., 2003. Production of controlled architectures of aligned carbon nanotubes by an injection chemical vapour deposition method. *Carbon*, Vol. 41, pp. 359-368.
114. Sircar, S., Golden, T. and Rao, M., 1996. Activated carbon for gas separation and storage. *Carbon*, Vol. 34, pp. 1-12.
115. Song, Y., Shao, M., Liu, Y., Lu, S., Kuster, W., Goldan, P. and Xie, S., 2007. Source apportionment of ambient volatile organic compounds in Beijing. *Environmental Science & Technology*, Vol. 41, Issue12, pp. 4348–4353.
116. Srivastava, A., Joseph, A. E., More, A., Patil, S., 2005. Emissions of VOCs at urban petrol retail distribution centres in India (Delhi and Mumbai). *Environmental Monitoring and Assessment*, Vol. 109, Issue 1–3, pp. 227–242.
117. Stenehjem, D. D., Bellows, B. K. and Yager, K. M., 2015. Cost-Utility of a Prognostic Test Guiding Adjuvant Chemotherapy Decisions in Early-Stage Non-Small Cell Lung Cancer. *Oncologist*.
118. Egbuchunama, T.O., Obia, G., Okieimenb, F.E. and Tihminliogluc, F., 2016. Removal of BTEX from Aqueous Solution Using Organokaolinite.

- International Journal of Applied Environmental Sciences, Vol. 11, pp. 505-513.
119. Tans, S.J., Devoret, M.H., Dai, H., Thess, A., Smalley, R.E., Geerlings, L. J. and Dekker, C., 1997. Individual single- wall carbon nano tubes as quantum wires. *Nature*, Vol. 386, pp. 474-477.
120. Tefera, D. T., Jahandar Lashaki, M., Fayaz, M., Hashisho, Z., Philips, J. H., Anderson, J. E. and Nichols, M., 2013. Two-dimensional modeling of volatile organic compounds adsorption onto beaded activated carbon. *Environmental science & technology*, Vol. 47, Issue 20, pp. 11700-11710.
121. Zhao, T., Zhang, Z., Peter, D., Zhang, W. K., Friedlander, M. and Xu, Y., 2015. Humanized Mice Reveal Differential Immunogenicity of Cells Derived from Autologous Induced Pluripotent Stem Cells. *Cell Stem Cell*, Vol. 17, pp. 353–359.
122. U.S. Environment Protection Agency Office of Air Quality, 2000. National Air Toxics Program: The Integrated Urban Strategy. Report to Congress, EPA 453-R-99-007. <http://www.epa.gov/urban-air-toxics>.
123. United States Environmental Protection Agency (USEPA), 2006. The clean air act amendments of 1990. Washington.
124. Uria-Tellaetxe, I., Navazo, M., de Blas, M., Durana, N., Alonso, L. and Iza, J., 2016. Gas-phase naphthalene concentration data recovery in ambient air and its relevance as a tracer of sources of volatile organic compounds. *Atmospheric Environment*, Vol. 131, pp. 279–288.

125. USEPA, 1990, Compendium of Methods for the Determination of Toxic Organic Compounds in Ambient Air, Second Edition Compendium Method TO-15, https://www.epa.gov/sites/production/files/2015-07/documents/epa-to-15_0.pdf
126. Chen, W., Duan, L. and Zhu, D., 2007. Adsorption of polar and nonpolar organic chemicals to carbon nanotubes. *Environ. Sci. Technol.*, Vol. 41, pp. 8295–8300.
127. Wallace, L., Pellizzari, E. and Wendel, C., 1991. Total organic concentrations in 2700 personal, indoor, and outdoor samples collected in the US EPA TEAM studies. *Indoor Air*, Vol. 1, Issue 4, pp. 465 - 477.
128. Wang, C. H., Hsiao, C. K. and Chen, C. L., 2007. A review of the epidemiologic literature on the role of environmental arsenic exposure and cardiovascular diseases. *Toxicology and Applied Pharmacology*, Vol. 222, pp. 315–326.
129. Wang, C. M., Chang, K. S., Chung, T. W. and Wu, H., 2004. Adsorption equilibria of aromatic compounds on activated carbon, silica gel, and 13X zeolite. *Journal of Chemical & Engineering Data*, Vol. 49, Issue 3, pp. 527-531.
130. Watson, J. G., Chow, J. C. and Pace, T. G., 1991. Chemical mass balance. In: Hopke PK (ed) *Receptor modeling for air quality management*. Elsevier Press, New York, NY, pp 83–116.
131. Watson, J. and Chow, J., 2007. Receptor models for source apportionment of suspended particles. *Environmental Science & Technology - Environmental Science & Technology*, Vol. 22, pp. 279-316.

132. Watson, J. G., Chow, J. C. and Fujita, E. M., 2001. Review of volatile organic compound source apportionment by chemical mass balance, *Atmospheric Environment*, Vol. 35, Issue 9, pp. 1567–1584.
133. WHO, 2000. The world health report - Health systems: improving performance, <http://www.who.int/whr/2000/en/>
134. Wibowo, N., Setyadhi, L., Wibowo, D., Setiawan, J. and Ismadji, S., 2007. Adsorption of benzene and toluene from aqueous solutions onto activated carbon and its acid and heat treated forms: influence of surface chemistry on adsorption. *Journal of Hazardous Materials*, Vol. 146, pp. 237–242.
135. Wu, F.C., Tseng, R.L. and Juang, R.S., 2009. Initial behavior of intraparticle diffusion model used in the description of adsorption kinetics. *Chemical Engineering Journal*, Vol. 153, pp. 1-8.
136. Zhang, X., Zhao, X., Hu, J., Wei, C. and Bi, H.T., 2011. Adsorption dynamics of trichlorofluoromethane in activated carbon fiber beds. *Journal of Hazardous Materials*, Vol. 186, pp. 1816-1822.
137. Xiang, L. I., Zhong, L. I. and Ling, ai LUO., 2006. Adsorption Kinetics of Dibenzofuran in Activated Carbon Packed Bed. *Chinese Journal of Chemical Engineering*, Vol. 16, Issue 2, pp. 203-208.
138. You, X., Senthilselvan, A., Cherry, N. M., Kim and H. G., Burstyn, I., 2008. Determinants of airborne concentrations of volatile organic compounds in rural areas of Western Canada. *Journal of Exposure Science & Environmental Epidemiology*, Vol. 18, Issue2, pp. 117–128.
139. Yu, F., Mie, J. and Wua, Y., 2011. Adsorption of toluene, ethylbenzene and m-xylene on multi-walled carbon nanotubes with different

- oxygen contents from aqueous solutions. *Journal of Hazardous Materials*, Vol. 192, pp. 1370– 1379.
140. Mèçabih Allabaksh, Z. M.B., Mandal, B.K., Kesarla, M.K., Kumar, K. S. and Reddy, P.S., 2010. Preparation of stable zerovalent iron nanoparticles using different chelating agents. *Journal of Chemical and Pharmaceutical Research*, Vol. 2, pp. 67–74.
141. Xiang, Z., Lu, Y., Gong, X. and Luo, G., 2010. Absorption and desorption of gaseous toluene by an absorbent microcapsules column. *Journal of Hazardous Materials*, Vol. 173, pp. 243-248.
142. Zhang, Y., Mu, Y., Liu, J. and Mellouki, A., 2012. Levels, sources and health risks of carbonyls and BTEX in the ambient air of Beijing, China. *Journal of Environmental Sciences*, Vol. 24, Issue 1, pp. 124–130.
143. Zhang, L., Weng, H. X., Gao, C. J. and Chen, H. L., 2002. Remove volatile organic compounds (VOCs) with membrane separation techniques. *Journal of Environmental Sciences*, Vol. 14, Issue 2, pp. 181-187.
144. Zhang, X., Gao, B., Zheng, Y., Hu, X., Creamer, A. E., Annable, M. D. and Li, Y., 2017. Biochar for volatile organic compound (VOC) removal: Sorption performance and governing mechanisms. *Bioresource technology*, Vol. 245, pp. 606-614.
145. Zhao, X. S., Ma, Q. and Lu, G. Q., 1998. VOC removal: comparison of MCM-41 with hydrophobic zeolites and activated carbon. *Energy & Fuels*, Vol. 12, Issue 6, pp. 1051-1054.

LIST OF PUBLICATIONS

Accepted and Communicated Research Papers

1. Srivastava, I. Mishra, S. Singh. P.K. Gupta T. and Sankararamakrishanan, N. Fast and efficient removal of Toluene, Ethylbenzene and O-Xylene from aqueous phase by functionalized carbon micro/nanocomposites – Journal of Environmental chemical engineering, ElsevierPublication (accepted).
2. Srivastava, I. Singh. P.K. Gupta T. and Sankararamakrishanan, N. (2018). Preparation of mesoporous carbon microspheres by floating catalytic chemical vapor deposition method and its highly enhanced removal capacity of VOC in air. (Communicated).
3. Srivastava, I. Mishra, S. Gupta T. and Sankararamakrishanan N. Studies on novel nano bio-metal doped cellulose nanofibres derived from agrowaste towards deflouridation Journal of carbohydrate polymers, Elsevier Publication (communicated).

Conferences

1. Srivastava, P.K. Singh. T. Gupta and N. Sankararamakrishanan, “Removal of Toluene, Ethyl Benzene and O – Xylene from aqueous solutions using carbon nano tubes prepared by floating catalytic chemical vapor deposition method” , Proceedings of International Conference on renewable energy, green technology and environmental science, ICREGTES, held at New Delhi 3rd December, 17.
2. Attend aInternational Seminar on Sources of Planet Energy, Environmental & Disaster Science: Challenges and Strategies, Organized by: Institute of Engineering & Technology, SMS, Lucknow, 09 - 10 Dec. 2017.
3. International Conference on Materials Engineering (ICME 2017) held at Indian Institute of technology Kanpur during 2 – 4 June 2017.
4. Assessing long-term performance of water sources in terms of quality and quantity and way to enhance water availability held at Indian Institute of technology Kanpur during, 12 – 14 April 2016.
5. Water quality, Its interpretation and sophisticated analysis of heavy metals and organics including pesticides and PAHs held at Indian Institute of technology Kanpur during 23 -27 march, 2015.